EVALUATION OF DUCTILITY OF REIFORCED CONCRETE STRUCTURES WITH SHEAR WALLS HAVING DIFFERENT THICKNESSES AND DIFFERENT POSITIONS

A THESIS SUBMITTED TO THE INSTITUTE OF GRADUATE STUDIES OF NEAR EAST UNIVERSITY

By
SHAHRAM JKHSI QASIM QASIM

In Partial Fulfilment of the Requirements for the Degree of Master of Science in Civil Engineering

NICOSIA, 2021

SHAHRAM JKHSI QASIM QASIM: EVALUATION OF DUCTILITY OF REINFORCED CONCRETE STRUCTURES WITH SHEAR WALLS HAVING DIFFERENT THICKNESSES AND DIFFERENT POSITIONS

Institute of Graduate Studies

Prof. Dr. K. Hüsnü Can Başer

We certify that this thesis is satisfactory for the award of the degree of Master of Science in Civil Engineering

Examining Committee in Charge:

Prof. Dr. Kabir Sadeghi	Committee Chairman, Department of Civil Engineering, NEU
Assoc. Prof. Dr. Rifat Reşatoğlu	Supervisor, Department of Civil Engineering, NEU
Assist. Prof. Dr. Ayten Akçay	Department of Architecture, NEU

I hereby declare that all information in this document has been obtained and presented in accordance with academic rules and ethical conduct. I also declare that, as required by these rules and conduct, I have fully cited and referenced all material and results that are not original to this work.

Name, Last name: SHAHRAM JKHSI QASIM QASIM

Signature: 

Date:

ACKNOWLEDGEMENTS

In the beginning, I would like to express great thanks to my thesis supervisor Assoc. Prof. Dr. Rifat Reşatoğlu for his helping, efforts, and supporting me all the time during my studying and he was a great supporter to me when I faced any problem during my thesis study. He brought my work to a higher level. I appreciate his guidance observed to me during my thesis. I'm happy that I choose not only the best supervisor but also the best motivator and mentor for my master thesis. And I want to thank my committee members.

I would like to thank Prof. Dr. Kabir Sadeghi for his helping and supporting me most of the time. And I want to gratitude to my family for their love, patience, and support. Also, I want to show my thanks to any of my friends for their helping, motivating, and supporting me all the time.

ABSTRACT

Reinforced concrete (RC) shear walls play an important role for taking lateral loads has been searched in this study. One of the main criteria that is required for designing earthquake resistant structures; ductility has been paid attention to. The structures need to be designed to have sufficient strength and ductility for overall safety against earthquake forces. Both the strength and the ductility are combined together to improve its seismic safety. Moreover, the location of the shear walls and shear wall thicknesses effects on ductility have been underlined in this study.

The non-linear static analysis (pushover) method has been selected to analyze and design 96 two-dimensional (2D) models of RC shear walls. Additionally, impacts of several other variables such as a number of stories, span lengths, and compressive strength (f'_C), have been compared. The commercial software program ETABS has been used to design and assess the models of the RC structures.

It is concluded that an increase in shear wall thickness causes a decrease in ductility values and a decrease in ductility value will also occur when shear wall position changes from edge to middle.

***Keywords**:* Ductility, RC, Non-linear static analysis, Earthquake design, Pushover curve, Shear wall, ETABS program

ÖZET

Bu çalışmada yanal yüklerin karşılanmasında önemli rol oynayan betonarme perde duvarlar araştırılmıştır. Depreme dayanıklı yapıların tasarlanması için gerekli olan ana kriterlerden biri; süneklik dikkate alınmıştır. Yapıların, deprem kuvvetlerine karşı genel güvenlik için yeterli dayanıma ve sünekliğe sahip olacak şekilde tasarlanması gerekmektedir. Sismik güvenliği artırmak adına, dayanım ve süneklik bir araya getirilmiştir. Ayrıca perde duvarların konumu ve perde duvar kalınlıklarının süneklik üzerindeki etkilerinin altı çizilmiştir.

Doğrusal olmayan statik analiz (itme) yöntemi, iki boyutlu (2D) betonarme (RC) perde duvar modellerini analiz etmek ve tasarlamak için seçilmiştir. Ek olarak, kat sayıları, açıklık uzunlukları ve basınç dayanımı (f'_C), gibi diğer birkaç değişkenin etkileri de karşılaştırılmıştır. Betonarme yapıların modellerini tasarlamak ve değerlendirmek için ticari yazılım programı ETABS kullanılmıştır.

Perde duvar kalınlığındaki bir artışın süneklik değerlerinde düşüşe neden olduğu ve perde duvar konumu kenardan ortaya değiştiğinde süneklik değerinde de düşüş olacağı sonucuna varılmıştır.

Anahtar Kelimeler: Süneklik, Betonarme yapılar, Doğrusal olmayan static analiz, Depres tasarımı, İtme eğrileri, Perde duvar, ETABS programı

TABLE OF CONTENTS

APPENDICES

LIST OF TABLES

LIST OF FIGURES

LIST OF ABBREVIATIONS

ACI:	American Concrete Institute
ASCE:	American Society for Civil Engineering
FEMA:	Federal Emergency Management Agency
MRFSW:	Moment Resisting Frame with Shear wall
RC:	Reinforced Concrete
2D:	Two-dimensional
SDC:	Seismic Design Category

CHAPTER 1
INTRODUCTION

1.1 General

Through recent earthquakes, several reinforced concrete structures have either failed or sustained separate degrees of destruction. Overall, knowing the seismic efficiency of structures has been a question for the science communities for rather a long period (Chou et al., 2016).

One of the most dangerous natural hazards causing a large percentage of losses of life and properties is earthquakes. In regards to safety and health, earthquakes will have disastrous consequences. Overall, knowing the seismic efficiency of buildings has been a problem for the scientific community for quite a long time (Yön et al., 2017).

through the past years, scientific understanding had achieved huge progress, but certain seismic engineering worries are still hard to evaluate simply and clearly. In a huge seismic, earthquake-resistant structural formations designed dependent upon standardized earthquake specifications improve the safety of live security (Furtado et al., 2018).

To evaluate the seismic behavior of a previous model and to adjust the function structural properties such as power, stiffness, and deflection to best reach the required quality requirements, it is important to build analytical modeling or physiological models (Ravikumara et al., 2015).

The destruction relies not just upon the earthquake's amount, but even on the form of a structural system. One of the most important types is the dual system (MRFSW), This dual system includes reinforced concrete frames reacting with RC shear walls. Dual structural frameworks, like structural reinforced concrete (RC) with shear walls, were generally utilized throughout operation as structural resistance frameworks to attraction and lateral forces (Zerbin et al., 2020).

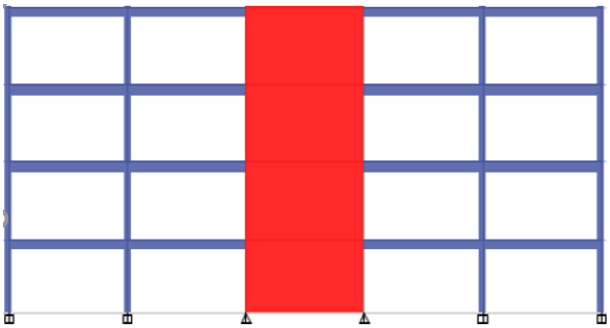

Figure 1.1: Dual system

The forms of structural system will be designed that deal against longitudinal forces of gravity and also horizontal loads affected via wind or earthquake action. The structural system contains mainly of members designed which hold loads, as well as the remaining members not included in the load holding process being related to as non-structural members. gravity forces (dead load, live load) and horizontal loads (wind loads, seismic loads) are the main loads of structures that are exposed to them (Rana ana Rana, 2014).

Shear wall devices are among the most widely applied systems in buildings to withstand lateral loads. The implementation of a shear wall is a functionally effective solution for stiffening a structure, as the major purpose of a shear wall is to raise lateral load tolerance stiffness (Madhu, 2018).

Shear walls were widely utilized as a longitudinal structural component across modern buildings to withstand the lateral loads that can be caused by the impact of winds and seismic. Reinforced concrete shear walls if built to become ductile, it already conducts significantly better. To increase the ductility of walls, the general geometric measurements of the wall, the form and quantity of reinforcement, and the relation against the other components through the building support (LovaRaju and Balaji, 2015). If shear walls were placed in good locations inside the building, via minimizing lateral deformations during seismic forces, they may create an effective lateral pressure resistance structure. Furthermore, this is also very important to establish an efficacious, impressive, and optimal shear wall position (Rokanuzzaman et al., 2017).

In earthquake-resistance design, the capacity of a device or structural component that undergo high-intensity cyclic displacements, under a provided ground motion, beyond extreme strength degradation is generally indicated more by the required ductility ratios, μ. Ductility proportion is identified by the ratio of maximal displacement (Δ_m) to the related displacement at the beginning of yield (Δ_y) (Mehta and Vasani, 2014).

With regards to strains, intervals, or deformations, this could be described. As ductile elements are being utilized to shape a structure, before collapse, the structure may undergo huge deformations. This is useful to the consumers of the structures, since if the structure is to fail during time of overloading, this will undergo big deformations till collapse and thus present the inhabitants with a notice (Vielma and Mulder, 2018).

Pushover analysis is a static nonlinear technique that progressively raises the amount of the horizontal loads, preserving a predetermined sequence of transmission throughout the height of the structure. Pushover analysis, considering the maximum load and the peak inelastic deformation, will define a building's performance. nonlinear influences were modified and once a collapsing mechanism is formed, that structure is stressed. To produce the pushover curve, a base shear and the roof displacement could be mapped for each stage. The primary benefit of pushover analysis is to obtain an over-strength estimation and then provide a sense of the general ability of the system to sustain inelastic deflection (Khoshnoudian et al., 2011).

Nonlinear pushover analysis offers sufficient knowledge regarding the building's durability and deformation capability and the discovery of the yield displaced as well as the ultimate displacement, and that is to discover the structure's ductility by dividing the max displacement by the displaced yield (Wang et al., 2020). The main goal of the pushover analysis is to assess the anticipated quality of structural systems by approximating the strength and deflection needs of the structural system through design seismic events by implies of a static inelastic analysis and by comparison those other requirements with the capacity obtainable at performance investment stages (Kadid and Bomrkik, 2008).

The Capability Curves or Pushover Curves illustrate the structure's nonlinear nature and is a base shear load-deformation curves toward the construction's lateral roof deformation. Structural capability is expressed via the pushover curve. By monitoring the base shear and the roof displacement, the most useful method to map the load-deformation curves was to track the base shear (Ghasemi Jouneghani et al., 2016)

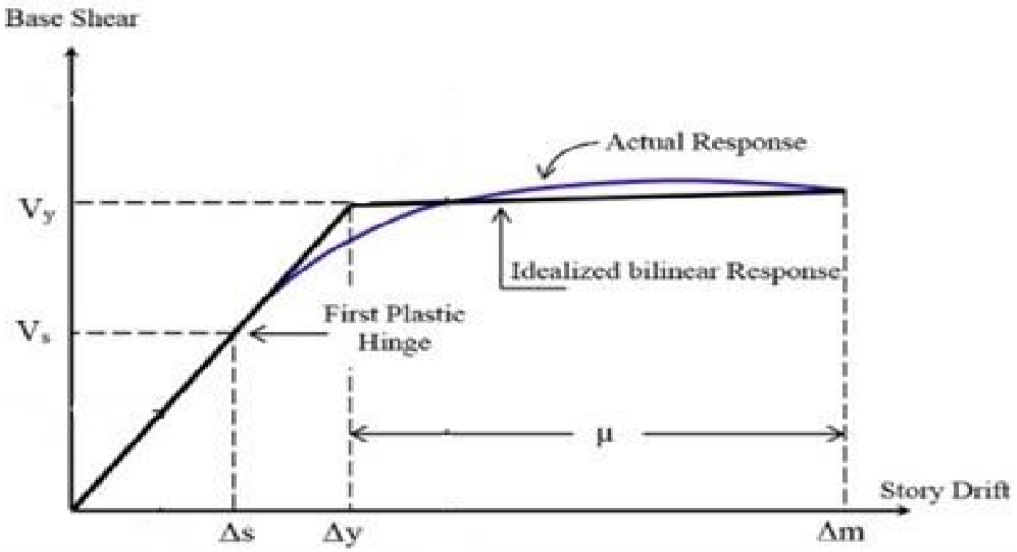

Figure 1.2: The pushover curve with bilinear

The equation for finding ductility ratio:

$$\mu = \frac{\Delta m}{\Delta y} \qquad (1.1)$$

1.2 Problem Statement

The impact of thickness and position of shear walls on ductility with the variation according to size and different parameters of buildings isn't very obvious so the ductility of the building structures will be determined by the different thicknesses and positions of shear wall and its influence will be explained.

1.3 Objective and Scope

This thesis aims to assess the ductility of RC structural buildings by using various types of parameters with a shear wall having different thicknesses and different positions. The research study aims to seismic assessment and discovering of ductility of the 2D models of dual system (MRFSW) through using the static non-linear methods and understanding the degree of impact of different categories: different span length different compressive strengths ($f'c$) of concrete different number of floors (low-rise, mid-rise, and high-rise building), and various thicknesses of the shear wall, and different positions of the shear wall, by using the software program (ETABS).

1.4 Hypothesis

- To carry out the earthquake analysis of (MRFSW) dual system with different thicknesses and positions of shear wall for low-rise buildings (4-story), mid-rise building (8-story), and high-rise building (12). withdrawing the pushover by using the software (ETABS).
- Finding the pushover curve for all buildings.
- Compression of achieved outcomes of various thicknesses and positions in shear walls.
- Compression of achieved outcomes of various parameters.
- Select the greatest suitable seismic lateral force resistance shear walls that may choose the best ductility.

1.5 Significance of the Study

The approach will be utilized to determine the building's displacement on different floors that are exposed to lateral loads. Ductility is one of the main significant factor in earthquake-resistant structural buildings and influences the performance of the building through the earthquake, therefore this research offers an assessment of the ductility of reinforced concrete

structures with shear walls having various thicknesses and positions and impacts the behavior of the building during the earthquake.

1.6 Organization of the Thesis

This thesis study is divided into 5 chapters: the first chapter provides a brief introduction about the study and aim of the study and also the significance of the study; chapter 2 presents previous studies about this study named literature review; chapter 3 contains the study's methodology; chapter 4 provides outcomes and discussion of the models of study; the last chapter that's chapter 5 includes conclusions and recommendations of the thesis study.

CHAPTER 2
LITERATURE REVIEW

2.1 General

This chapter defined prior authors and studies on seismic-resistant designs, reinforced concrete frame structure, Reinforced concrete shear wall, Effect of different locations of shear wall, Effects of different thicknesses of shear wall, non-linear static pushover analysis, and ductility of reinforced concrete structures.

2.2 Earthquake-resisting Buildings

The designs of earthquake-resistant were primarily given for the orbital impact correlated with the abnormalities resulting from the earthquake's moving structure. And for most of the overall destruction occurring, this orbital influence provides a cause. Only in a rare case, however, there is limited inertial influence resulted in important damage (Omer and Amine, 2013)

Jamnani et al. (2018) these researchers evaluated the diffusion of energy in reinforced concrete shear wall-structural frames exposed to multiple earthquakes, taking into focus the impact of multiple earthquakes through evaluating the performance of the structures. The nonlinear action and power distribution of the RC shear wall-structural frames exposed to several global earthquakes were examined by this research. Rather accurate outcomes may be predicted by analyzing the impact of repetitive earthquakes against structures compared to the study of the main shock alone. Normally, as the structures were exposed to frequent earthquakes, the faded inelastic power rises. Its inherent rate reduces due to structural failure while the structure achieves the nonlinear level. Besides that, the rate difference rises, as well as the repetition probability reduces. The growth in drifting demand will be The effect of the cumulative structural destruction caused by repetition earthquakes.

The plastic joints are the primary cause of power absorption to produce a ductile reaction across the load period of the earthquake, which is utilized in current design training. Cautious

information must also be presented to predict potential positions for all the plastic hinges. Structures must withstand mild to severe earthquakes beyond loss or, at the most, without extreme loss or failure, all in compliance with the requirements of seismic architecture in the current structural buildings code (Mantawy, 2015)

Tafheem and Khusru (2013) concentrated on studying how well the structural reliability of a building utilizing a 6-floor building system is influenced by dead load, live load and wind loading, and horizontal seismic. Depending on how the structural buildings reacted since readied with HSS parts, V-type and cross X bracings regarding bent moment, axial and drifted pressure, and floor displacement, the reliability for the building has been assessed. This was observed how X-braced structures have been comparatively stiffer and also had a greater ability to displace further lateral forces.

Venkatesh and Bay (2011) their study's points are concentrated on the concept that earthquakes tend to collapse every structural building, mainly one which is not designed to handle horizontal forces. The significance of providing load resistant solutions like steel braces, extrusion frames, and shear walls was therefore emphasized. To evaluate the beam power, supporting reaction, and joints displaced rates of the 3 structures with inner and outer steel braces and a moment resisting reinforced concrete structures, the models were subjected to linear dynamic analysis. The results showed which steel bracings provide a large capacity to enhance the capacity of a structure to withstand horizontal forces. It has also been recognized that internally and externally braces are being used to boost the ultimate overall load resistance capacity. Nevertheless, the usage of internally and externally braces needs that the systems, whether retrofitted or modified, have been adequately paired.

Chandiwala (2012) it has been noted that the desire for safe buildings that will resist an earthquake is rising. Was believed to have resulted in an increase in price for systems of moment carrying. He emphasized, however, the significance of cost savings and the necessity should achieve optimal solutions with the usage of steel and also the correct size of suitable concrete walls. This was observed that throughout earthquake actions, the external sections of

a flange usually move a bit and that providing an "L" section wall with just an F-shear wall would help improve a structure's reliability.

Wang et al. (2020) study provides a mechanism to examine the structural quality of buildings exposed to the collective effect of winds and seismic. The research utilizes a pushover analysis to measure the intensity of low-rise and mid-rise concrete buildings and equate their strength with their strength. Double reinforced concrete buildings of Five and Eight floors had been analyzed using the 3-dimension finite element process, taking into consideration fix-base and flexible requirements. For all fix-base and flexible building structures, the present earthquake design code suggests the same strength reducing factors. This principle explicitly suggests that in either elastic and inelastic structural building reliability, the lowering of design base shear was equivalent. The conclusions findings, nevertheless, indicate that SSI's effect on inelastic efficiency wasn't as obvious as it would be for elastic efficiency.

The earthquake that destroyed most of northern Algeria had created concerns towards the sufficiency of framed structures to withstand great shakes, as several building structures have sustained huge loss or fallen. A nonlinear static pushover analysis was performed to assess the efficiency of framed structural buildings during predicted future seismic. 3 frame buildings of 6, 9, and Twelve floors collectively had been examined to reach this target. The outcomes of the research indicate that underneath earthquake loading, adequately designed frames can operate well (Kadid et al., 2008)

2.3 Reinforced Concrete Frame Structure

Bertagnoli et al. (2016) in this work a computational study of reinforced concrete frame is presented. The structure studied is a beam-column assembly that presents a portion of the structural framing system of a ten-story reinforced concrete frame building and is subjected to distributed loads and to monotonically increasing vertical displacement of the Centre column to simulate a column removal scenario. A computerized analysis of reinforced concrete frames is discussed in this article. The structure described was a beam-column ensemble that provides a percentage of structural building frame of 10-floor RC structural

frame buildings and is also exposed to spread forces and geometrically growing longitudinal displacement of the center column to replicate a situation of column elimination.

Ghaffarzadeh et al. (2013) an earthquake demand assessment of RC moment framings with intermediate ductility was proposed by these authors. Compared to the findings of time background evaluation on several frames, the precision of using simplified nonlinear static analysis was measured. To determine earthquake demands, displaced patterns, drifting demand and peak plastic rotating had been determined. In this research, via comparing the results generated by pushover loaded behaviors, the nonlinear static conduct of RC structural frames with intermediate ductility had also been evaluated. As a result, eight recordings of seismic acceleration, chosen and sized for compliance within a design range, were used. Through nonlinear static analysis, utilizing the fixed pressure template leads to a large oversimplification of inter-floor drifts throughout the smaller stories. In higher frames, it's mostly noticeable since greater lateral force was added throughout the below floors across such a uniformly distributed. Utilizing the standardized load pattern, internal story drifting demands throughout the top floor had been overlooked. When the heights of a structure rises, the tolerance of the demand forecasts to separate load patterns produced for nonlinear static analysis becomes important. Ignoring the influence of the upper mode throughout the assessment step will lead to an important undervaluation of the structure's earthquake demands.

2.4 Reinforced Concrete Shear Wall

Ozkul et al. (2019) the impact of shear wall upon the seismic efficiency of RC frame building structures is presented by these authors. In this research 2 RC building structures with sheer walls that had been destroyed by the Van earthquake in 2011 were identified and the current losses were determined using Van 2011 seismic accelerator data using nonlinear period background evaluation. Besides, material properties are raised and shear walls were constructed for two buildings corresponding to the specifications of the Turkish Earthquake Code 2007. For the upgraded buildings, nonlinear time history was performed and loss

distribution was calculated. Therefore, destruction distributions of current and improved buildings had been compared and an estimate was made for the dispersion of losses including if just suitable concrete and reinforced materials and shear wall besides beams and columns have been utilized throughout the design of the structural buildings. Due to research findings, usage of appropriate material of structural buildings and shear walls may escape hard destruction perhaps seismic reactions of column and beam components were weak.

Mid-rise reinforced concrete frame residential buildings in metropolitan parts of India including stories ranging around eight to ten or twelve will become common. To lateral force tolerance, mid-rise reinforced concrete frames having shear walls were supplied. The shear walls were also supplied with having openings, so the influence of that on the story drift, floor stiff, moment, and shear as well as upon the pressure inside the shear walls must be studied. For the design of the shear wall throughout the building structure, a 3-D analysis was taken out. The impact of the scale and positions of all these openings are protected by this research (Varma and Kumar, 2020)

Fahjan et al. (2010) the adequate model of shear walls has been described to be very necessary for analyses of linear and non-linear structural buildings. Shear walls of reinforced concrete are designed using various strategies through linear structure analysis, whether utilizing shell components or a mixture of frame components. The nonlinear substance design of the shakier frame was usually dependent upon the idea of the plastic hinge positioned on the plastic regions at the ends of the structural components or spread across the length of the component span throughout the nonlinear analysis. Utilizing a multi-layer shield component with a layer substance design, the nonlinear action of the shell components was typically designed. Throughout this method, the concrete and reinforcement being designed through various layers inside of the structural components, In this research, various methods to linear and non-linear shear wall models were discussed and implemented to RC shear wall building works through structural experiments of buildings. In consideration of the total performance of the systemic structures, the analyses resulting from various methods had been compared.

Kaplan et al. (2011) in this research, through inverted cyclic charging, a new strengthening solution for RC building structures, including external shear walls, was already experimentally tested. It can strengthen building structures utilizing the suggested methodology without disrupting their consumers or subletting the building under restoration. Shear walls are built with the external faces of the building throughout this methodology. The use of external shear walls was already noticed to substantially boost the capability and motion rigidity of RC structures. To replicate earthquake loadings, structures of a 2-floor structural frames template had been evaluated under the applied reverse cyclic horizontal sway. As anticipated, this was noted that the deployment of shear walls to a structural framework had already boosted the ability of the base frame.

2.5 Effect of Different Positions of Shear Wall

Anshuman et al. (2011) those authors defined the option dependent on its elastomeric and elastoplastic habits for shear wall position throughout multi-story buildings. The seismic load was measured and added to a 50-floors building situated in region V. Elastoplastic and elastic tests were conducted onto the computer programs utilized by both STAAD Pro and SAP 2000. In both ways, shear force, story drift, and bent moment had been measured, and depending on the following simulations, the position of a shear wall has been calculated. To conduct this research, the concept of the buildings that having shear walls and the buildings that haven't shear walls were discussed. The allowable deflection was reached by the peak deflection (while the direction of the earthquake forces will into the smaller dimension).

Rokanuzzaman et al. (2017) these authors focus on the influence of the shear wall positions upon the building structural frames when exposed to lateral forces. A residence building with such a common story height of ten (ft.) was viewed for the (16-floor) structure. Throughout this article, for crucial variables such as displaced and base shear during lateral forces 8, 12, and 16-floor buildings had been designed utilizing software programs and 3 different designs have been evaluated with various shear wall positions in the building structural frames. The investigation was conducted utilizing the ETABS program and similar static methods have

been utilized for analysis. Three forms of models were evaluated (one of them has no shear wall, one of them having a shear wall located in the center of four peripheral faces, one having an L-shaped shear wall located at four corners). In this research, it was discovered that the Second model (those with a shear wall positioned in the center of 4 peripheral sides) gives the perfect efficiency in terms of maximum displacement and base shear.

This observed assessment aims to investigate the efficient position of the shear wall for a multi-story structural building. The study begins with a non-linear structural frame analysis for different shear wall places throughout a framed building structure. A bare framed structure framework is termed model one as well as the other 3 types are dual structural systems. A seismic load was added to a building structure of eight-floor has been placed in region II, Region IV, and region V according to code requirement IS189002. The studies were conducted out by utilizing programs from ETABS. For different models, a pushover curve was being built and compared. This had been discovered that in the situation of base shear and displacement building structures having a shear wall for an acceptable place is much more necessary (LovaRaju and Blaji, 2015)

Tarigan et al. (2018) those authors defined the impact of the position of shear wall in seismic resistance. The usage of the shear wall will efficiently decrease the structure's displacement and story drifting. It would decrease the damage caused by lateral forces like a seismic. Previous research reported that, depending upon the place in structures, the shear wall provides distinct efficiency. Throughout this article, for various models of structures, earthquake evaluation was implemented utilizing the response spectrum process; the opened frame, the shear walls in the circumference perfectly proportionally, the shear walls at the circumference proportionally, and the shear wall at the circumference unevenly. The outcomes are obtained by comparison of the displacement and the story drift. Dependent on the study the positioning of the central shear wall of the structures evenly provides the finest performance that decreases the displacement and story-drift.

2.6 Effects of Different Thicknesses of Shear Wall

Shinde and Raut (2016) the authors studied the varying shear wall thicknesses throughout similar buildings at different peaks, preserving the places around similar positions and their impact on the deformation of multi-storied buildings. In this research analysis, G+24 floor building in the region has been defined with certain examination that are designed via having to change the shear wall thickness at periods of each five floors throughout the exact building to determine variables such as shear story, story drift, and deflection utilizing SAP and ETABS. Throughout this study, the shear walls places that are established for longitudinal rise at the building's corner and also in the middle part of the building were unchanged. Giving shear walls in corners greatly decreases the displacement related during the seismic, as well as the proportion of horizontal drift and displacement. It’s discovered according to the following findings that the thickness already raises the rigidity. And when we raise the height and thickness, the deformation of a shear walls decreases.

Sengupta (2014) the author explores the impact on multi-story buildings including its various thickness and associated reinforcement ratios needed for shear walls. Shear wall structural building templates were designed by ETABS. The position of the shear walls has been preserved the similar and a comparison evaluation for separate shear wall thicknesses for various building floors 5-floors, 10 floors, and 15 floors is conducted. The correlating reinforcement amounts needed in any of the cases were defined. It's also identified that reinforcement proportion rises with an increment in seismicity and floor numbers for a steady shear wall thickness. This was also noted that when the shear wall thickness grows for the same degree of thickness and therefore reduces for a specific range of thickness, the reinforcement proportion rises for all areas. The findings therefore demonstrate that for seismic-resistant design, increasing shear wall thickness may not usually be efficient.

2.7 Non-linear Static Pushover Analysis

Wang et al. (2020) this authors provides a framework for investigating the structural efficiency of buildings exposed to the collective behavior of wind and seismic. The research

utilizes a pushover examination to assess the stability of low-rise and mid-rise structural concrete to make a comparison of their strength, which is derived from the Chinese earthquake code requirements. The suggested technique indicates that by raising ductility criteria, evaluation of seismic and wind concurrent impacts may change performance ranges utilized during design. This demonstrates that under existing design guidelines, structures placed throughout regions seismic prone have been allowable to unpredictable destruction rates.

Huang and Kuang (2010) the suitability of pushover analysis has been discussed for seismic evaluation of med-rise-to-high-rise shear wall building structures and showed that pushover analysis understates the inner story drifts and rollouts, especially those which are upon the top floors of structure buildings, and overstates inelastic maximum roof movement.

Babu et al. (2012) non-linear study of different symmetric and oblique building structures built on flat and sliding down ground exposed to different types of forces has been clarified. Throughout the current analysis, separate structures built on planes ground and inclination earth with a slope of 30o are identified. Through plan symmetric and even oblique, different structural buildings are taken into consideration with variations in bay dimensions in shared directions. Utilizing SAP and ETABS programs, the study was conducted. For separate instances, pushover curves are being built and contrasted. It was found that structures with longitudinal irregularities are much rather important than structures with irregularities in the plan.

Shah et al. (2011) the nonlinear static analysis described is an incremental process, and therefore that is hard to accomplish with hand measurement which is how nonlinear static analysis needs software. ETABS program has been features that permit nonlinear static analysis to be conducted out. It is a method of doing nonlinear static analysis in simplified and efficient ways.

Khoshnoudian et al. (2011) described the suggested lateral force model for pushover analysis in certain types for symmetric structural concrete buildings for low-rise, mid-rise, and high-

rise buildings. In contrast to traditional loading patterns, like triangle and uniform loading patterns, these types provide further practical outcomes. The supposed concrete structure buildings of 4, 12, 20, and 30-floors were specific moment frames that had been planned accordingly using the standardized 2800. The pushover analysis was then conducted utilizing traditional load conditions and proposed load patterns, and the outcomes were contrasted to the findings of the nonlinear time background analysis. In contrast to load patterns suggested via guidelines like FEMA456, the findings indicate the precision of the provided load pattern.

Rahman et al. (2012) introduces the 3D static nonlinear study of a current 8-floor reinforced concrete framed shear wall structural building through Madinah for earthquake efficiency assessment. At various floor rates, the building also has a roof, framed RC, elevated shafts, and plain slab structures. A 3D pushover analysis being used to achieve the earthquake displacement reaction of the RC framed structural building having a shear wall. Utilizing SAP2000 integrating inelastic substance actions for concrete and steel, the 3D static pushover study has been conducted out. Utilizing the mid-pier technique, the shear wall has been modeled. The phases of destruction involve a series of yielding and collapse of components and structural rates have been achieved for the desired displacement required underneath the seismic design and evaluation of refitting techniques to increases the strength of the structure.

Abhilash and Biju (2010) the pushover analysis discussed is indeed a fixed nonlinear approach from which the amplitude of the structural loads per some predetermined formula has been progressively enhanced. Poor connections and failure modes of the structure were discovered with the rise in the size of a load capacity. Static nonlinear pushover evaluation is an effort to determine the actual stability of the structure within the structural engineer's community and that guarantees to become a helpful and efficient method for efficiency-based design. The structure efficiency factor relies on the lateral load template added through the structure. Popularly implemented force patterns are Reversed triangles and equally distributed.

Sattar and Liel (2016) to evaluate the efficacy of brickwork infill walls towards minimizing the probability of falling nonlinear structural building models once exposed to earthquake impacts, efforts were created. Regardless of the walls collapsing, the efficiency of the bare frame has been found to being smaller than those of the infilled frames throughout connection to both the quantity of power displacement, rigidity and preliminary strength Results from the dynamic evaluation demonstrated that throughout a structure equipped with naked frames, the influence of aseismic was strong. That's why they're weak in strength and also have a weaker capability that dissipates power.

Dhileep et al. (2011) the author's emphasis was focused upon large modal rate nonlinear earthquake facets as well as their potential for response. While their ideas indicate which could be correlated with a range of inaccuracy regarding the response of greater mode, the usage of pushover analysis has been recognized to provide the greatest outcomes. In the consequence, a limited amount of smaller ordered modes has been expected to have been utilized to determine the total receptive capability to achieve a high degree of performance. However, it has been still best to account for the influence of nonlinear impacts and frequency types. It has been documented that throughout irregular or rigid structures, large frequency patterns were a popular aspect.

2.8 Ductility of Reinforced Concrete Structures

Rao et al. (2008) in their article those authors focused on ductility and assessment of minimal flexural reinforcements in reinforced concrete beams. Researches upon this layout of RC components have shown that beams including various flexural reinforcement size and proportions display various flexural behavior. Ductility of the modifications of the RC component within a scale of a member and also concrete capacity. The collapse of reinforced concrete beams does not demonstrate any size dependency on the traditional strength or yielding requirement, nor will the magnitude of the beam get any impact upon the ductility. The findings indicate that strength of flexural crack dependent upon the magnitude of the beam. The impact of beam magnitude and flexural reinforcement ratio on the standardized overall strength of RC beams was important. Although when the depth of the beam rises, it

reduces. While the ratio of flexural reinforcement rises, the reinforced concrete beam ductility enhances.

Shedid et al. (2008) researched upon ductility of RC masonry having shear wall underneath earthquake loads. The probability of obtaining a higher degree of ductility in completely braced RC masonry having shear walls via flexural yields has been assessed. To examine the impact of the quantity and sharing of longitudinal reinforcing and the degree of axial compressive pressure upon this inelastic action and ductility of RC masonry shear walls, 6 huge walls have been examined for collapse against inverted cyclic lateral forces. The study findings showed that at the beginning of the longitudinal reinforcement yields, the upper wall displaced is largely based upon the quantity of reinforcement and weakly influenced by the axial compressive degree.

Teixeira and Bernardo (2018) the ductility of (RC) rectangle crossed part beams has been examined. For that, it collected and evaluated the laboratory findings of many reinforced concrete beams available throughout the paper. To quantify the torsional ductility for the examined beams, a torsional ductility chart has been employed. The research suggested the preceding parameters: compressive strength of concrete, torsional reinforcing percentage, and form of cross-sectional (dull or empty). The impact of each parameter analysis upon torsional ductility has been evaluated and significant results are highlighted that would assist throughout the torque design of reinforced concrete beams. The extra comparison analysis was also conducted using the guidelines through certain codes of training that are being used. It has been observed that, in total, through terms of maximal torsional reinforcement, the codes have become too limiting. As a result, this may relate to many beams with ductile actions being unsupported.

Vielma and Mulder (2018) some of the major ductility processes are updated and contrasted throughout this article, and then changes are made to certain processes to evaluate the displaced ductility. A modern mechanism has been therefore applied, which uses the earthquake failure threshold and the yielding displacement to calculate the peak displacement,

obtaining the equilibrium of vanished energy. The technique was utilized to measure the ductility of RC structural buildings for displacement. the finding ratios of displaced ductility determined per the suggested method are almost constant in the normal direction of the cases researched and also had values that differ slightly throughout the irregular path of the study. Those values are higher than the ductility ratio that the builder expects the structures will grow during a serious seismic and are compatible with the response reducing factor values calculated through previous studies with the most detailed and therefore time-consuming study.

Carrillo et al. (2014) those authors researched displaced ductility for earthquake design of reinforced concrete walls for low-rise building houses the study contrasts and explains the ductility value of RC walls generally utilized in one-floor and two-floor building houses. By evaluating the response calculated onto 38 walls examined against moving table vibrations and static lateral forces, ductility has been studied. The size proportion and walls that have openings, concrete forms, steel percentage, and web reinforcement method have been the parameters examined. It proposes a formula to calculate the usable ductility of a wall. Ductility capabilities suggested throughout this research will be utilized to logically estimate the variables of power modification and displacement amplification.

The reinforced concrete is widely used, and shear walls are used in most of them for carrying the seismic loads. Shear walls have an enormous impact on the building and huge effects on the way of designing the buildings. According to recent studies, the effect of the different parameters on the performance of shear walls is studied, and the ductility of the structures during seismic loads is checked. Some recent studies use pushover analysis to analyze the impacts of lateral loads on the structures' ductility.

Different codes have been used in the previous studies. Moreover, various number of stories are conducted. 3D models are considered in the most of the previous works. In the present work 2D dual system, moment resisting frame with shear wall (MRFSW) systems are selected. The 4-stories, 8- stories, and 12- stories models have been used throughout this study.

The mentioned parameters have a remarkable effects on the ductility of the structures during earthquakes, and considering the combined effect of these parameters on the concrete structures causes designing high-performance buildings. During this study, different parameters are gathered, and their simultaneous impacts were considered with each other. In other words, different span lengths, different number of stories, and different compressive strengths of concrete were considered as well, and the results show the simultaneous impacts of them on the structure.

The thickness and position of shear walls have the most critical impact on ductility and the behavior of shear walls. Therefore, the concentration of the study is on the effects of these two parameters together. Besides, the effects of other mentioned parameters were controlled as well.

CHAPTER 3
METHODOLOGY

3.1 Introduction

The static and dynamic analysis of structures has been the primary concern of structural engineers. The key parameters of the seismic study of structures are loads carrying ability, ductility, stability. Throughout this chapter, the RC dual system (MRFSW) will be studied, and an analysis to evaluate the yield displacement, maximum displacement, and ductility ratio of different models has been carried out. 96 2D models were designed to recognize ductility with different thickness and positions of shear wall, different stories, span length, and compressive strengths. In this analysis, ACI 318-08, ASCE 7-10 codes were used. Any structure must be built by how to withstand lateral forces include seismic. The ETABS program is being utilized during this study to designing and analyzing the models.

3.2 Building Arrangement

In this thesis, one type of structural system is used: dual system (MRFSW) for low-rise (4), mid-rise (8), and high-rise (12) buildings. Having 5(N) spans with various span lengths 5m, 5.5m, 6m, and 7m for typical story height 3.2m and ground floor height 4m.

In this study, the normal concrete with two different compressive stress is used, which are 250 and 300 kgf/cm^2 respectively. The maximum span length while the normal concrete is used is around 7 meters, and for longer span lengths, usually pre-stressed concrete is used. Therefore, in this study, the maximum length for the span is assumed as 7 meters.

Depending on some studies, it is observed each country has its own method of calculating the number of stories for the designation of a specific building form. There have been no universally agreed descriptions for low-rise, mid-rise, and high-rise building structures, and these descriptions are changed from one place to another. In this study, 4-story, 8-story, and 12-story buildings were selected. The lowest one is 4-story and considered a low-rise building, and the highest one is 12-story and considered a high-rise building structure.

3.2.1 Material properties

The materials and the properties of this thesis are shown in below Table 3.1.

Table 3.1: Material properties of models

Material	**Value**
Fy of reinforcement steel	420 N/mm^2
Compressive strength ($f'c$)	250, 300 kgf/cm^2
Modulus of elasticity of steel	200,000 N/mm^2
Modulus of elasticity of concrete	23500 and 25743 N/mm^2
Unit weight of concrete	24 kN/m^3
Shear modulus, G	99847.2, 109377 kgf/cm^2

3.2.2 Details of the models

The details of the models for low, mid, and high-rise buildings are shown in Table 3.2.

Table 3.2: Details of the buildings: low-rise, medium-rise, and high-rise buildings

Number of models			Story height (m)	Number of span	Span length (m)	$f'c$ kgf/cm^2	fy kgf/cm^2	Thickness of the shear wall (m)	Position of the shear wall
Low-rise building (4)	Mid-Rise building (8)	High-rise building (12)							
1	**33**	**65**	3.2	5	5	250	4200	0.250	Edge
2	**34**	**66**	3.2	5	5.5	250	4200	0.250	Edge
3	**35**	**67**	3.2	5	6	250	4200	0.250	Edge
4	**36**	**68**	3.2	5	7	250	4200	0.250	Edge
5	**37**	**69**	3.2	5	5	250	4200	0.250	Middle
6	**38**	**70**	3.2	5	5.5	250	4200	0.250	Middle
7	**39**	**71**	3.2	5	6	250	4200	0.250	Middle
8	**40**	**72**	3.2	5	7	250	4200	0.250	Middle
9	**41**	**73**	3.2	5	5	250	4200	0.300	Edge
10	**42**	**74**	3.2	5	5.5	250	4200	0.300	Edge
11	**43**	**75**	3.2	5	6	250	4200	0.300	Edge
12	**44**	**76**	3.2	5	7	250	4200	0.300	Edge
13	**45**	**77**	3.2	5	5	250	4200	0.300	Middle
14	**46**	**78**	3.2	5	5.5	250	4200	0.300	Middle
15	**47**	**79**	3.2	5	6	250	4200	0.300	Middle
16	**48**	**80**	3.2	5	7	250	4200	0.300	Middle
17	**49**	**81**	3.2	5	5	300	4200	0.250	Edge
18	**50**	**82**	3.2	5	5.5	300	4200	0.250	Edge
19	**51**	**83**	3.2	5	6	300	4200	0.250	Edge
20	**52**	**84**	3.2	5	7	300	4200	0.250	Edge
21	**53**	**85**	3.2	5	5	300	4200	0.250	Middle
22	**54**	**86**	3.2	5	5.5	300	4200	0.250	Middle
23	**55**	**87**	3.2	5	6	300	4200	0.250	Middle
24	**56**	**88**	3.2	5	7	300	4200	0.250	Middle
25	**57**	**89**	3.2	5	5	300	4200	0.300	Edge
26	**58**	**90**	3.2	5	5.5	300	4200	0.300	Edge
27	**59**	**91**	3.2	5	6	300	4200	0.300	Edge
28	**60**	**92**	3.2	5	7	300	4200	0.300	Edge
29	**61**	**93**	3.2	5	5	300	4200	0.300	Middle
30	**62**	**94**	3.2	5	5.5	300	4200	0.300	Middle
31	**63**	**95**	3.2	5	6	300	4200	0.300	Middle
32	**64**	**96**	3.2	5	7	300	4200	0.300	Middle

3.3 Reinforcement Details of the Models

The buildings have been built as per code ACI318-14, the beams and columns were configured

as per method to capability design. The reinforcement details of beam and columns for low-rise, mid-rise, and high-rise buildings are shown in those below Tables in this section.

Table 3.3: Reinforcement details of beams in low-rise buildings (4-story)

Number of models	Section size (mm)	Longitudinal Bars		Stirrups
		Top	Bottom	
1	350*400	6Ø16	4Ø16	Ø10@150mm
2	350*400	6Ø16	4Ø16	Ø10@150mm
3	350*400	6Ø16	4Ø16	Ø10@150mm
4	350*400	6Ø16	4Ø16	Ø10@150mm
5	350*400	6Ø16	4Ø16	Ø10@150mm
6	350*400	6Ø16	4Ø16	Ø10@150mm
7	350*400	6Ø16	4Ø16	Ø10@150mm
8	350*400	6Ø16	4Ø16	Ø10@150mm
9	350*400	6Ø16	4Ø16	Ø10@150mm
10	350*400	6Ø16	4Ø16	Ø10@150mm
11	350*400	6Ø16	4Ø16	Ø10@150mm
12	350*400	6Ø16	4Ø16	Ø10@150mm
13	350*400	6Ø16	4Ø16	Ø10@150mm
14	350*400	6Ø16	4Ø16	Ø10@150mm
15	350*400	6Ø16	4Ø16	Ø10@150mm
16	350*400	6Ø16	4Ø16	Ø10@150mm
17	350*400	5Ø18	5Ø16	Ø10@150mm
18	350*400	5Ø18	5Ø16	Ø10@150mm
19	350*400	5Ø18	5Ø16	Ø10@150mm
20	350*400	5Ø18	5Ø16	Ø10@150mm
21	350*400	5Ø18	5Ø16	Ø10@150mm
22	350*400	5Ø18	5Ø16	Ø10@150mm
23	350*400	5Ø18	5Ø16	Ø10@150mm
24	350*400	5Ø18	5Ø16	Ø10@150mm
25	350*400	5Ø18	5Ø16	Ø10@150mm
26	350*400	5Ø18	5Ø16	Ø10@150mm
27	350*400	5Ø18	5Ø16	Ø10@150mm
28	350*400	5Ø18	5Ø16	Ø10@150mm
29	350*400	5Ø18	5Ø16	Ø10@150mm
30	350*400	5Ø18	5Ø16	Ø10@150mm
31	350*400	5Ø18	5Ø16	Ø10@150mm
32	350*400	5Ø18	5Ø16	Ø10@150mm

Table 3.4: Reinforcement details of columns in low-rise buildings (4-story)

Number of models	Section size (mm)	Longitudinal bars	Stirrups
1	400*400	10Ø20	Ø10@125mm
2	400*400	10Ø20	Ø10@125mm
3	400*400	10Ø20	Ø10@125mm
4	400*400	10Ø20	Ø10@125mm
5	400*400	10Ø20	Ø10@125mm
6	400*400	10Ø20	Ø10@125mm
7	400*400	10Ø20	Ø10@125mm
8	400*400	10Ø20	Ø10@125mm
9	400*400	10Ø20	Ø10@125mm
10	400*400	10Ø20	Ø10@125mm
11	400*400	10Ø20	Ø10@125mm
12	400*400	10Ø20	Ø10@125mm
13	400*400	10Ø20	Ø10@125mm
14	400*400	10Ø20	Ø10@125mm
15	400*400	10Ø20	Ø10@125mm
16	400*400	10Ø20	Ø10@125mm
17	400*400	12Ø16	Ø10@150mm
18	400*400	12Ø16	Ø10@150mm
19	400*400	12Ø16	Ø10@150mm
20	400*400	12Ø16	Ø10@150mm
21	400*400	12Ø16	Ø10@150mm
22	400*400	12Ø16	Ø10@150mm
23	400*400	12Ø16	Ø10@150mm
24	400*400	12Ø16	Ø10@150mm
25	400*400	12Ø16	Ø10@150mm
26	400*400	12Ø16	Ø10@150mm
27	400*400	12Ø16	Ø10@150mm
28	400*400	12Ø16	Ø10@150mm
29	400*400	12Ø16	Ø10@150mm
30	400*400	12Ø16	Ø10@150mm
31	400*400	12Ø16	Ø10@150mm
32	400*400	12Ø16	Ø10@150mm

Table 3.5: Reinforcement details of beams in mid-rise buildings (8-story)

Number of models	Section size (mm)	Longitudinal Bars		Stirrups
		Top	Bottom	
1	350*450	5Ø20	4Ø20	Ø10@125mm
2	350*450	5Ø20	4Ø20	Ø10@125mm
3	350*450	5Ø20	4Ø20	Ø10@125mm
4	350*450	5Ø20	4Ø20	Ø10@125mm
5	350*450	5Ø20	4Ø20	Ø10@125mm
6	350*450	5Ø20	4Ø20	Ø10@125mm
7	350*450	5Ø20	4Ø20	Ø10@125mm
8	350*450	5Ø20	4Ø20	Ø10@125mm
9	350*450	5Ø20	4Ø20	Ø10@125mm
10	350*450	5Ø20	4Ø20	Ø10@125mm
11	350*450	5Ø20	4Ø20	Ø10@125mm
12	350*450	5Ø20	4Ø20	Ø10@125mm
13	350*450	5Ø20	4Ø20	Ø10@125mm
14	350*450	5Ø20	4Ø20	Ø10@125mm
15	350*450	5Ø20	4Ø20	Ø10@125mm
16	350*450	5Ø20	4Ø20	Ø10@125mm
17	350*450	5Ø20	5Ø16	Ø10@125mm
18	350*450	5Ø20	5Ø16	Ø10@125mm
19	350*450	5Ø20	5Ø16	Ø10@125mm
20	350*450	5Ø20	5Ø16	Ø10@125mm
21	350*450	5Ø20	5Ø16	Ø10@125mm
22	350*450	5Ø20	5Ø16	Ø10@125mm
23	350*450	5Ø20	5Ø16	Ø10@125mm
24	350*450	5Ø20	5Ø16	Ø10@125mm
25	350*450	5Ø18	4Ø18	Ø10@125mm
26	350*450	5Ø18	4Ø18	Ø10@125mm
27	350*450	5Ø18	4Ø18	Ø10@125mm
28	350*450	5Ø18	4Ø18	Ø10@125mm
29	350*450	5Ø18	4Ø18	Ø10@125mm
30	350*450	5Ø18	4Ø18	Ø10@125mm
31	350*450	5Ø18	4Ø18	Ø10@125mm
32	350*450	5Ø18	4Ø18	Ø10@125mm

Table 3.6: Reinforcement details of columns in mid-rise buildings (8-story)

Number of models	Section size (mm)	Longitudinal bars	Stirrups
1	400*650	12Ø20	Ø10@100mm
2	400*650	12Ø20	Ø10@100mm
3	400*650	12Ø20	Ø10@100mm
4	400*650	12Ø20	Ø10@100mm
5	400*650	12Ø20	Ø10@100mm
6	400*650	12Ø20	Ø10@100mm
7	400*650	12Ø20	Ø10@100mm
8	400*650	12Ø20	Ø10@100mm
9	400*650	12Ø20	Ø10@125mm
10	400*650	12Ø20	Ø10@125mm
11	400*650	12Ø20	Ø10@125mm
12	400*650	12Ø20	Ø10@125mm
13	400*650	12Ø20	Ø10@125mm
14	400*650	12Ø20	Ø10@125mm
15	400*650	12Ø20	Ø10@125mm
16	400*650	10Ø20	Ø10@125mm
17	400*650	10Ø20	Ø10@100mm
18	400*650	10Ø20	Ø10@100mm
19	400*650	10Ø20	Ø10@100mm
20	400*650	10Ø20	Ø10@100mm
21	400*650	10Ø20	Ø10@100mm
22	400*650	10Ø20	Ø10@100mm
23	400*650	10Ø20	Ø10@100mm
24	400*650	10Ø20	Ø10@100mm
25	400*650	10Ø20	Ø10@125mm
26	400*650	10Ø20	Ø10@125mm
27	400*650	10Ø20	Ø10@125mm
28	400*650	10Ø20	Ø10@125mm
29	400*650	10Ø20	Ø10@125mm
30	400*650	10Ø20	Ø10@125mm
31	400*650	10Ø20	Ø10@125mm
32	400*650	10Ø20	Ø10@125mm

Table 3.7: Reinforcement details of beams in high-rise buildings (12-story)

Number of models	Section size (mm)	Longitudinal Bars		Stirrups
		Top	Bottom	
1	400*500	6Ø20	4Ø20	Ø10@100mm
2	400*500	6Ø20	4Ø20	Ø10@100mm
3	400*500	6Ø20	4Ø20	Ø10@100mm
4	400*500	6Ø20	4Ø20	Ø10@100mm
5	400*500	6Ø20	4Ø20	Ø10@100mm
6	400*500	6Ø20	4Ø20	Ø10@100mm
7	400*500	6Ø20	4Ø20	Ø10@100mm
8	400*500	6Ø20	4Ø20	Ø10@100mm
9	400*500	6Ø20	4Ø20	Ø10@100mm
10	400*500	6Ø20	4Ø20	Ø10@100mm
11	400*500	6Ø20	4Ø20	Ø10@100mm
12	400*500	6Ø20	4Ø20	Ø10@100mm
13	400*500	6Ø20	4Ø20	Ø10@100mm
14	400*500	6Ø20	4Ø20	Ø10@100mm
15	400*500	6Ø20	4Ø20	Ø10@100mm
16	400*500	6Ø20	4Ø20	Ø10@100mm
17	400*500	6Ø18	4Ø18	Ø10@150mm
18	400*500	6Ø18	4Ø18	Ø10@150mm
19	400*500	6Ø18	4Ø18	Ø10@150mm
20	400*500	6Ø18	4Ø18	Ø10@150mm
21	400*500	6Ø18	4Ø18	Ø10@150mm
22	400*500	6Ø18	4Ø18	Ø10@150mm
23	400*500	6Ø18	4Ø18	Ø10@150mm
24	400*500	6Ø18	4Ø18	Ø10@150mm
25	400*500	6Ø18	4Ø18	Ø10@150mm
26	400*500	6Ø18	4Ø18	Ø10@150mm
27	400*500	6Ø18	4Ø18	Ø10@150mm
28	400*500	6Ø18	4Ø18	Ø10@150mm
29	400*500	6Ø18	4Ø18	Ø10@150mm
30	400*500	6Ø18	4Ø18	Ø10@150mm
31	400*500	6Ø18	4Ø18	Ø10@150mm
32	400*500	6Ø18	4Ø18	Ø10@150mm

Table 3.8: Reinforcement details of columns in high-rise buildings (12-story)

Number of models	Section size (mm)	Longitudinal bars	Stirrups
1	400*800	12Ø25	Ø10@100mm
2	400*800	12Ø25	Ø10@100mm
3	400*800	12Ø25	Ø10@100mm
4	400*800	12Ø25	Ø10@100mm
5	400*800	12Ø25	Ø10@100mm
6	400*800	12Ø25	Ø10@100mm
7	400*800	12Ø25	Ø10@100mm
8	400*800	12Ø25	Ø10@100mm
9	400*800	10Ø25	Ø10@100mm
10	400*800	10Ø25	Ø10@100mm
11	400*800	10Ø25	Ø10@100mm
12	400*800	10Ø25	Ø10@100mm
13	400*800	10Ø25	Ø10@125mm
14	400*800	10Ø25	Ø10@125mm
15	400*800	10Ø25	Ø10@125mm
16	400*800	10Ø25	Ø10@125mm
17	400*800	12Ø20	Ø10@100mm
18	400*800	12Ø20	Ø10@100mm
19	400*800	12Ø20	Ø10@100mm
20	400*800	12Ø20	Ø10@100mm
21	400*800	10Ø20	Ø10@100mm
22	400*800	12Ø20	Ø10@100mm
23	400*800	12Ø20	Ø10@100mm
24	400*800	12Ø20	Ø10@100mm
25	400*800	10Ø20	Ø10@125mm
26	400*800	10Ø20	Ø10@125mm
27	400*800	10Ø20	Ø10@125mm
28	400*800	10Ø20	Ø10@125mm
29	400*800	10Ø20	Ø10@125mm
30	400*800	10Ø20	Ø10@125mm
31	400*800	10Ø20	Ø10@125mm
32	400*800	10Ø20	Ø10@125mm

3.4 Attraction Loads

Dead load(DL), super dead load(SDL), and live loads(LL) were set for all modeling's and also deemed the same to all of the modeling's. Masonry load, live load, super dead load, and dead load (self-weight of the structure) were the attraction loads regarded throughout this thesis, the software ETABS automatically measures the structure's self-weight. But masonry load, LL, and SDL have been identified and applied to the program ETABS as shown: The live load is 5 kN/m, super dead load 15 kN/m, and masonry load is 14 kN/m are identified and applied to the structure buildings.

3.5 Model Description

This research just includes a moment-resistant frame with the shear wall MRFSW (Dual System). The supporting form has been presumed to be fixed for all the modeling's as well as the corresponding different parameters are listed throughout this thesis:

- The number of stories (S): Low-rise (4-story), medium-rise (8-story), and high-rise building (12-story).

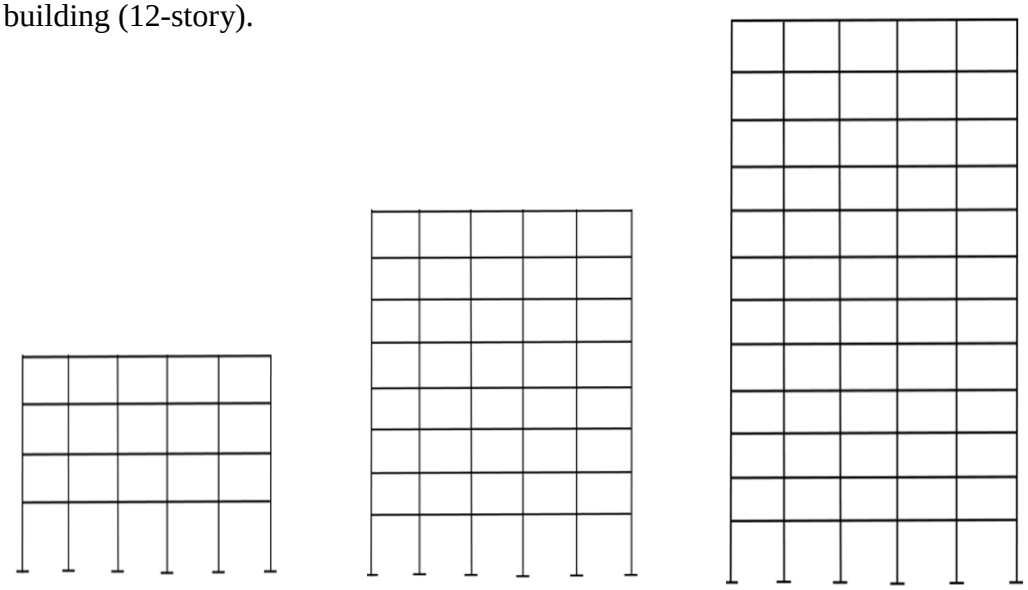

Figure 3.1: Number of stories

- Number of spans(N): 5-span

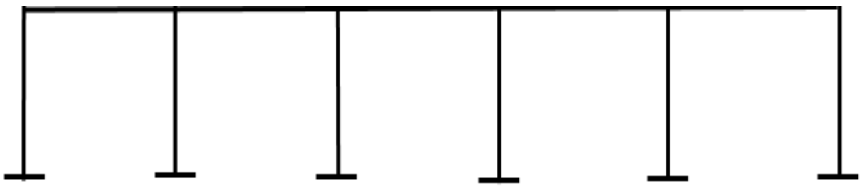

Figure 3.2: Number of spans

- Height of stories (H): Typical story height 3.2m, Ground floor height 4m.

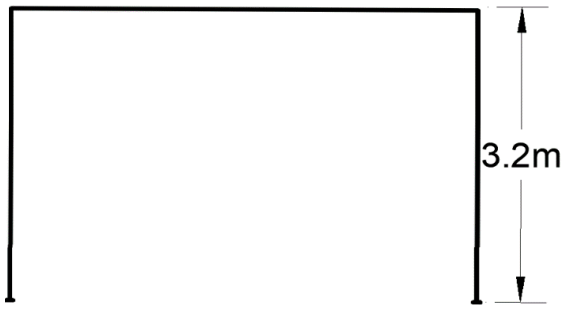

(a) Typical story height

(b) Ground floor height

Figure 3.3: Story heights: (a) typical story height (b) ground floor height

- Span length(L): 5m, 5.5m, 6m, and 7m

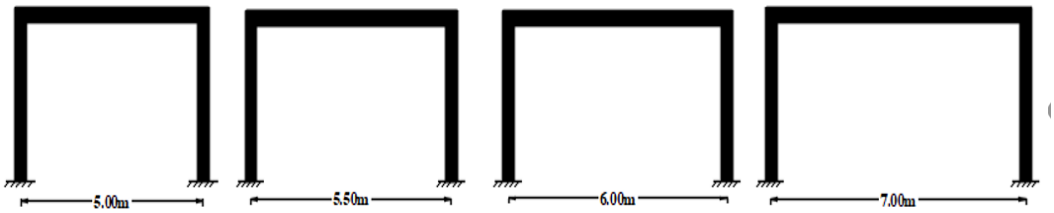

Figure 3.4: Different span lengths

- Different positions of shear wall: edge, middle

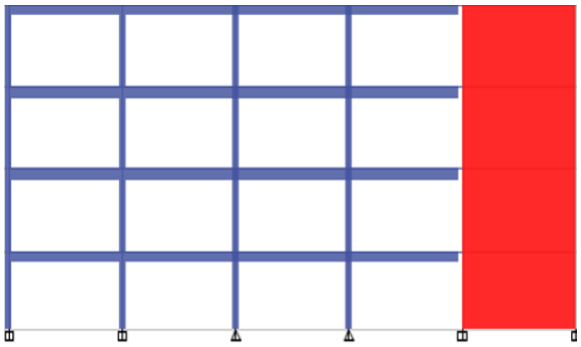

(a) Edge

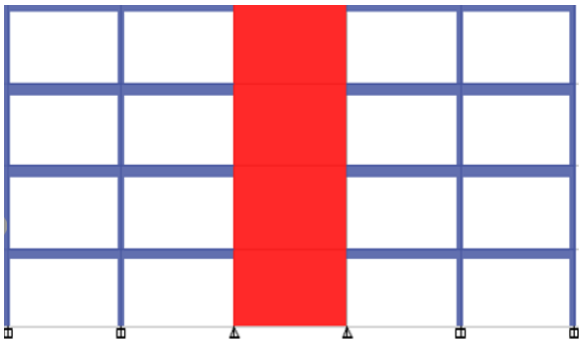

(b) Middle

Figure 3.5: Different positions of shear wall: (a) edge, (b) middle

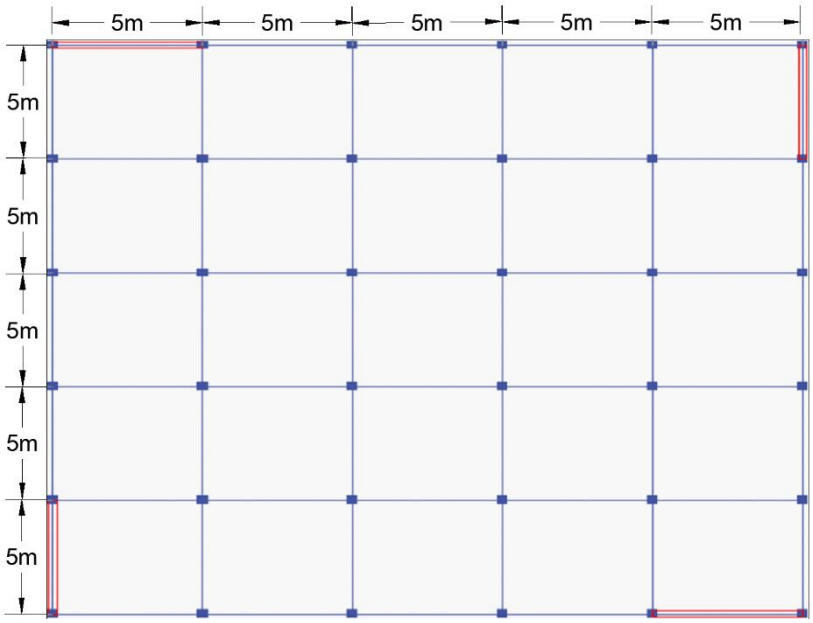

(a) Edge

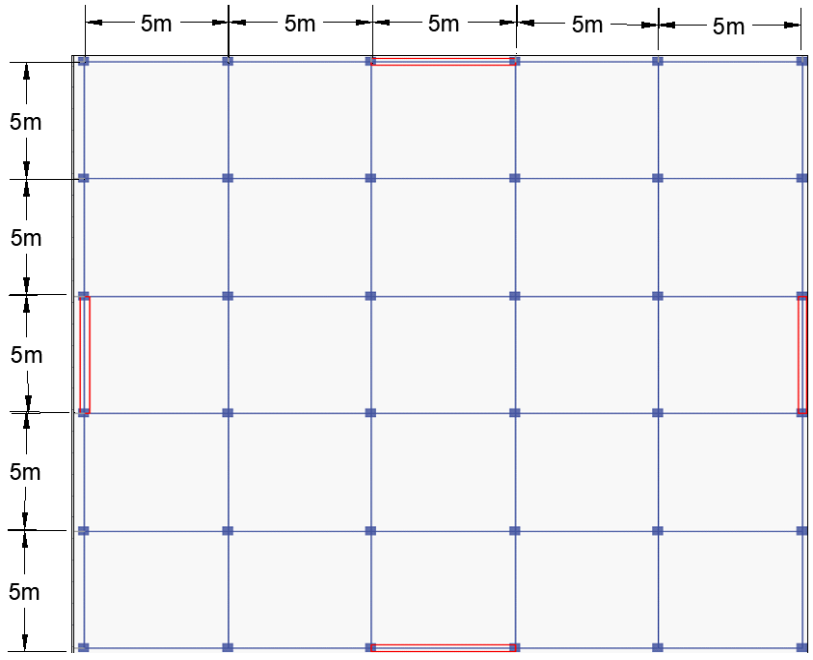

(b) Middle

Figure 3.6: Plan view of different positions of shear wall: (a) edge, (b) middle

- Different thicknesses of shear wall**:** 250mm, 300mm
- Different compressive strengths ($f'c$) : (250, 300 kgf/cm^2)
- The number of models by ETABS are: 96 models
- Location of buildings: Washington DC, USA

3.6 Seismic Analysis Methods

The earthquake loads had been defined per the requirements of ASCE 7-10 throughout this thesis. Seismic analysis is divided into four methods, the method of earthquake analysis which may be utilized to evaluate the structure relies on dynamic characteristics, the classification of the seismic layout of the structure, consistency, and structural framework.

The various processes for analysis are:

- Linear Static Analysis
- **Nonlinear Static Analysis**
- Linear Dynamic Analysis
- Nonlinear Dynamic Analysis

Static non-linear analysis was chosen because it is simpler than better and more precise dynamic analysis.

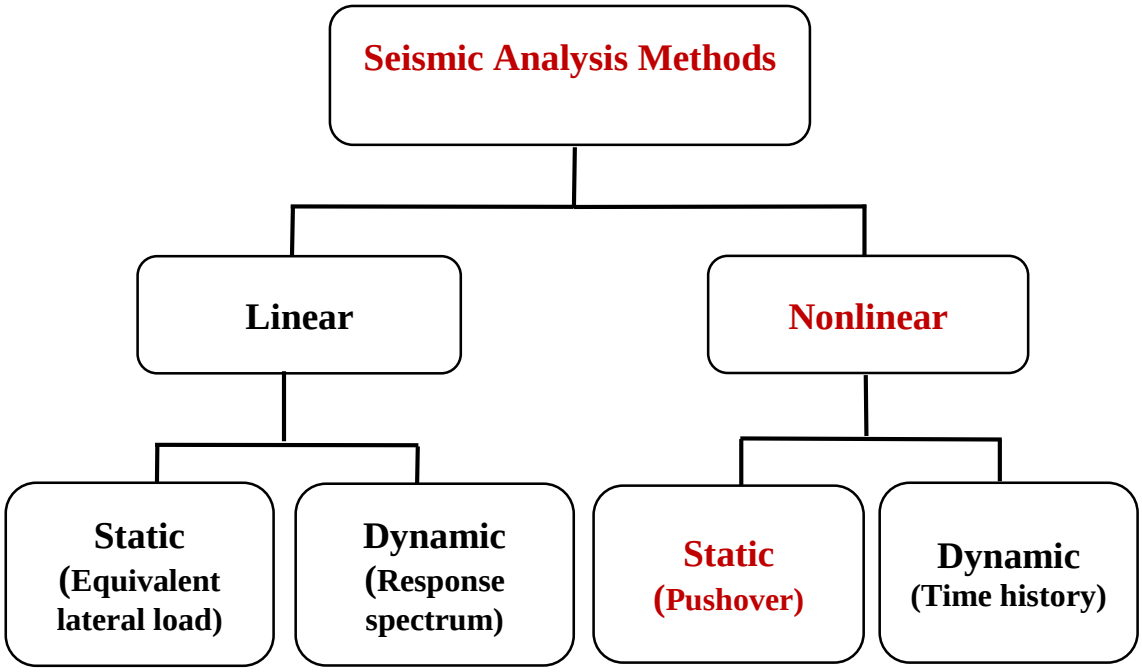

Figure 3.7: Seismic analysis methods

By the numerous recovery guidelines and standards for seismic efficiency assessment of structures, Pushover evaluation has been the appropriate approach because its algorithmically and functionally easy. Pushover analysis allows the mechanism of component and structural stage yield and breakdown to being traced and the progress of the average pushover curve of the system to be tracked. Pushover analysis had been an efficient method of determining the actions of the building, underlining the cracking trend of the component and yielding while the base shear level rises. The primary benefit of pushover analysis would be to obtain an over-strength calculation and to gain a sense of the total capabilities of the structure to withstand inelastic deforming.

3.7 Seismic Design Category (SDC)

Depending upon the magnitude of the layout seismic ground movement in the sites as well as its occupation, structures were allocated to an SDC.

3.7.1 Procedure for calculation of seismic design category according to ASCE 7-10

1- Through this analysis, risk category I is utilized throughout Table 1.5-1 of ASCE 7-10 code, as the structures being perceived to be built for residential buildings, so the significant factor was 1 due to Table 1.5-2 in ASCE 7-10.

2- Depending upon the building position, the map MCER spectral response acceleration parameters for short periods (S-S) and the map MCER spectral response acceleration parameters for a time of 1 second (S-1) are calculated. In this study (S-S) and (S-1) results have been drawn from the United States of America from Washington City, which are 0.5 g and 0.2 g.

3- The site category has been defined from the characteristics of the soil as well as the soil type name. Class C is being utilized throughout the research site and while the position is uncertain, ASCE 7-10 is required to use.

4- After that, the MCER spectral responded acceleration parameters for short periods (SMS) and at 1 second (SM1) are modified for Site Category impacts equations (3.1) and (3.2) in compliance with ASCE 7-10 section 11.4. 3.

$$S_{MS} = F_a\, S_S \qquad (3.1)$$

$$S_{M1} = F_v\, S_1 \qquad (3.2)$$

According to ASCE 7-10 code, site parameters F_a and F_v are listed in Tables 11.4-1 and 11.4-2, and those tables are shown in tables 3.9 and 3.10 separately throughout this study.

Table 3.9: Site coefficient (F_a)

Site class	Mapped MCE_R spectral response acceleration parameters at short period				
	$S_S \leq 0.25$	$S_S = 0.5$	$S_S = 0.75$	$S_S = 1.0$	$S_S \geq 1.25$
A	0.8	0.8	0.8	0.8	0.8
B	1	1	1	1	1
C	1.2	1.2	1.1	1	1
D	1.6	1.4	1.2	1.1	1
E	2.5	1.7	1.2	0.9	0.9
F	See ASCE 7-10 segment 11.4.7				

Table 3.10: Site coefficient (F_v)

Site class	Mapped MCE_R spectral response acceleration parameters at 1-s periods				
	$S_1 \leq 0.1$	$S_1 = 0.2$	$S_1 = 0.3$	$S_1 = 0.4$	$S_1 \geq 0.5$
A	0.8	0.8	0.8	0.8	0.8
B	1	1	1	1	1
C	1.7	1.6	1.5	1.4	1.3
D	2.4	2	1.8	1.6	1.5
E	3.5	3.2	2.8	2.4	2.4
F	See ASCE 7-10 segment 11.4.7				

5- SDS at short time and 1-s period SD1, seismic layout spectral response acceleration parameters had been calculated via equations (3.3) and (3.4).

$$S_{DS} = 2/3\ S_{MS} \quad (3.3)$$

$$S_{D1} = 2/3\ S_{M1} \quad (3.4)$$

6- Identify seismic design category per Tables (11.6.1) and (11.6.2) of ASCE7-10 and Tables 3.11 and 3.12 of this study.

Table 3.11: SDC depending on short-period response acceleration parameter

Values of S_{DS}	Risk Category	
	I or II or III	IV
S_{DS}<0.167	A	A
0.167≤ S_{DS}<0.33	B	C
0.33≤ S_{DS} <0.5	C	D
0.5≤ S_{DS}	D	D

Table 3.12: SDC based on 1-s period response acceleration parameter

Values of S_{D1}	Risk Category	
	I or II or III	IV
S_{D1}<0.067	A	A
0.067≤ S_{D1}<0.133	B	C
0.133≤ S_{D1} <0.2	C	D
0.2≤ S_{D1}	D	D

3.7.2 Determination of seismic design category for all models.

- Risk category = III
- S_S = 0.5g, S_1 = 0.2g
- Site class = C
- Fa= 1.2 from Table (11.4-1) and F_v=1.6 from Table (11.4-2) from ASCE 7-10
- S_{MS}=1.2 * 0.5g = 0.6g

  S_{M1}=1.6 * 0.2g = 0.32g
- S_{DS} = 2/3 *0.6 = 0.4g

  S_{D1} = 2/3 *0.32= 0.213g

7- Seismic design category is dependent upon tables (11.6-1) and (11.6-2) from ASCE7-10 and tables 3.5 and 3.6 throughout this study, in accordance with SDS and SD1 results. The SDC of all buildings is type C, relying upon the tables.

The seismic design category for all the buildings in this study is type C, which is observed before.

3.8 Seismic Parameters

Further information is required to define earthquake forces and designing the models, the following seismic parameters were used to calculate seismic loads and design for all modeling's:

- Importance factor (residential building): 1
- Response modification factor: 5
- Over strength factor: 2.5
- Deflection implication factor: 4.5

3.9 Modeling of the Different Story Numbers of Dual Systems (MRFSW)

This part includes modeling's of different numbers of stories of dual system (MRFSW) with different locations of shear wall which is designed and analyzed by ETABS program.

- Low-rise building

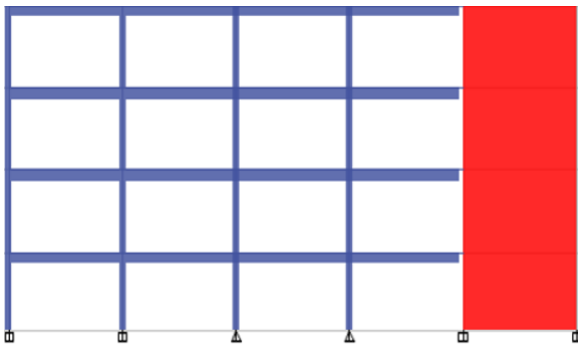

Figure 3.8: 2D model for low-rise building (4-story), shear wall position (edge)

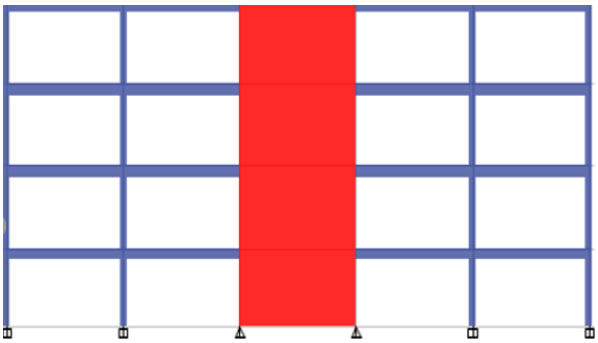

Figure 3.9: 2D model for low-rise building (4-story), shear wall position (middle)

- Mid-rise building

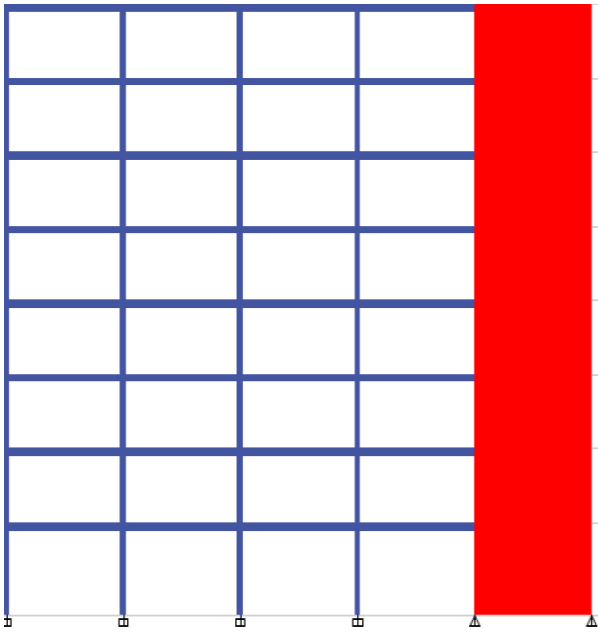

Figure 3.10: 2D model for mid-rise building (8-story), shear wall position (edge)

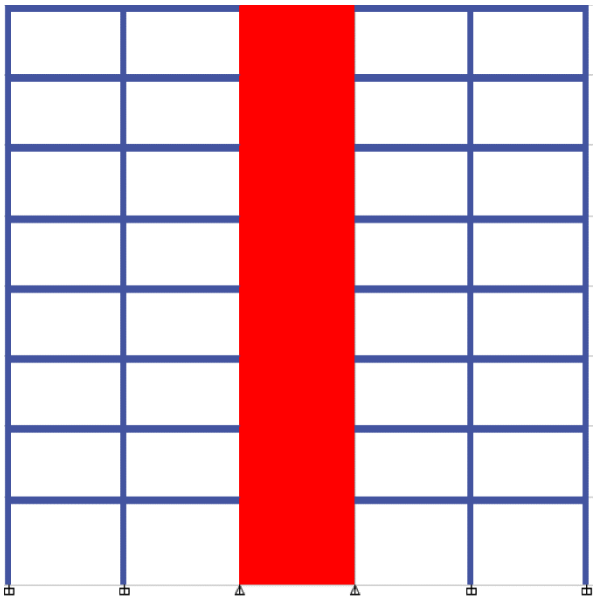

Figure 3.11: 2D model for mid-rise building (8-story), shear wall position (middle)

- High-rise building

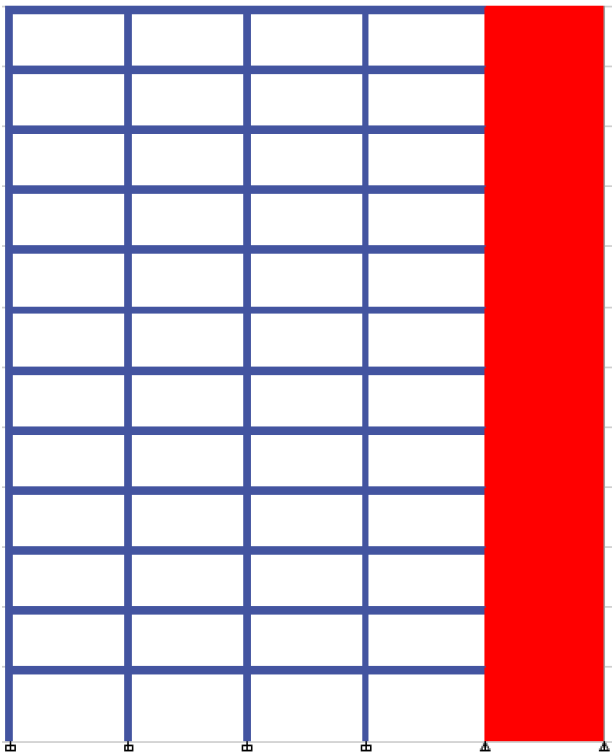

Figure 3.12: 2D model for high-rise building (12-story), shear wall position (edge)

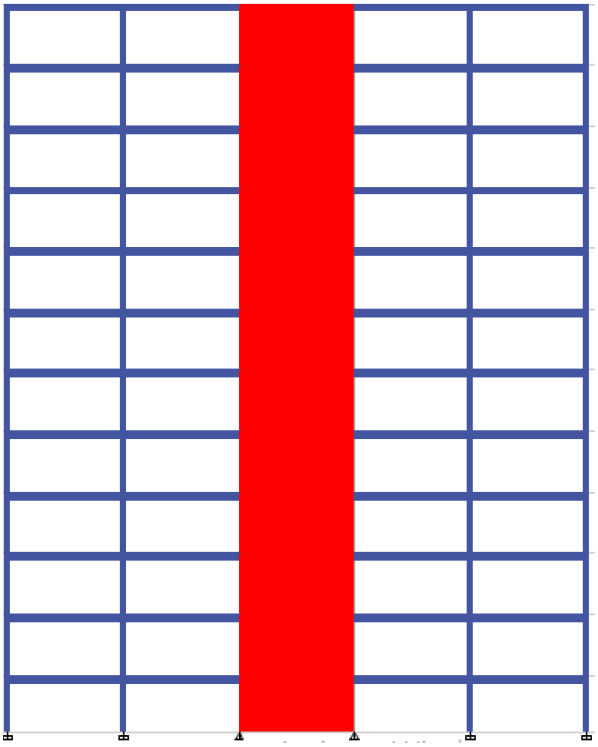

Figure 3.13: 2D model for high-rise building (12-story), shear wall position (middle)

3.10 Bilinear Curve of Pushover Curve

The request for an easy approach to estimate the non-linear actions of a structure against earthquake loading, from which is widely recognized as the pushover study. Pushover Curves illustrates the structure's nonlinear nature and also is a base shear deformed curve against the construction's lateral floor displacement. The study of Pushover has been dependent upon the concept that one prevailing Eigen value and mode form is through the structure.

This method is dependent upon the principles of FEMA356, assuming equal regions underneath the main and bilinear curves, but there were some variations, primarily with regard to the 'highest point concept and the yield branching slopes. To every method of design buildings, bilinear pushover curve has been constructed and reflect different stages of

earthquake layout and building efficiency. So each curve has been defined via 2 points: yields of capability and ultimate capacity. The yield points were determined by the conjunction of the preliminary tangent stiff within the proposed strength, the intersections of the secant rigidity with the proposed strength throughout the initial yield.

The maximal capacity was achieved after the general structural framework has been developed as a total approach and a 15 percentage reduce in strength had occurred through the failing of certain components to reach the deformation capability. Consequently, the strength referring to the optimum capacity doesn't always correlate with the actual highest power reported through the study. Furthermore, the yield capability is not really the power of the building while the initial yield of a member occurs.

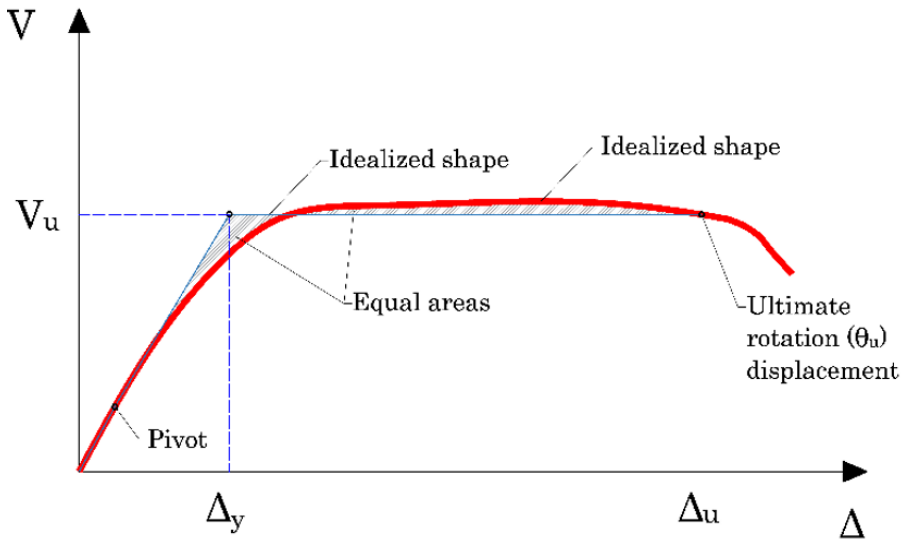

Figure 3.14: The bilinear curve of pushover curve (Vielma-Perez and Mulder, 2018)

3.10.1 Sample of the bilinear curve of capacity curve

Which can be seen in Figure 3.15 below, the bilinear curve with pushover curve demonstrates which the amount of the region under the pushover curve must be similar with the area located above the pushover curve and also that area calculation was carried out using AutoCAD program. For this purpose, the pushover curve is exported from ETABS to Microsoft Excel

and then was transferred to AutoCAD. In this stage, a horizontal line was drawn from the point of 85% of the maximum base shear of the pushover curve. This line was intersected the pushover curve and is passed it. Another line is drawn from the coordinate center and intersected with the drawn horizontal line. In the next stage, the area below the pushover and above the pushover curves are compared with each other, and the position of the second drawn line is changed until both areas had the almost same area.

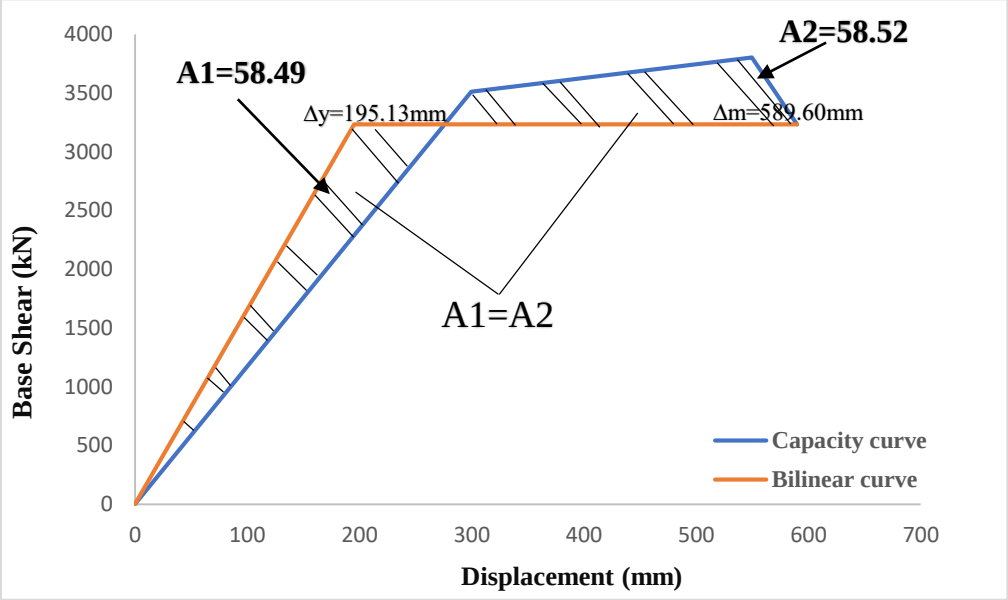

Figure 3.15: The area above capacity curve and area below the bilinear curve

CHAPTER 4
RESULTS AND DISCUSSION

4.1 Introduction

When the structure lacks elasticity, the deformation underneath the seismic loads can rise considerably. Besides, any structure's tolerance to every lateral force without failure has been recognized as ductility, which can be identified by the peak displacement of the building, dividing on the displacement at the beginning of the fracture (Δu/Δy). Using (ETABS) program, capability (pushover) curves have been obtained for the various 2D RC buildings. The findings of 2D RC structures have been compared and assessed through this chapter including figures and tables for the effect of various variables. The important variables are shear wall thickness and position, as well as other parameters including span length, compressive strength, and number of stories. The results of this research involve peak displacement, yield displacement, maximum base shear, and ductility value.

4.2 Results

The results of yield displacement, maximum displacement, maximum base shear, and ductility ratio obtained by pushover analysis in Appendix 1, 2, and 3 are shown in the given table below. For low-rise buildings with different compressive strengths, the results achieved are summarized in Table 4.1 and Table 4.2, and Table 4.3 and Table 4.4 for mid-rise buildings with various compressive strengths, as well as Table 4.5 and Table 4.6 for high-rise buildings for various compressive strengths.

Table 4.1: Results of nonlinear static analysis for low-rise models at compressive strength $(f'c)$, 250 kgf/cm^2

No. of models	Span length(m)	Thickness of shear wall (mm)	Position of shear wall	Δ_y (mm)	Δ_m (mm)	V_m (kN)	μ
1	5	250	Edge	120.44	311.62	8683.96	2.58
2	5.5	250	Edge	118.50	324.70	8617.29	2.74
3	6	250	Edge	116.45	332.19	8573.91	2.85
4	7	250	Edge	103.91	351.82	8497.85	3.38
5	5	250	Middle	70.43	154.51	9887.37	2.19
6	5.5	250	Middle	67.55	163.34	9725.80	2.41
7	6	250	Middle	62.17	169.12	9561.29	2.72
8	7	250	Middle	53.95	176.23	9372.13	3.26
9	5	300	Edge	86.34	203.28	9164.85	2.35
10	5.5	300	Edge	85.26	214.97	9107.88	2.52
11	6	300	Edge	80.85	223.17	9045.28	2.76
12	7	300	Edge	74.19	242.63	8939.80	3.27
13	5	300	Middle	77.20	144.38	9997.85	1.87
14	5.5	300	Middle	70.59	155.28	9889.92	2.19
15	6	300	Middle	64.20	160.72	9681.94	2.50
16	7	300	Middle	56.11	174.28	9544.57	3.10

Table 4.2: Results of nonlinear static analysis for low-rise models at compressive strength $(f'c)$, 300 kgf/cm^2

No. of models	Span length(m)	Thickness of shear wall (mm)	Position of shear wall	Δ_y (mm)	Δ_m (mm)	V_m (kN)	μ
17	5	250	Edge	128.30	296.81	8601.37	2.31
18	5.5	250	Edge	123.23	305.63	8556.48	2.48
19	6	250	Edge	118.11	319.15	8497.08	2.70
20	7	250	Edge	106.12	340.23	8579.72	3.20
21	5	250	Middle	77.61	149.74	10298.90	1.92
22	5.5	250	Middle	70.42	158.83	10148.58	2.25
23	6	250	Middle	64.64	163.29	10008,28	2.53
24	7	250	Middle	54.81	172.37	9905.42	3.14
25	5	300	Edge	51.01	112.78	10269.37	2.21
26	5.5	300	Edge	50.21	120.85	10203.72	2.40
27	6	300	Edge	49.32	129.44	10154.38	2.62
28	7	300	Edge	47.12	148.23	10066.38	3.14
29	5	300	Middle	76.24	136.62	10579.29	1.79
30	5.5	300	Middle	69.12	145.29	10362.57	2.10
31	6	300	Middle	63.15	152.47	10301.24	2.41
32	7	300	Middle	55.90	169.22	10181.38	3.02

Table 4.3: Results of nonlinear static analysis for mid-rise models at compressive strength $(f'c)$, 250 kgf/cm^2

No. of models	Span length(m)	Thickness of shear wall (mm)	Position of shear wall	Δ_y (mm)	Δ_m (mm)	V_m (kN)	μ
33	5	250	Edge	98.15	317.73	3832.46	3.23
34	5.5	250	Edge	93.02	330.76	3768.28	3.55
35	6	250	Edge	88.22	346.63	3692.27	3.92
36	7	250	Edge	82.39	367.81	3588.08	4.46
37	5	250	Middle	126.35	389.7	4842.19	3.08
38	5.5	250	Middle	122.14	406.39	4765.38	3.32
39	6	250	Middle	119.46	423.97	4698.22	3.54
40	7	250	Middle	111.42	451.83	4608.23	4.05
41	5	300	Edge	104.99	316.91	4255.19	3.01
42	5.5	300	Edge	100.22	334.89	4184.11	3.34
43	6	300	Edge	97.26	351.34	4074.28	3.61
44	7	300	Edge	87.91	370.18	4019.50	4.19
45	5	300	Middle	147.14	382.70	5695.18	2.60
46	5.5	300	Middle	144.32	401.18	5612.98	2.77
47	6	300	Middle	141.37	418.91	5532.17	2.96
48	7	300	Middle	130.25	437.11	5419.06	3.35

Table 4.4: Results of nonlinear static analysis for mid-rise models at compressive strength $(f'c)$, 300 kgf/cm^2

No. of models	Span length(m)	Thickness of shear wall (mm)	Position of shear wall	Δ_y (mm)	Δ_m (mm)	V_m (kN)	μ
49	5	250	Edge	102.07	306.39	4243.18	3.00
50	5.5	250	Edge	101.25	326.63	4139.55	3.22
51	6	250	Edge	100.01	340.13	4051.73	3.40
52	7	250	Edge	85.06	361.68	3937.39	4.25
53	5	250	Middle	142.05	380.48	5184.21	2.67
54	5.5	250	Middle	140.19	394.31	5129.08	2.81
55	6	250	Middle	129.13	407.55	5095.45	3.15
56	7	250	Middle	112.2	430.00	4983.65	3.83
57	5	300	Edge	105.49	296.34	4913.55	2.80
58	5.5	300	Edge	100.30	318.20	4801.40	3.17
59	6	300	Edge	102.60	332.62	4729.11	3.24
60	7	300	Edge	89.65	355.00	4615.11	3.95
61	5	300	Middle	169.44	366.70	6055.46	2.16
62	5.5	300	Middle	158.41	384.28	5986.35	2.42
63	6	300	Middle	153.10	399.69	5912.45	2.61
64	7	300	Middle	134.01	423.80	5853.70	3.16

Table 4.5: Results of nonlinear static analysis for high-rise models at compressive strength $(f'c)$, 250 kgf/cm^2

No. of models	Span length(m)	Thickness of shear wall(mm)	Position of shear wall	Δ_y (mm)	Δ_m (mm)	V_m (kN)	μ
65	5	250	Edge	115.6	589.96	2390.34	5.11
66	5.5	250	Edge	115.09	598.72	2311.56	5.20
67	6	250	Edge	113.21	612.16	2266.39	5.40
68	7	250	Edge	112.10	627.34	2191.22	5.59
69	5	250	Middle	156.16	673.66	2855.67	4.31
70	5.5	250	Middle	147.71	685.37	2764.94	4.63
71	6	250	Middle	145.37	699.38	2708.26	4.81
72	7	250	Middle	137.12	721.24	2641.96	5.25
73	5	300	Edge	107.05	429.79	2690.88	4.01
74	5.5	300	Edge	104.10	441.92	2617.18	4.24
75	6	300	Edge	98.11	454.27	2556.13	4.62
76	7	300	Edge	90.30	470.45	2470.19	5.21
77	5	300	Middle	204.15	638.36	3496.39	3.12
78	5.5	300	Middle	198.11	651.17	3401.33	3.28
79	6	300	Middle	183.49	669.77	3281.11	3.65
80	7	300	Middle	166.14	698.28	3186.04	4.20

Table 4.6: Results of nonlinear static analysis for high-rise models at compressive strength $(f'c)$, 300 kgf/cm^2

No. of models	Span length(m)	Thickness of shear wall (mm)	Position of shear wall	Δ_y (mm)	Δ_m (mm)	V_m (kN)	μ
81	5	250	Edge	103.12	521.45	2503.55	5.05
82	5.5	250	Edge	104.92	545.32	2409.17	5.19
83	6	250	Edge	106.32	566.45	2343.19	5.32
84	7	250	Edge	110.87	615.16	2245.44	5.47
85	5	250	Middle	159.51	639.68	3332.45	4.01
86	5.5	250	Middle	150.20	663.20	3215.99	4.41
87	6	250	Middle	152.01	684.15	3101.58	4.50
88	7	250	Middle	143.25	719.45	2931.10	5.02
89	5	300	Edge	87.02	399.28	3000.56	3.95
90	5.5	300	Edge	106.59	426.88	2890.34	4.00
91	6	300	Edge	100.04	443.96	2714.89	4.43
92	7	300	Edge	93.12	466.56	2621.01	5.01
93	5	300	Middle	195.13	589.60	3802.78	3.02
94	5.5	300	Middle	190.12	605.43	3678.34	3.18
95	6	300	Middle	185.05	659.45	3511.28	3.56
96	7	300	Middle	168.64	692.04	3406.46	4.00

4.3 Discussion of the Results

This segment identifies the findings in three sections: (a) the discussion of the influence of certain variables on the ductility value in the first part; (b) the discussion of the effect of the difference in shear wall thicknesses on the ductility ratio in the second part; (c) the discussion of the impact of the difference in shear wall position on the ductility value in the third part.

4.3.1 The effect of some parameters on ductility value

This section provides an evaluation of the influence of certain parameters on the value of ductility, span length, number of stories, and compressive strength are parameters. this segment includes 3 parts The first part discusses the influence of span length on ductility value, the second part describes the effect of the number of stories on the value of ductility, and the third part describes the effect on ductility of the difference in compressive strength.

a) The effect of span length on ductility value and the capacity curves

The effect of span length on ductility values and capability curves at different shear wall thicknesses and positions with different numbers of stories will be described in this section. Table 4.7, Table 4.8, Figure 4.1, and Figure 4.2 shows the ductility values with different span length for models (4-story), models (8-story), and models (12-story) with different thicknesses and positions of shear wall, and Figure 4.3, Figure 4.4 and Figure 4.5 shows the difference in the capacity (pushover) curve with different span length.

As shown in Table 4.7 and Figure 4.1 when span length increases from 5m to 5.5m for 4-story cause an increase in ductility values by 6%, to 6m increased by 10.5%, and to 7m increased by 31%, when span length increases from 5m to 5.5m for 8-story cause an increase in ductility values by 10%, to 6m increased by 21%, and to 7m increased by 38%, when span length increases from 5m to 5.5m for 8-story cause an increase in ductility values by 2%, to 6m increased by 6%, and to 7m increased by 10%, and as shown in Table 4.8 and Figure 4.2, ductility will increase by increasing span length as well, this is because of increased stiffness of the building. Increasing span length allows a reduction in yield displacement and increase

in maximum displacement for 4-story, 8-story, and 12-story, as shown in Figure 4.3 Figure 4.4 and Figure 4.5, so the value of ductility rises. And by increasing the span length cause a decrease in maximum base shear.

Used parameters in this section: compressive strength ($f'c$) = 250 kgf/cm^2, shear wall thickness = 250 mm and shear wall position = edge, shear wall thickness = 300mm and shear wall position = middle

Table 4.7: Results of ductility ratios of buildings with different span lengths at shear wall thickness (250mm) and shear wall position (edge)

	Span length			
No. of stories	**5m**	**5.5m**	**6m**	**7m**
4-story	2.58	2.74	2.85	3.38
8-story	3.23	3.55	3.92	4.46
12-story	5.11	5.20	5.40	5.59

Table 4.8: Results of ductility ratios of buildings with different span lengths at shear wall thickness (300mm) and shear wall position (middle)

	Span length			
No. of stories	**5m**	**5.5m**	**6m**	**7m**
4-story	1.87	2.19	2.50	3.10
8-story	2.60	2.77	2.96	3.35
12-story	3.12	3.28	3.65	4.20

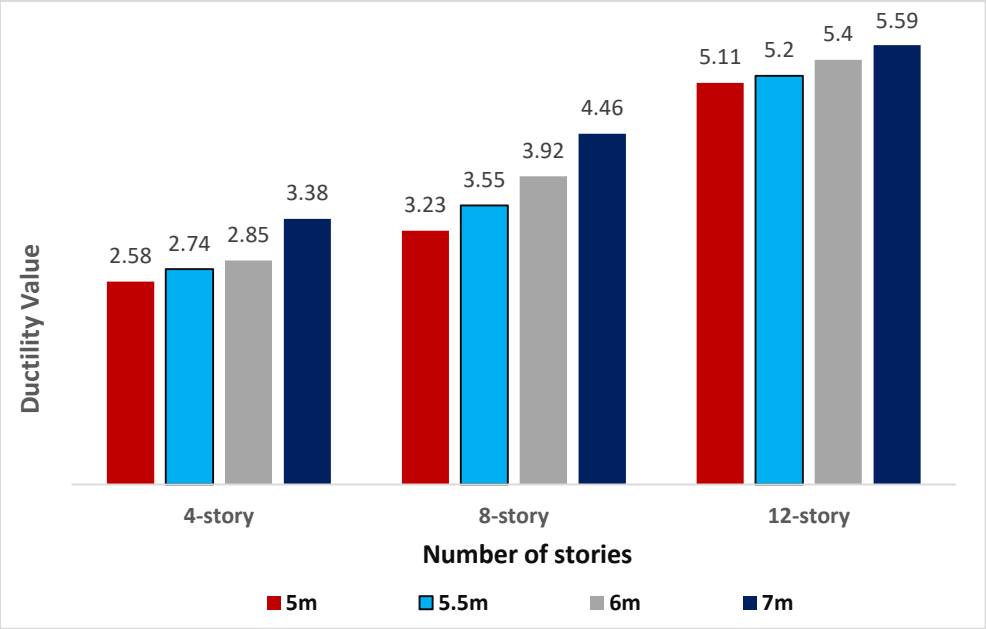

Figure 4.1: A comparison of the values of ductility of different span lengths at shear wall thickness (250mm) and shear wall position (edge)

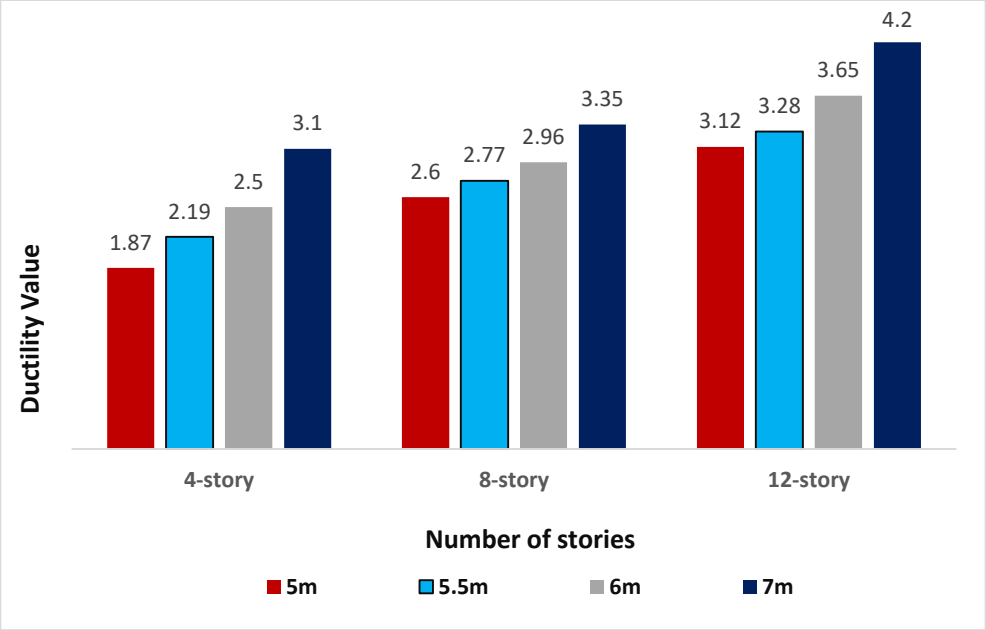

Figure 4.2: A comparison of the values of ductility of different span lengths at shear wall thickness (300mm) and shear wall position (middle)

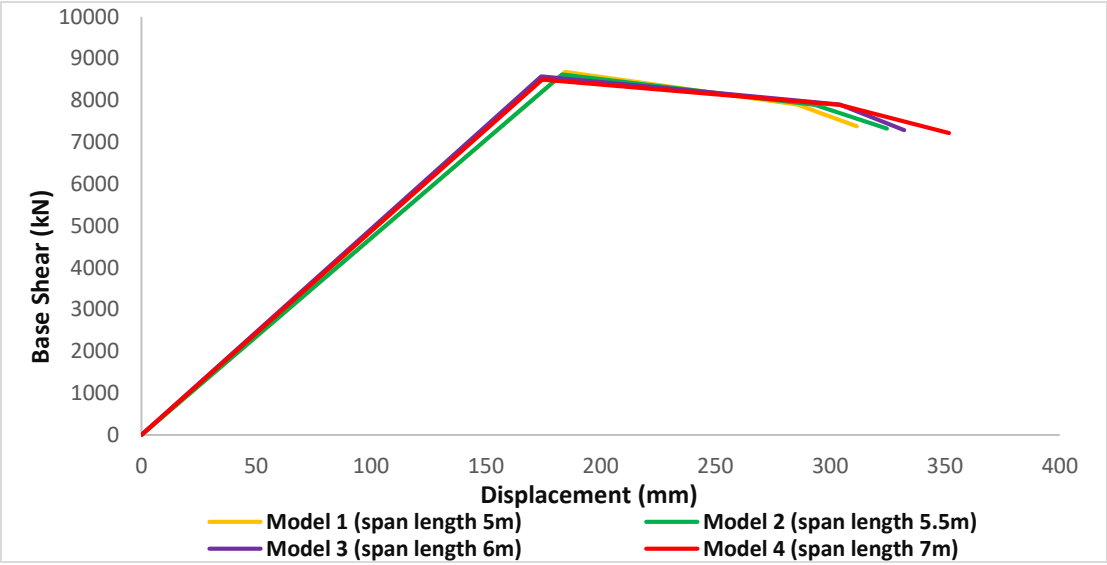

Figure 4.3: The effect of the different span length on the capacity curve of the low-rise building (4-story)

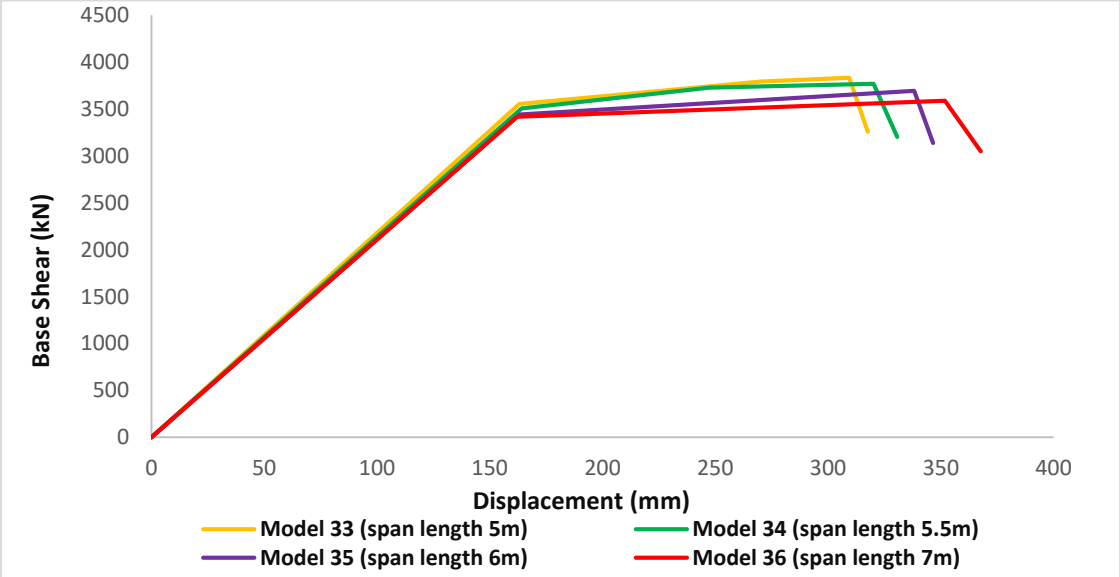

Figure 4.4: The effect of the different span length on the capacity curve of the mid-rise building (8-story)

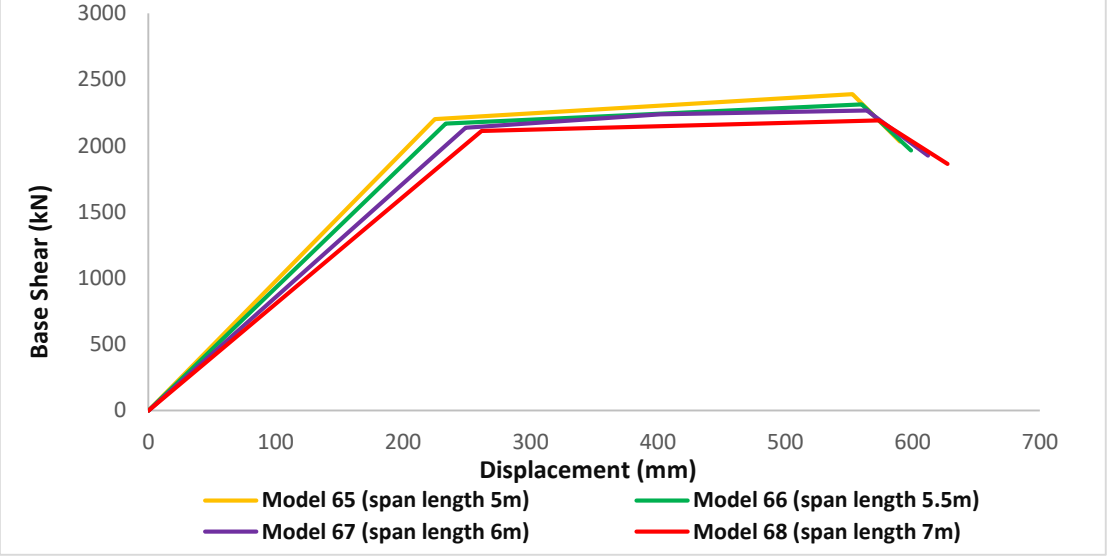

Figure 4.5: The effect of the different span length on the capacity curve of the high-rise building (12-story)

b) The effect of the number of stories on ductility value and the capacity curves

The impact of various stories upon ductility values and capability curves at various shear wall thicknesses and positions will be explained throughout this section. Table 4.9, Table 4.10, Figure 4.6 and Figure 4.7 illustrates the ductility values for different number of stories for models (4-story), models (8- story), and models (12-story) with different thicknesses and positions of shear wall, and Figure 4.8 and Figure 4.9 illustrates the difference in the capacity (pushover) curve with different number of stories.

As seen in Table 4.9 and Figure 4.6 as the number of stories rises for span length 5m from 4-story to 8-story, ductility value increases by 33%, and 12-story ductility values increases by 71%, also as seen in Table 4.10 and Figure 4.7 changing numbers of stories from low-rise to mid-rise cause an increase in ductility value by 5% and high-rise buildings increases by 32%, this is due to decreasing stiffness when the number of story increases.

As seen in Figure 4.8 and Figure 4.9, an increasing number of stories lead to an increase in both yield displacement and ultimate displacement, which is how ductility value rises, and also by increasing the number of stories cause a decrease in maximum base shear.

Used parameters in this section: compressive strength ($f'c$) = 300 kgf/cm^2, shear wall thickness = 250 mm and shear wall position = edge, shear wall thickness = 300mm and shear wall position = middle

Table 4.9: Results of values of ductility of buildings with different number of stories at shear wall thickness (250mm) and shear wall position (edge)

Span length	No. of stories		
	4-story	8-story	12-story
5m	2.31	3.00	5.05
5.5m	2.48	3.22	5.19
6m	2.70	3.40	5.32
7m	3.20	4.25	5.47

Table 4.10: Results of values of ductility of buildings with different number of stories at shear wall thickness (300mm) and shear wall position (middle)

Span length	No. of stories		
	4-story	8-story	12-story
5m	1.79	2.16	3.02
5.5m	2.10	2.42	3.18
6m	2.41	2.61	3.56
7m	3.02	3.16	4.00

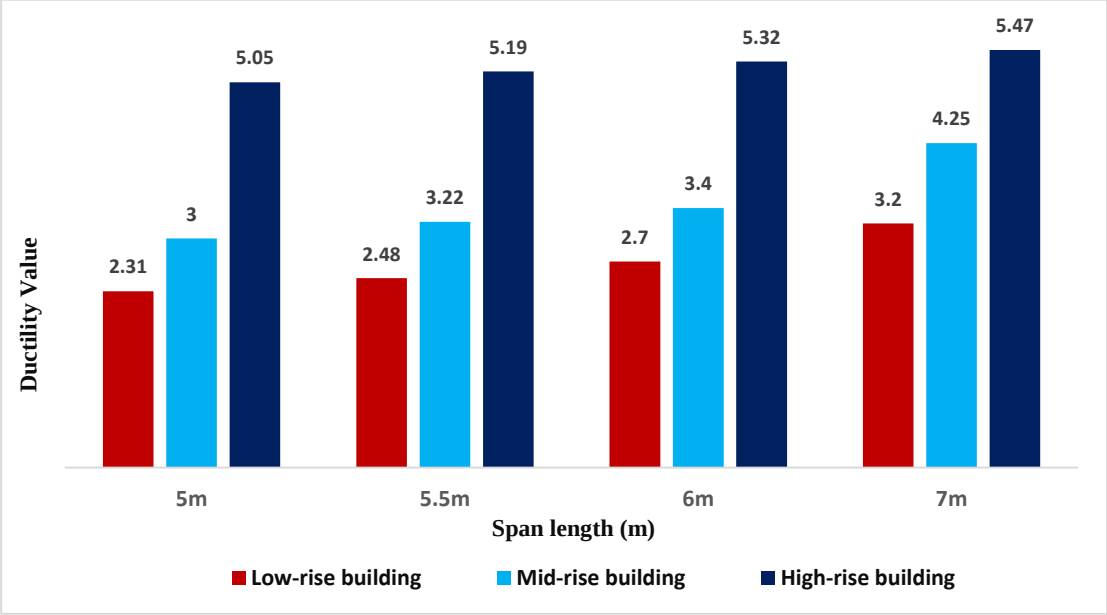

Figure 4.6: A comparison of the values of ductility of different number of stories at shear wall thickness (250mm) and shear wall position (edge)

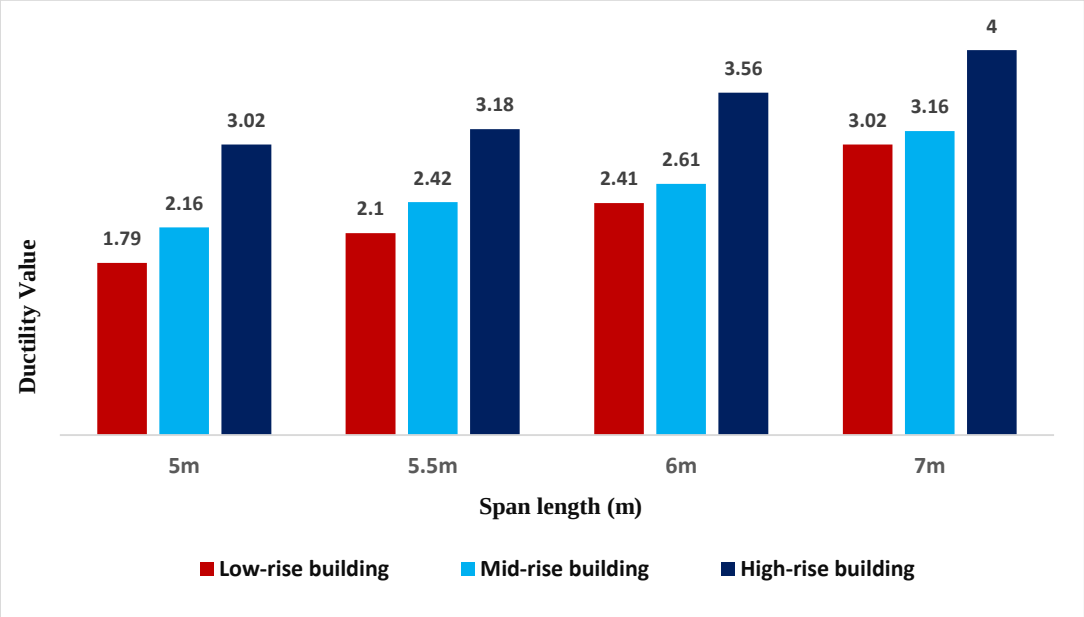

Figure 4.7: A comparison of the values of ductility of different number of stories at shear wall thickness (300mm) and shear wall position (middle)

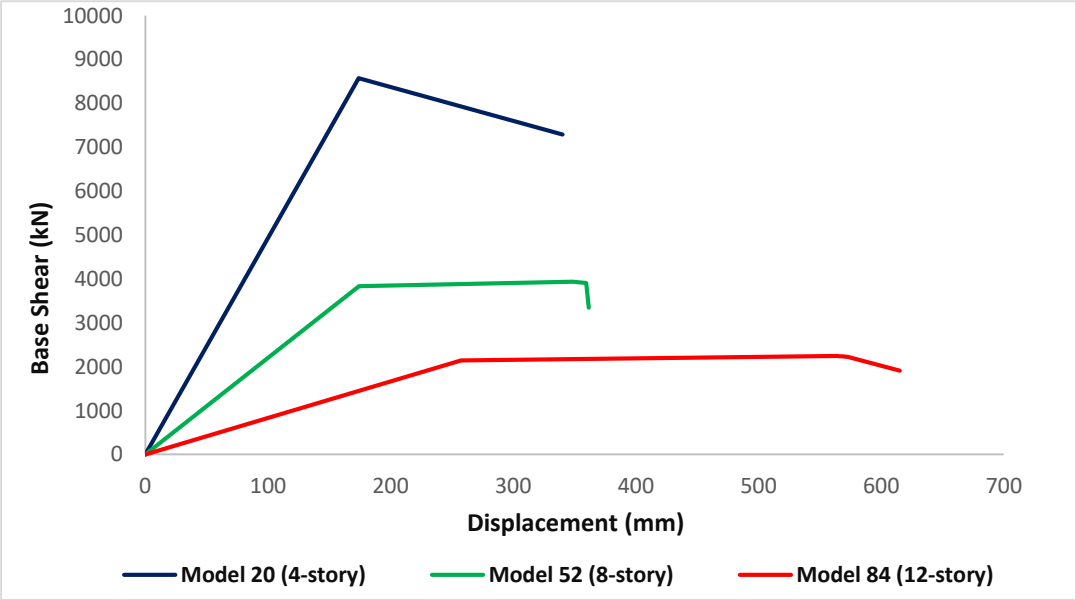

Figure 4.8: The impact of the various number of stories on the capacity curve at shear wall thickness (250mm) and shear wall position (edge)

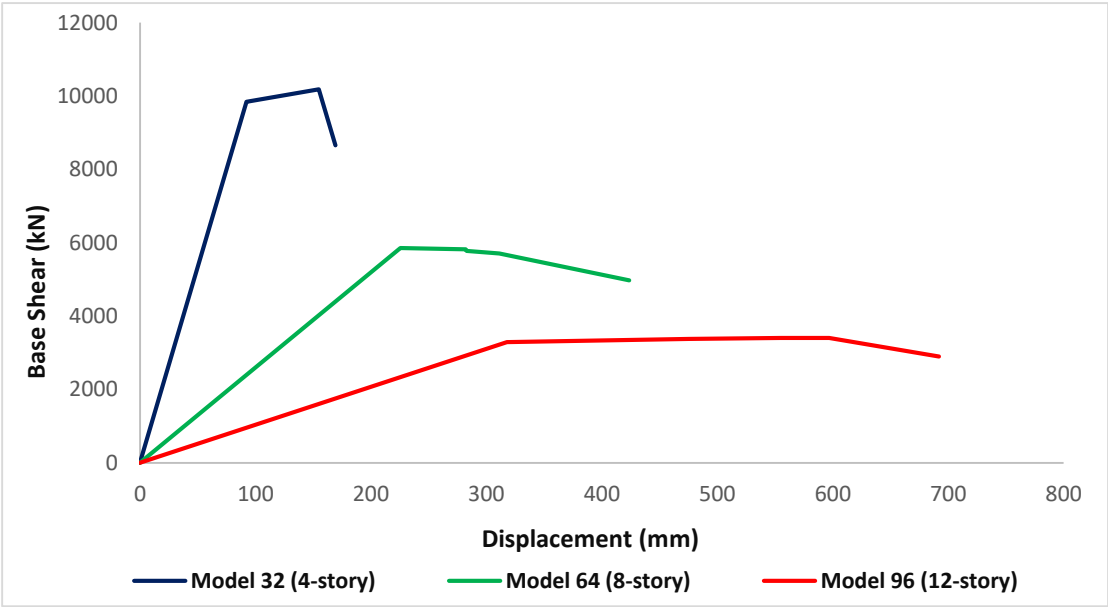

Figure 4.9: The impact of the various number of stories on the capacity curve at shear wall thickness (300mm) and shear wall position (middle)

c) The effect of the compressive strength ($f'c$) on ductility value and the capacity curves

The difference in compressive strength ($f'c$) has been known as one of the main significant variables that influence the behavior and ductility values of the building and therefore it is understood that either the compressive strength changes negatively or positively impacts the value of ductility. The ductility values with variations in compressive strength ($f'c$) at shear wall thickness (250 mm) and shear wall position (edge) are shown in Table 4.11 and Figure 4.10, and the ductility values with variations in compressive strength at shear wall thickness (300 mm) and shear wall position (middle) are seen in Table 4.12 and Figure 4.11, and the difference in capability is demonstrated in Figure 4.12 and Figure 4.13.

As illustrated in Table 4.11 and Figure 4.10, compressive strength changes from $250\ kgf/cm^2$ to $300\ kgf/cm^2$ at shear wall thickness (250mm) and shear wall position (edge) generate a reduction in ductility rates by 7% for span length 5m, 9% for span length 5.5, 13% for span length 6m, and 5% for span length 7m, and as shown in Table 4.12 and Figure 4.11 for shear wall thickness (300mm) and shear wall position (middle) when compressive strength changes from $250\ kgf/cm^2$ to $300\ kgf/cm^2$ cause a reduction in ductility value by 17% for 5m, 13% for 5.5m, 12% for 6m, 6% for 7m, and this is due to increasing the strength of the building that can reduce the ductility so its good point.

Also as shown in Figure 4.12 and Figure 4.13, compressive strength changes from $250\ kgf/cm^2$ to $300\ kgf/cm^2$ yield displacement (Δ_y) would increase and a reduction in ultimate displacement (Δ_m) will lead to a decrease in ductility value and cause an increase in ultimate base shear.

Used parameters in this section: number of stories = 8-stories (mid-rise building), shear wall thickness = 250 mm and shear wall position = edge, shear wall thickness = 300mm and shear wall position = middle

Table 4.11: Results of values of ductility of buildings with different compressive strengths at shear wall thickness (250mm) and shear wall position (edge)

Span length	Compressive strength	
	$\mathbf{250\ kgf/cm^2}$	$\mathbf{300\ kgf/cm^2}$
5m	3.23	3.00
5.5m	3.55	3.22
6m	3.92	3.40
7m	4.46	4.25

Table 4.12: Results of values of ductility of buildings with different compressive strengths at shear wall thickness (300mm) and shear wall position (middle)

Span length	Compressive strength	
	$\mathbf{250\ kgf/cm^2}$	$\mathbf{300\ kgf/cm^2}$
5m	2.60	2.16
5.5m	2.77	2.42
6m	2.96	2.61
7m	3.35	3.16

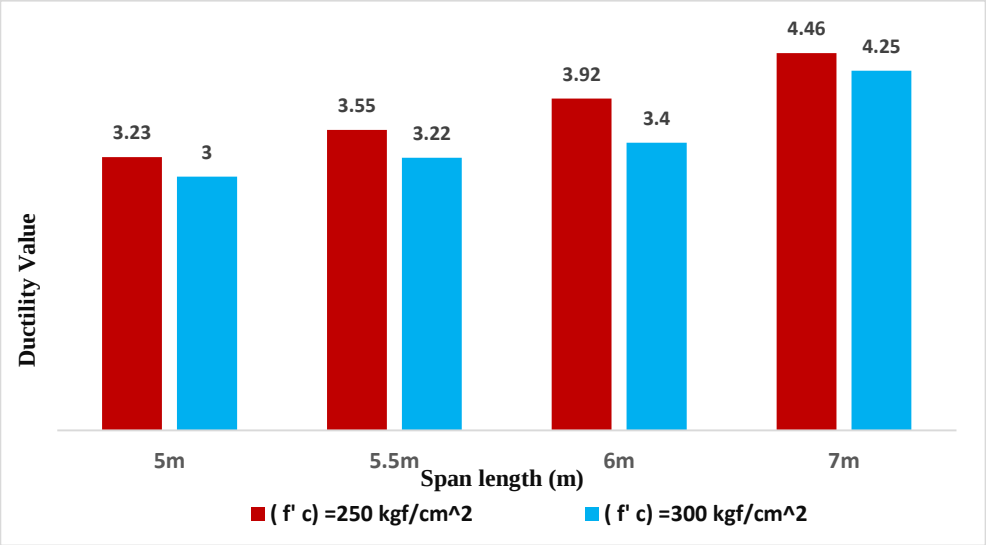

Figure 4.10: Comparison between the values of ductility of different compressive strengths at shear wall thickness (250mm) and shear wall position (edge)

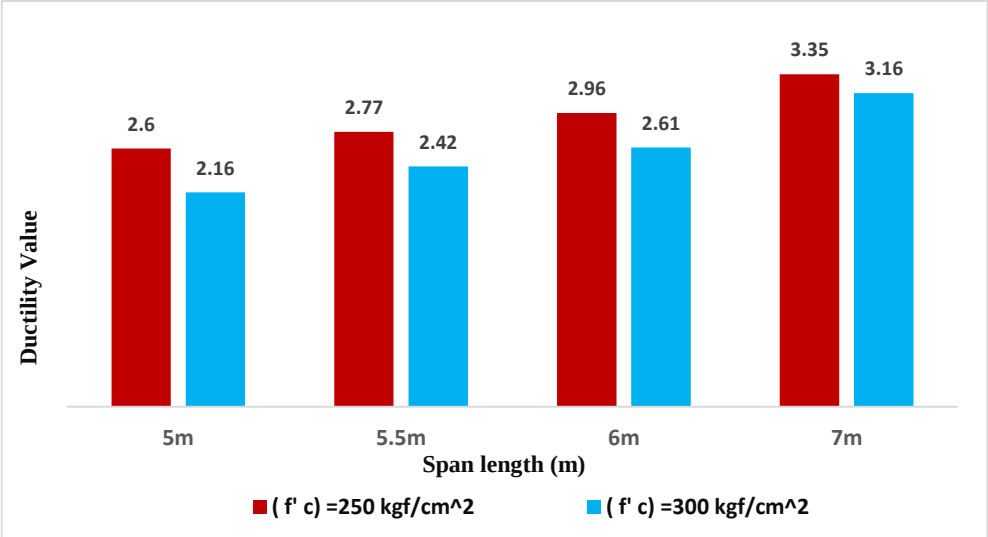

Figure 4.11: Comparison between the ductility values of different compressive strengths at shear wall thickness (300mm) and shear wall position (middle)

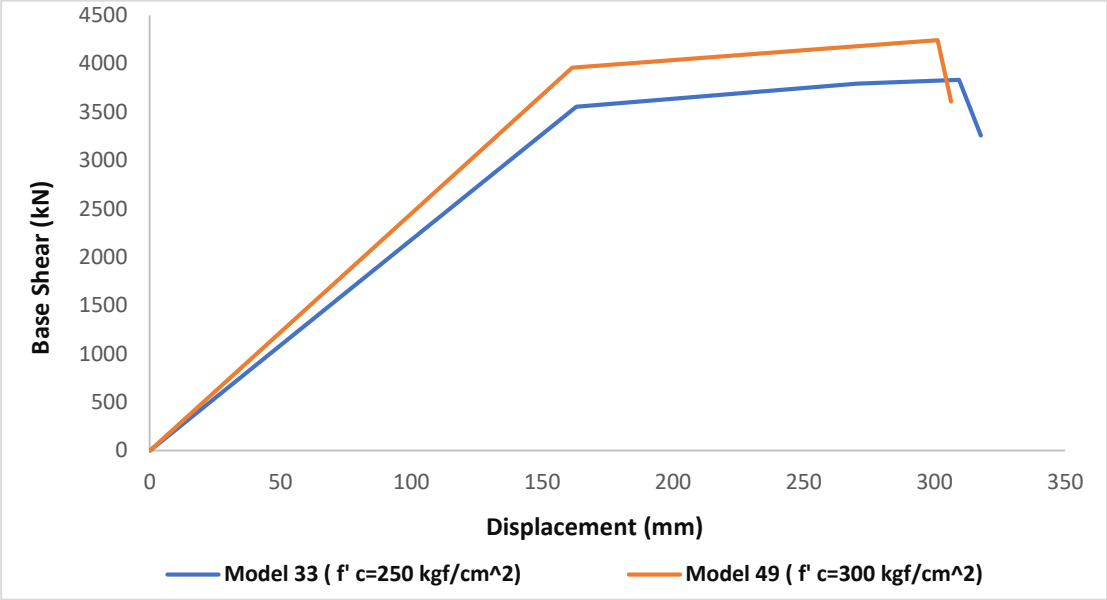

Figure 4.12: The impact of the different compressive strengths on capacity curve at shear wall thickness (250mm) and shear wall position (edge)

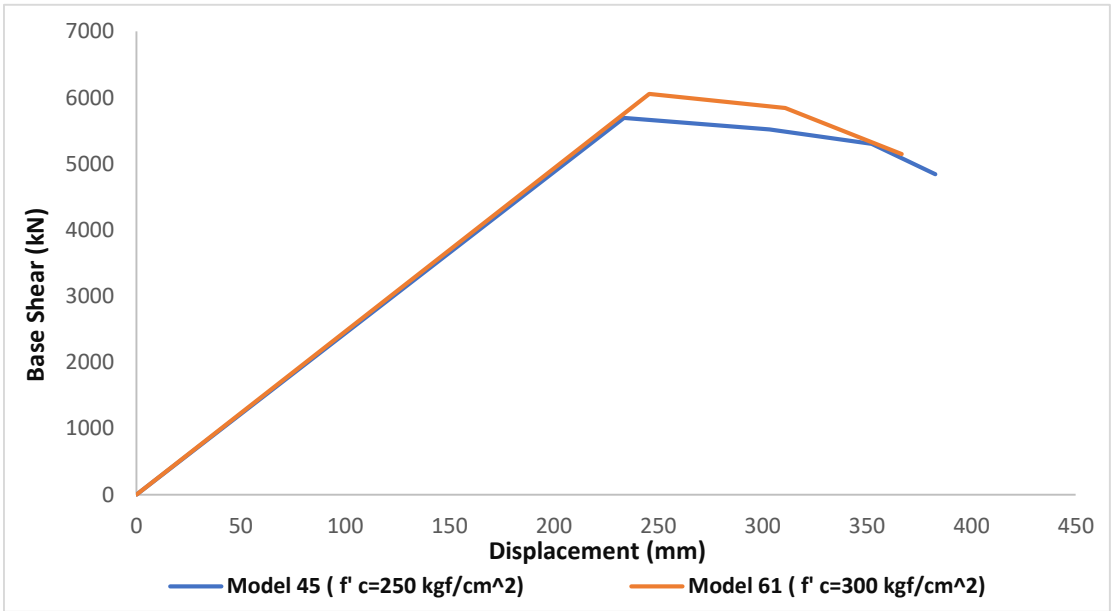

Figure 4.13: The impact of the different compressive strengths on capacity curve at shear wall thickness (300mm) and shear wall position (middle)

4.3.2 The effect of the difference in the shear wall thicknesses on ductility value

An investigation on the effect of the various shear wall thicknesses on the ductility value has been presented in this section. This segment contains two parts; the first part addresses the effect on ductility value of various shear wall thicknesses with compressive strength of 250 kgf/cm^2, part 2 describes the effect on values of ductility of various shear wall thicknesses with compressive strength of 300 kgf/cm^2.

a) ***The effect of the difference in the shear wall thicknesses on ductility value and the capacity curve with compressive strength*** $\mathbf{250\ kgf/cm^2}$

One of the most significant variables that influence the ductility and action of the building is the variation in shear wall thickness. Table 4.13 and Figure 4.14 indicate the ductility rates at various shear wall thicknesses with compressive strength ($f'c$) 250 kgf/cm^2 and Figure 4.15 shows the difference in capability (pushover) curve with compressive strength ($f'c$) 250 $kgf/cm^2$for various shear wall thicknesses.

As can be seen in Table 4.13 and Figure 4.14, as shear wall thickness increases from 250 mm to 300 mm, a drop in ductility value will occur by 15% for 4-story and 16%, 28% for 8-story and 12-story respectively this was due to stiffness of the building by increasing thickness of shear wall, and as shown by the Figure 4.15, while rising shear wall thickness from 250 mm to 300 mm, yield displacement (Δ_y) will increase and a decrease in ultimate displacement (Δ_m) will occur that is contributed to a decline in ductility values, and a rise in shear wall thickness causes maximum base shear to increase.

Used parameters in this section: compressive strength ($f'c$) = 250 kgf/cm^2, span length = 5m, shear wall position = middle, number of stories for pushover curve = 8-stories (mid-rise building)

Table 4.13: Results of values of ductility of buildings with different shear wall thicknesses at compressive strengths ($f'c$) 250 kgf/cm^2

No. of stories	Shear wall thickness	
	250 mm	300 mm
4-story	2.19	1.87
8-story	3.08	2.60
12-story	4.31	3.12

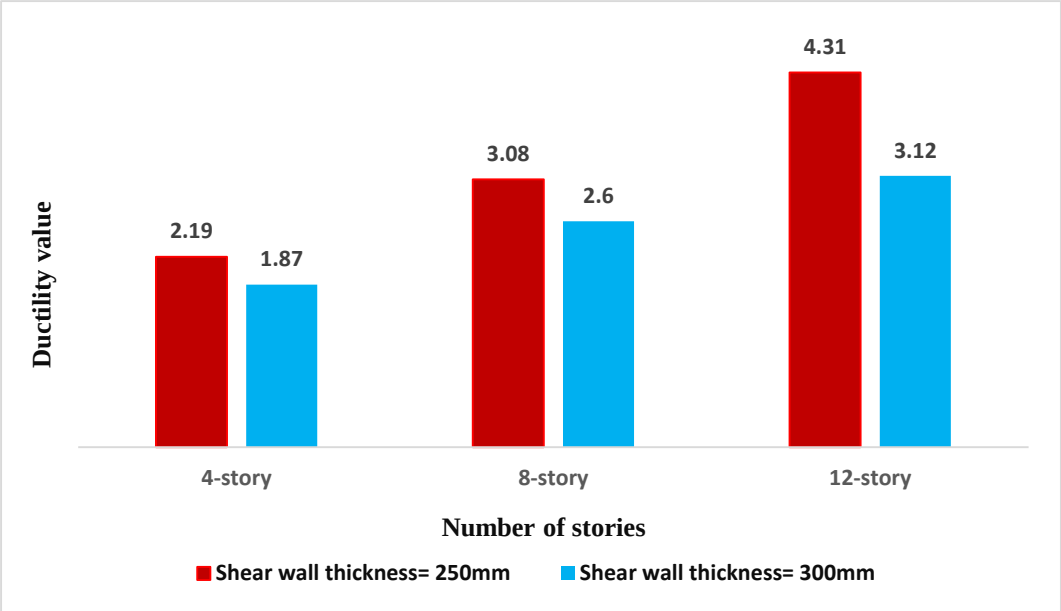

Figure 4.14: Comparison of the ductility values of different thicknesses of shear wall at compressive strength 250 kgf/cm^2

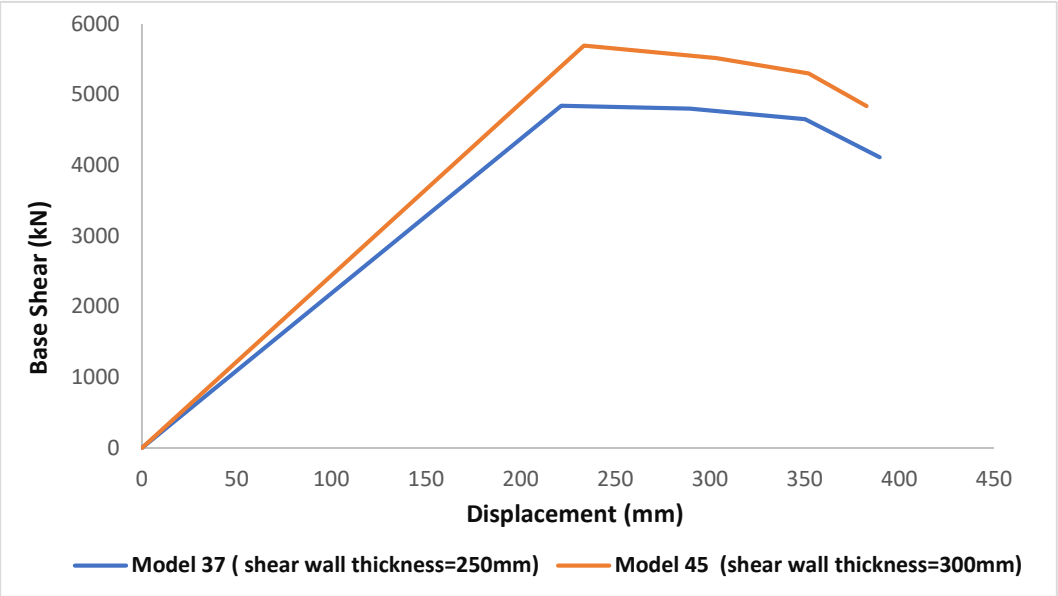

Figure 4.15: The impact of the different thicknesses of shear wall at compressive strengths 250 kgf/cm^2 on a capacity curve

b) The effect of the difference in the shear wall thicknesses on ductility value and the capacity curve with compressive strength $\mathbf{300\ kgf/cm^2}$

Table 4.14 and Figure 4.16 illustrates the values of ductility at different shear wall thicknesses with compressive strength of 300 kgf/cm^2 and Figure 4.17 displays the difference in the capacity (pushover) curve for different shear wall thicknesses with compressive strength ($f'c$) 300 kgf/cm^2.

As seen in the Table 4.14 and Figure 4.16, while shear wall thickness increases from 250mm to 300mm, a decline in ductility value will occur by 7% for low-rise, 19% for mid-rise, and 25% for high-rise building, and this decreasing percentage is because of increased stiffness of the buildings. As seen in Figure 4.17, by increasing shear wall thickness from 250mm to 300mm, yield displacement (Δ_y) will rise and a decrease in maximum displacement (Δ_m) will occur that's resulted in a reduction in ductility values, and increasing shear wall thickness causes an increase in maximum base shear.

Used parameters in this section: compressive strength ($f'c$) = 300 kgf/cm^2, span length = 5m, shear wall position = middle, number of stories for pushover curve = 8-stories (mid-rise building)

Table 4.14: Results of values of ductility of buildings with different shear wall thicknesses at compressive strengths ($f'c$) 300 kgf/cm^2

No. of stories	Shear wall thickness	
	250 mm	300 mm
4-story	1.92	1.79
8-story	2.67	2.16
12-story	4.01	3.02

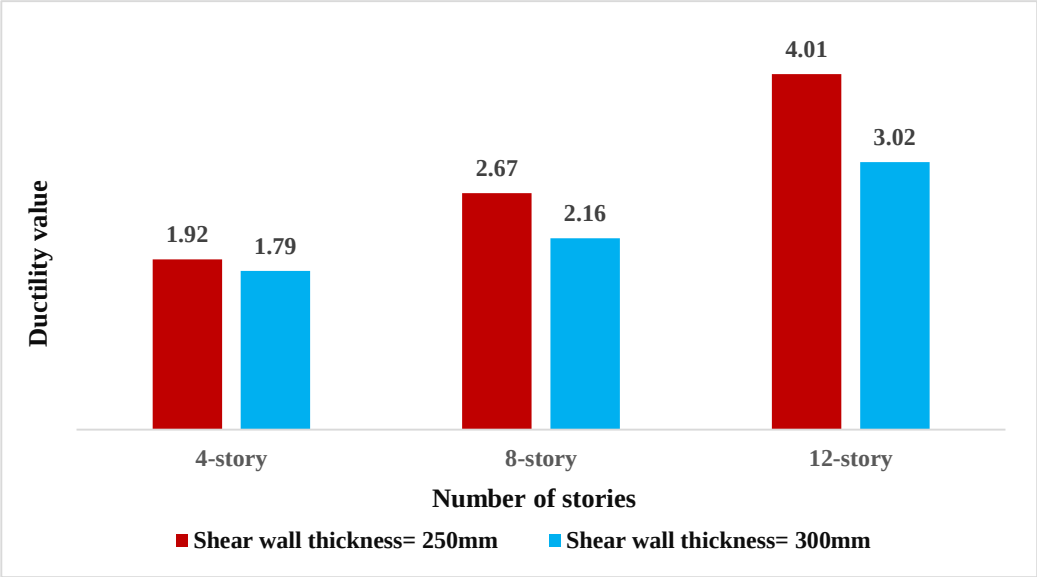

Figure 4.16: Comparison between the values of ductility for different thicknesses of shear wall at compressive strength 300 kgf/cm^2

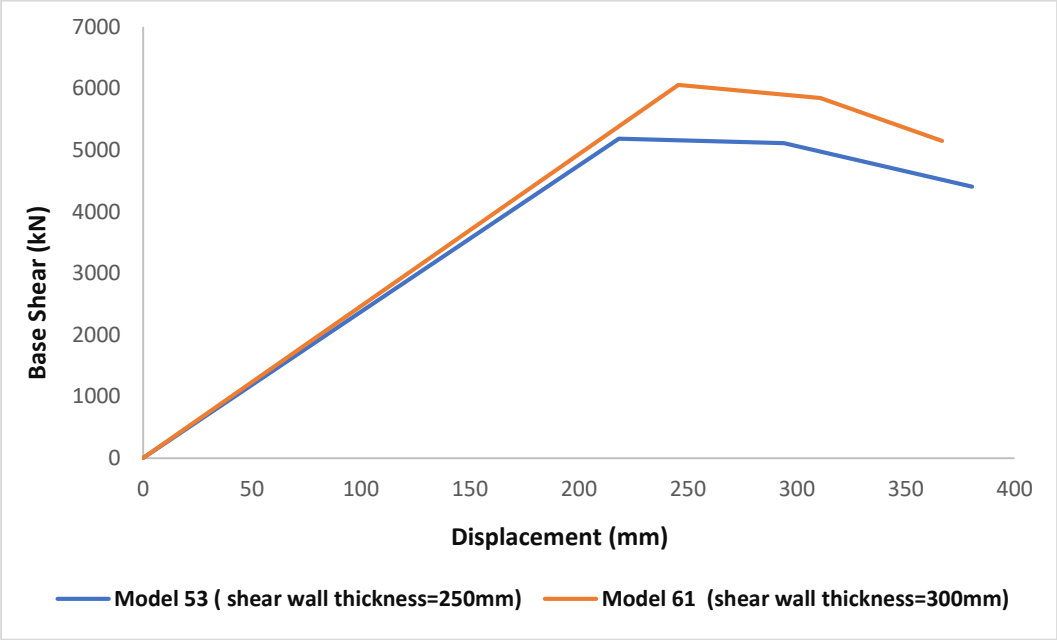

Figure 4.17: The impact of the different thicknesses of shear wall at compressive strengths 300 kgf/cm^2 on a capacity curve

4.3.3 The effect of the difference in the shear wall positions on ductility value

This section provides a study of the effect on the ductility value of the various positions of the shear wall. This segment contains two parts, the first part addresses the effect on ductility value of various shear wall positions having compressive strength of 250 kgf/cm^2, the second part describes the effect on ductility value of different shear wall positions having a compressive strength of 300 kgf/cm^2.

a) The effect of the different positions of shear wall on ductility value and the capacity curve with compressive strength $\mathbf{250\ kgf/cm^2}$

It is very important to performing shear walls in an appropriate position of buildings that can affect the performance of buildings when exposed to seismic loads. Table 4.15 and Figure 4.18 demonstrates the values of ductility at different shear wall positions with compressive strength of 250 kgf/cm^2 and Figure 4.19 demonstrates the difference in the capacity

(pushover) curve for different shear wall positions with compressive strength ($f'c$) 250 kgf/cm^2.

As indicated in Table 4.15 and Figure 4.18 by changing shear wall position from edge to middle position a reduction in ductility value will happen by 20% for 4-story, by 14% for 8-story, and 22% for 12-story, the position of shear wall will effect on the stability of the building if it located in the middle it has more stiffness and more stable so ductility was decreasing when the position changed to the middle. As shown in Figure 4.19 changing the position of the shear wall from edge to middle can cause an increase in both yield displacement (Δ_y) and maximum displacement (Δ_m), and leads to an increase in maximum base shear.

Used parameters in this section: compressive strength ($f'c$) = 250 kgf/cm^2, span length = 5m, shear wall thickness = 300 mm, number of stories for pushover curve = 8-stories (mid-rise building)

Table 4.15: Results of ductility ratios of buildings with different shear wall positions having compressive strengths ($f'c$) 250 kgf/cm^2

No. of stories	Shear wall position	
	Edge	**Middle**
4-story	2.35	1.87
8-story	3.01	2.60
12-story	4.01	3.12

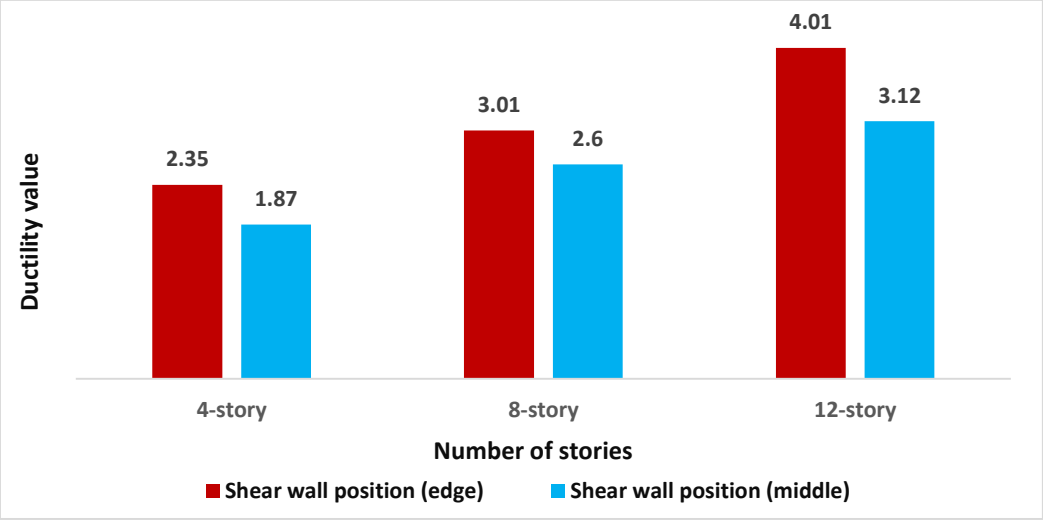

Figure 4.18: A comparison of the ductility values of different positions of shear wall with compressive strength 250 kgf/cm^2

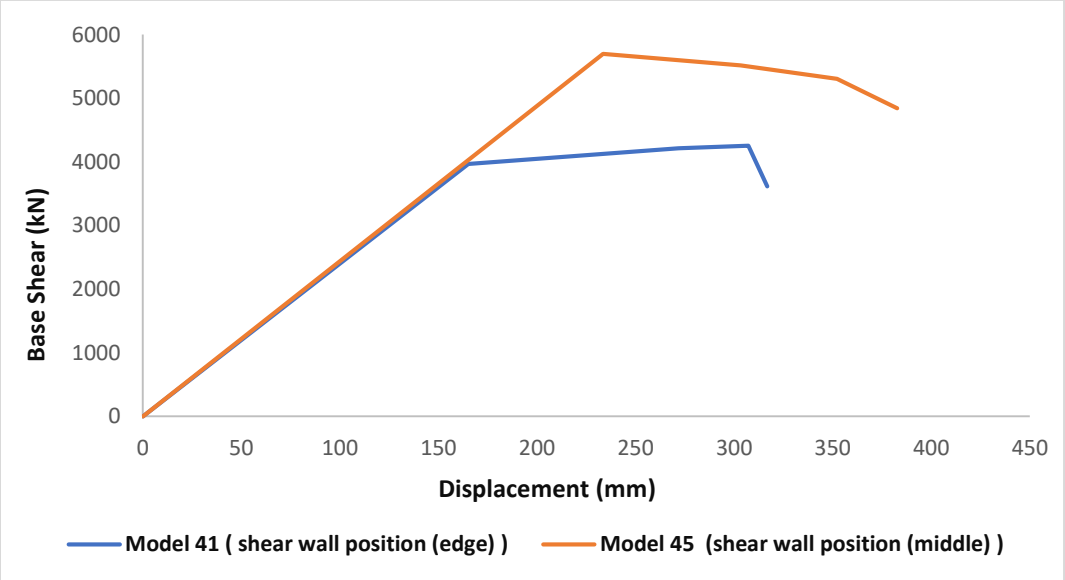

Figure 4.19: The impact of the different positions of shear wall with compressive strengths 250 kgf/cm^2 on a capacity curve

b) The effect of the different positions of shear wall on ductility value and the capacity curve with compressive strength $300\ kgf/cm^2$

The ductility values at different shear wall positions with compressive strength $300\ kgf/cm^2$ are shown in Table 4.16 and Figure 4.20, and the difference in the capacity (pushover) curve for different positions of shear wall with compressive strength ($f'c$) $300\ kgf/cm^2$ shown in Figure 4.21.

As shown in Table 4.16 and Figure 4.20, a decrease in ductility value will occur when the position of shear walls shifts from edge to middle by 19% for 4-story, by 23% for 8-story, and 24% for 12-story, this is due to the position of shear wall that will effect on the stability of the building if it located in the middle it has more stiffness and more stable so ductility was decreased when the position changed to the middle. As seen in Figure 4.21, a change in shear wall position from edge to middle causes an increase in both yield displacement (Δ_y), and ultimate displacement (Δ_m), and a change in shear wall position from edge to middle induces an increase in maximum base shear.

Used parameters in this section: compressive strength ($f'c$) = 300 kgf/cm^2, span length = 5m, shear wall thickness = 300 mm, number of stories for pushover curve = 8-stories (mid-rise building)

Table 4.16: Results of ductility ratios of buildings with different shear wall positions at compressive strengths ($f'c$) $300\ kgf/cm^2$

No. of stories	Shear wall position	
	Edge	**Middle**
4-story	2.21	1.79
8-story	2.80	2.16
12-story	3.95	3.02

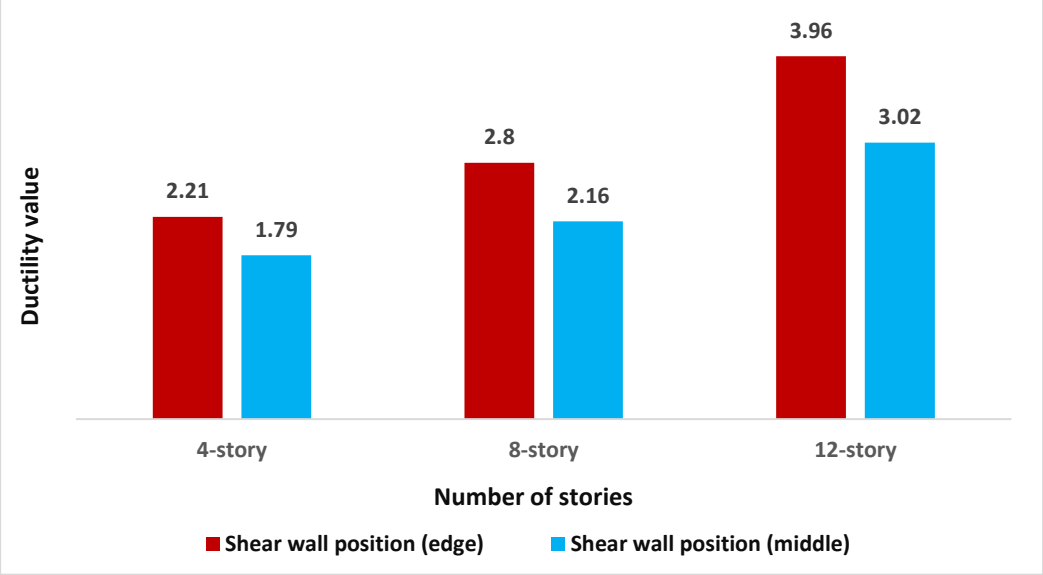

Figure 4.20: A comparison of the ductility values of different positions of shear wall with compressive strength 300 kgf/cm^2

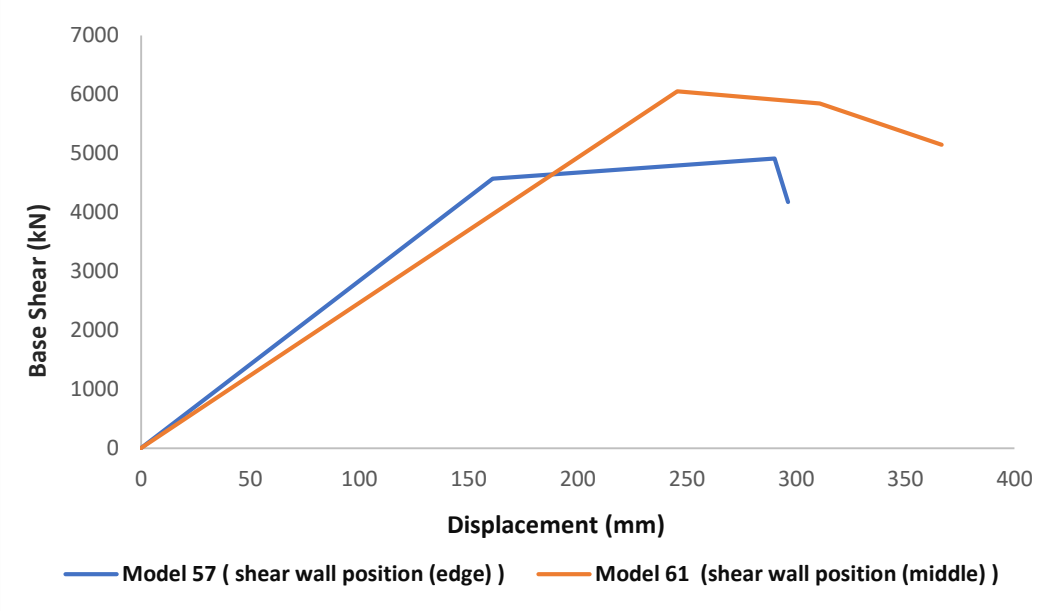

Figure 4.21: The impact of the different positions of shear wall with compressive strengths 300 kgf/cm^2 on a capacity curve

CHAPTER 5
CONCLUSIONS AND RECOMMENDATIONS

5.1 Conclusions

Throughout this research, the 2D dual system (MRFSW) was investigated. To determine the ductility value, ultimate displacement, yield displacement, and maximum base shear, the models of RC structures were designed and evaluated for different shear wall thicknesses and positions. 96 ETABS models are developed and analyzed after that pushover curves are withdrawn to evaluate all requested variables. The impacts of all parameters have been examined, assessed, and compared after obtaining pushover curves, then the influence of various parameters had been clarified, the important parameter in this analysis is the impact of shear wall thickness and position, other parameters involving different number of stories, span length, and compressive strength. The detailed conclusion of this study is as follows, depending on the outcomes achieved:

- When span length increases with different thicknesses and positions of shear wall causes increasing ductility value.
- Increasing span length causes an increase in ductility value for low, mid, and high-rise models for all used parameters.
- When span length increase allows a reduction in yield displacement (Δ_y) and increase in maximum displacement (Δ_m) to (4) stories, (8) stories, and (12) stories with different positions and thicknesses of shear wall.
- Maximum base shear (V_m) for all used parameters decreases when span length is increased for low-rise buildings and more decreases for mid, and high-rise models.

- By changing story numbers at low to mid, and high-rise RC structures ductility value increased for all different parameters.

- The increasing ratio of ductility in models of high-rise is higher than low and mid-rise building structures including different shear wall thicknesses and positions.
- An increase in both yield displacement (Δ_y) and ultimate displacement (Δ_m) will happen during an increasing number of stories from (4) stories to (8) stories, and (12) stories for all used parameters.
- The increasing number of stories causes a decrease in maximum base shear (V_m) with various shear wall thicknesses and positions for all parameters.

- When compressive strength ($f'c$) changes from 250 kgf/cm^2 to 300 kgf/cm^2 causes a decrease in ductility value for different numbers of stories and other parameters.
- Yield displacement (Δ_y) would increase and a reduction in ultimate displacement (Δ_m) would happen by increasing compressive strength for different thicknesses and positions of the shear wall.
- Changing compressive strength ($f'c$) from 250 kgf/cm^2 to 300 kgf/cm^2 leads an increase in maximum base shear (V_m) for various thicknesses and positions of shear and all other parameters.

- When increasing shear wall thickness from 250mm to 300mm, ductility value would decrease for different number of stories. And this reduction in low-rise building is much more than the models with more stories.
- While rising shear wall thickness from 250 mm to 300 mm, yield displacement (Δ_y) will increase and a decrease in ultimate displacement (Δ_m) would occur that is contributed to a reduction in ductility values.
- Changing shear wall thickness from 250mm to 300mm causes an increase in maximum base shear (V_m). And this increase is much more in less number of stories.
- Ductility rate was noticed to decrease in both shear wall positions and other parameters by increasing shear wall thickness.

- The ductility value of the buildings decreases by changing shear wall position from (edge) to (middle) in both thicknesses of shear wall and other parameters, this reduction was more in the case of more stiff buildings.
- Changing the position of shear wall from (edge) to (middle) can cause an increase in both yield displacement (Δ_y) and maximum displacement (Δ_m),
- When shear wall position changes from (edge) to (middle) an increase in maximum base shear (V_m) would occur in both thicknesses of shear wall and other used parameters.
- The reduction in the ductility rate of the building having less number of stories is higher than the buildings have more number of stories, by changing position of shear wall from (edge) to (middle).

- Locating a shear wall in the middle of the building is better than locating it in the edge in case of ductility influence.
- Increasing shear wall thickness was a good reason to decrease the ductility of the buildings considering suitable parameters.
- The stiffness of the building has the most effect on the ductility of the buildings including all used parameters.

5.2 Recommendations

i. In this study 2D models of RC structures are used, the 3D models and steel structures can be studied.

ii. The models that are used in this study is only dual system (MRFSW) the other structural systems can be considered in the future studies.

iii. Shear walls were without openings, the openings in the shear walls can be considered in future studies.

iv. The number of spans that are used are 5 spans and the same spans, so more number of spans and different spans also should be used in future researches.

v. The (4) stories, (8) stories, and (12) stories models have been used throughout this study, also the yield strength effect on ductility is not used through this study, so more stories and the effect of yield strength can be considered in future studies.

REFERENCES

Abhilash, R., & Biju, V. (2010). Effect of lateral load patterns in pushover analysis. *10th National Conference on Technological Trends.*

Anshuman, S., Dipendu, B., & Bhavin, R. (2011). Solution of shear wall location in Multi-storey building. *International Journal of Civil & Structural Engineering*, *2*(2), 493-506.

ASCE (American Society of Civil Engineers). (2010). Minimum Design Loads and associated criteria for Buildings and Other Structures, Standard ASCE/SEI 7–10. Reston, VA: ASCE.

BABU, N. J., Balaji, K. V. G. D., & Gopalaraju, S. S. S. V. (2012). Pushover analysis of unsymmetrical framed structures on sloping ground. *International Journal of Civil, Structural, Environmental and Infrastructure Engineering Research and Development (IJCSEIERD), 2*(4), *45-54*.

Bertagnoli, G., Giordano, L., La Mazza, D., & Mancini, G. (2016). Reinforced Concrete Frame Structures. *Procedia engineering*, *161*, 1013-1017.

Carrillo, J., González, G., & Rubiano, A. (2014). Displacement ductility for seismic design of RC walls for low-rise housing. *Latin American Journal of Solids and Structures, 11*(4), 725-737.

Chandiwala, A. (2012). Earthquake analysis of building configuration with different position of shear wall. *International Journal of Emerging Technology and Advanced Engineering, 2*(12), 391-399.

Chou, C. C., Tsai, W. J., & Chung, P. T. (2016). Development and validation tests of a dual-core self-centering sandwiched buckling-restrained brace (SC-SBRB) for seismic resistance. *ScienceDirect*, 121(15), 30-41.

Dhileep, M., Trivedi, A., & Bose, P. R. (2011). Behavior of high frequency modal responses in nonlinear seismic analysis. *International Journal of Civil and Structural Engineering, 1*(4), 723.

Fahjan, Y. M., Kubin, J., & Tan, M. T. (2010, August). Nonlinear analysis methods for reinforced concrete buildings with shear walls. In *14th European Conference on Earthquake Engineering*, 17(7), 156-172.

Furtado, A., Rodrigues, H., Arêde, A., Varum, H., Grubišić, M., & Šipoš, T. K. (2018). Prediction of the earthquake response of a three-story infilled RC structure. *Engineering Structures*, *171*, 214-235.

Ghaffarzadeh, H., Talebian, N., & Kohandel, R. (2013). Seismic demand evaluation of medium ductility RC moment frames using nonlinear procedures. *Earthquake Engineering and Engineering Vibration*, *12*(3), 399-409.

Ghasemi Jouneghani, H., Haghollahi, A., Moghaddam, H., & Sarvghad Moghadam, A. (2016). Study of the seismic performance of steel frames in the elliptic bracing. *Journal of Vibroengineering*, *18*(5), 2974-2985.

Huang K and Kuang JS (2010), "On the Applicability of Pushover Analysis for Seismic Evaluation of Medium- and High-rise Buildings," *The Structural Design of Tall and Special Buildings*, 19: 573–588

Jamnani, H. H., Amiri, J. V., & Rajabnejad, H. (2018). Energy distribution in RC shear wall-frame structures subject to repeated earthquakes. *Soil Dynamics and Earthquake Engineering*, *107*, 116-128.

Kadid, A., & Boumrkik, A. (2008). Pushover analysis of reinforced concrete frame structures. *Asian Journal of Civil Engineering*, *9*(1), 75-83.

Kaplan, H., Yilmaz, S., Cetinkaya, N., & Atimtay, E. (2011). Seismic strengthening of RC structures with exterior shear walls. *Sadhana*, *36*(1), 17.

Khoshnoudian, F., Mestri, S., & Abedinik, F. (2011). Proposal of lateral load pattern for pushover analysis of RC buildings. *Computational Methods in Civil Engineering*, *2*(2), 169-183.

Lovaraju, k. (2013). Effective location of shear walls on performance of building frame subjected to lateral load. *Journal of Engineering Science and Technology, 13*(5), 1206-1215.

LovaRaju, K., & Balaji, D. K. (2015). Effective location of shear walls on performance of building frame subjected to earthquake load. *International Advanced Research Journal in Science, Engineering and Technology*, *2*(1).

LovaRaju, K., & Balaji, D. K. (2015). Effective location of shear walls on performance of building frame subjected to earthquake load. *International Advanced Research Journal in Science, Engineering and Technology*, *2*(1).

Madhu, S. (2018). Optimum location of a shear walls in a R.C building. *International Journal of Scientific & Engineering Research, 9(7*), 2229-5518.

Mantawy, A., & Anderson, J. (2015, September). Ductility of reinforced concrete frame buildings subjected to the recent New Zealand earthquakes. *International Association for Bridge and Structural Engineering, 105*(11), 1-8.

Mehta, B. B. Prof. PC Vasani. (2014). Ductility requirements for buildings. *Applied Mechanics Department*, 216, 113-122.

Omer, S., Amine, M. (2013). Seismic Design of Reinforced Concrete Structures. *Structures Congress, 1*(3), 7-29.

Ozkul, T. A., Kurtbeyoglu, A., Borekci, M., Zengin, B., & Kocak, A. (2019). Effect of shear wall on seismic performance of RC frame buildings. *Engineering Failure Analysis*, *100*, 60-75.

Rahman, M. K., Ajmal, M., Baluch, M. H., & Celep, Z. (2012). Nonlinear Static Pushover Analysis of an Eight Story RC Frame-Shear Wall Building in Saudi Arabia. *Proceedings of 15th World Conference on Earthquake Engineering*.

Rana, E. N., & Rana, S. (2014). Structural Forms Systems for Tall Building Structures. *SSRG International Journal of Civil Engineering*, *1*(4), 33-35.

Rao, G. A., Vijayanand, I., & Eligehausen, R. (2008). Studies on ductility and evaluation of minimum flexural reinforcement in RC beams. *Materials and Structures*, *41*(4), 759-771.

Ravikumara, H. S., Kulkarni, S. R., & KS, B. N. A. (2015). Study of plastic hinge formation in R.C frames with non-linear static analysis. An International Journal of Research in Engineering and Technology, 4(9), 179-182.

Rokanuzzaman, M., Farjana, K., Anik, D., Reza, S. (2017). Effective location of shear walls on performance of building frame subjected to lateral loading. *International Journal of Advances in Mechanical and Civil Engineering, 4*(6).

Sattar, S., & Liel, A. B. (2016). Seismic Performance of Nonductile Reinforced Concrete Frames with Masonry Infill Walls—II: Collapse Assessment. *Earthquake Spectra*, *32*(2), 819-842.

Sengupta, S. (2014). Study of shear walls in multi-storied buildings with different thickness and reinforcement percentage for all seismic zones in India. *International Journal of Research in Engineering and Technology (IJRET)*, *3*(11), 197-204.

Shah, M. D., & Patel, S. B. (2011). Nonlinear static analysis of RCC frames (software implementation ETABS 9.7). In *National Conference on Recent Trends in Engineering & Technology*, 1-6.

Shedid, M. T., Drysdale, R. G., & El-Dakhakhni, W. W. (2008). Ductility of reinforced concrete masonry shear walls under seismic loading. In *The 14th World conference on earthquake engineering, China*, 12-17.

Shinde, S. B., & Raut, N. B. (2016). Effect of Change in Thicknesses and Height in Shear Wall on Deflection of Multistoried Buildings. *International Journal of Civil Engineering and Technology, 7*(6), 587-591.

Tafheem, Z., & Khusru, S. (2013). Structural behavior of steel building with concentric and eccentric bracing: A comparative study. *International Journal of Civil & Structural Engineering, 4*(1), 12-19.

Tarigan, J., Manggala, J., & Sitorus, T. (2018). The effect of shear wall location in resisting earthquake. *MS&E*, *309*(1), 012077.

Teixeira, M. M., & Bernardo, L. F. A. (2018). Ductility of RC beams under torsion. *Engineering Structures*, *168*, 759-769.

Varma, V. N. K., & Kumar, U. P. (2020). Seismic response on multi-storied building having shear walls with and without openings. *Materials Today: Proceedings*, 124-135.

Venkatesh, S. V., & Bai, H. S. (2011). Effect of Internal & External Shear Wall on Performance of Building Frame Subjected to Lateral Load. *International Journal of Earth Sciences and Engineering* ISSN, 974, 571-576.

Vielma-Perez, J. C., & Mulder, M. M. (2018). Improved procedure for determining the ductility of buildings under seismic loads. *Revista Internacional de Métodos Numéricos para cálculo y diseño en Ingeniería*, *34*(1).

Wang, Z., Martinez-Vazquez, P., & Zhao, B. (2020). Pushover analysis of structures subjected to combined actions of earthquake and wind. *Engineering Structures*, *221*, 111034.

Yön, B., Sayın, E., & Onat, O. (2017). Earthquake and structural damages. *Earthquakes-Tectonics, Hazard and Risk Mitigation*, 319-339.

Zerbin, M., Aprile, A., & Spacone, E. (2020). New formulation of ductility reduction factor of RC frame-wall dual systems for design under earthquake loadings. *Soil Dynamics and Earthquake Engineering*, *138*, 106279.

APPENDICES

APPENDIX 1

Pushover curves (capacity curves) for all models at low-rise (4-story) buildings

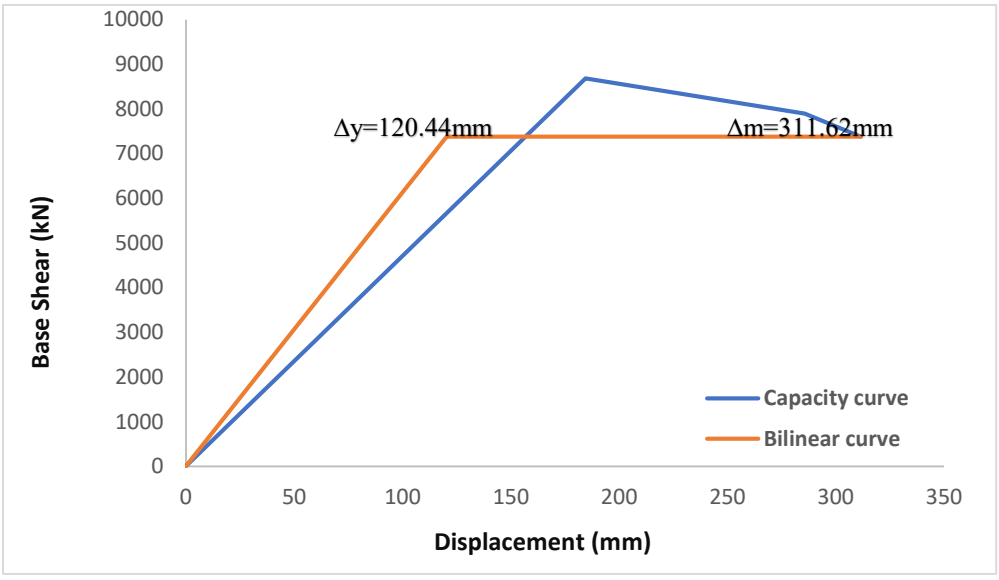

a) Model 1 (span length= 5m)

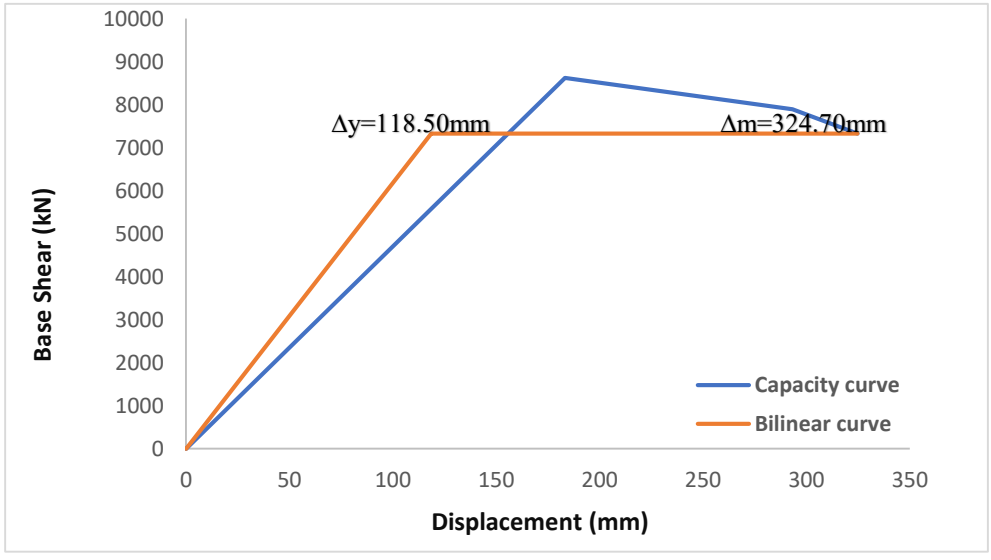

b) Model 2 (span length= 5.5m)

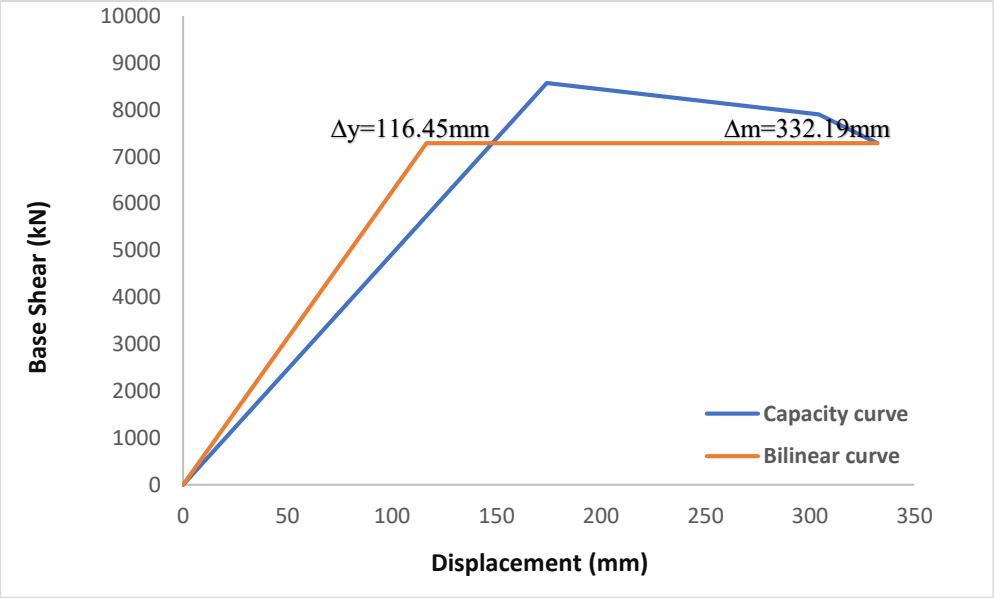

c) Model 3 (span length= 6m)

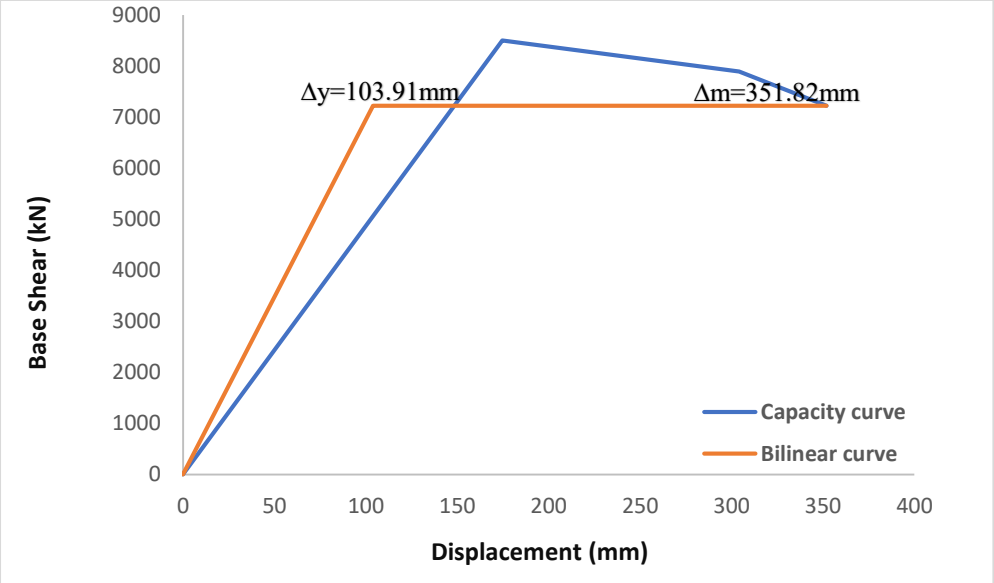

d) Model 4 (span length= 7m)

Figure A.1.1: Pushover (capacity) curve with bilinear curve for (4-story) with (($f'c$)= 250 kgf/cm^2, shear wall thickness = 250mm, shear wall position = edge)

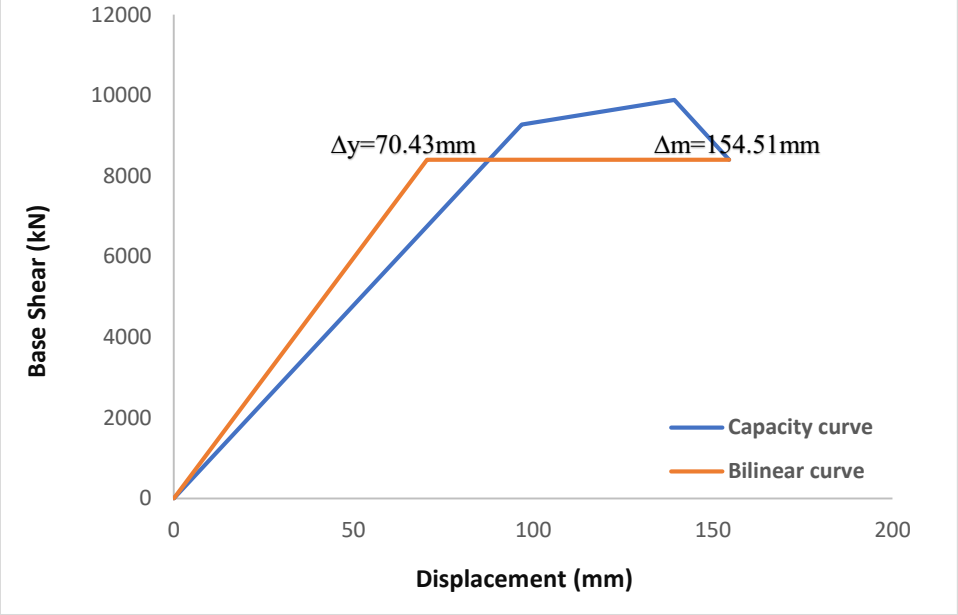

a) Model 5 (span length= 5m)

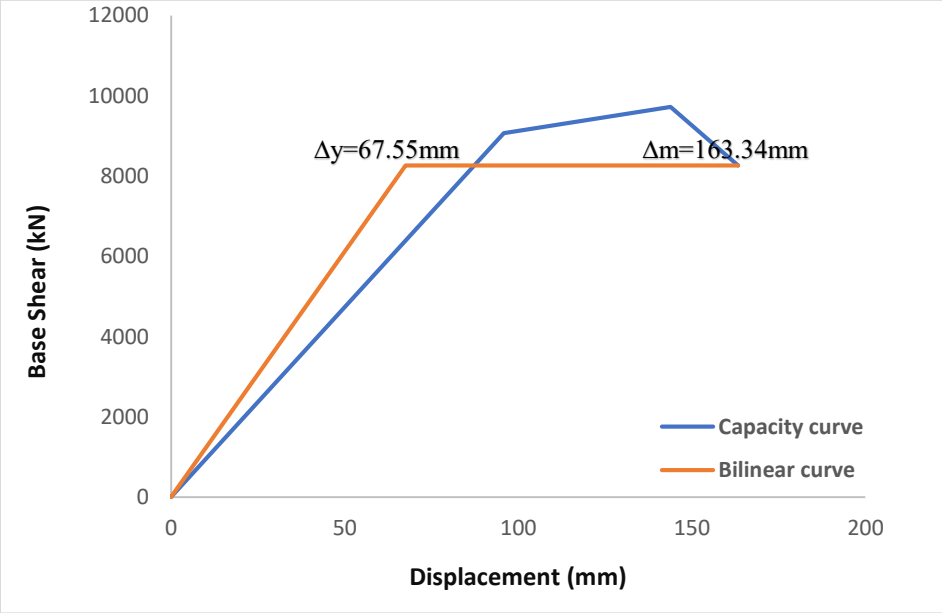

b) Model 6 (span length= 5.5m)

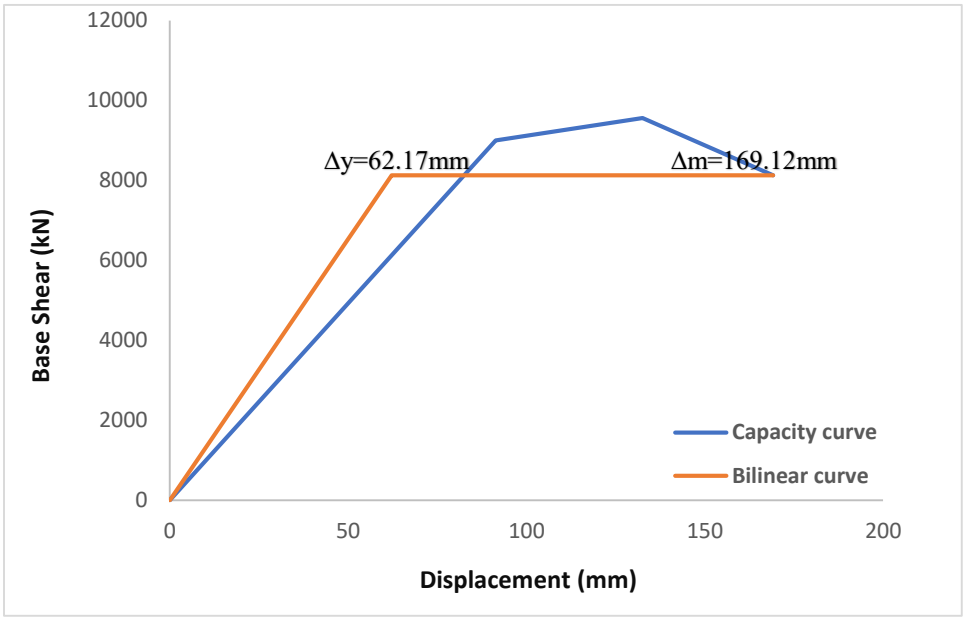

c) Model 7 (span length= 6m)

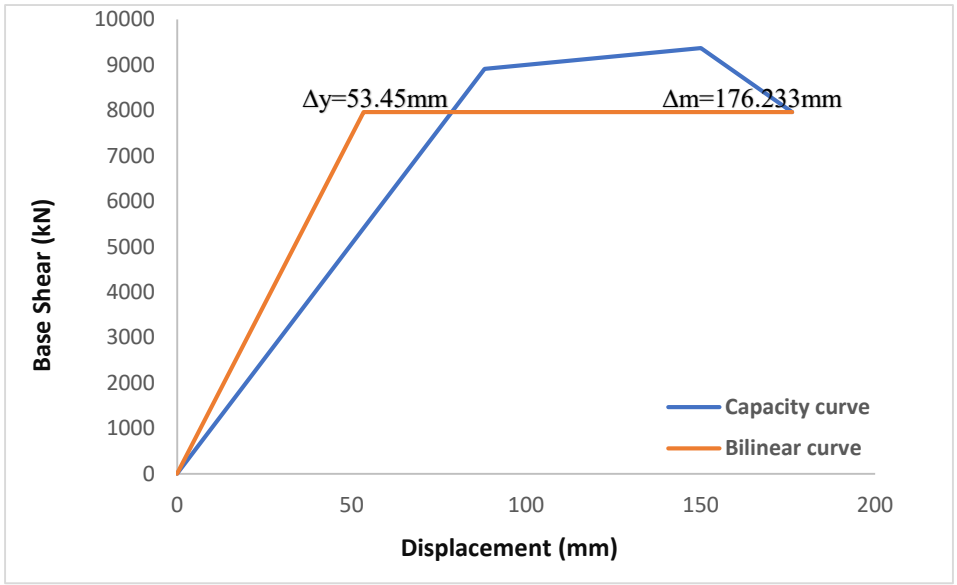

d) Model 8 (span length= 7m)

Figure A.1.2: Pushover (capacity) curve with bilinear curve for (4-story) with (($f'c$)= 250 kgf/cm^2, shear wall thickness = 250mm, shear wall position = middle)

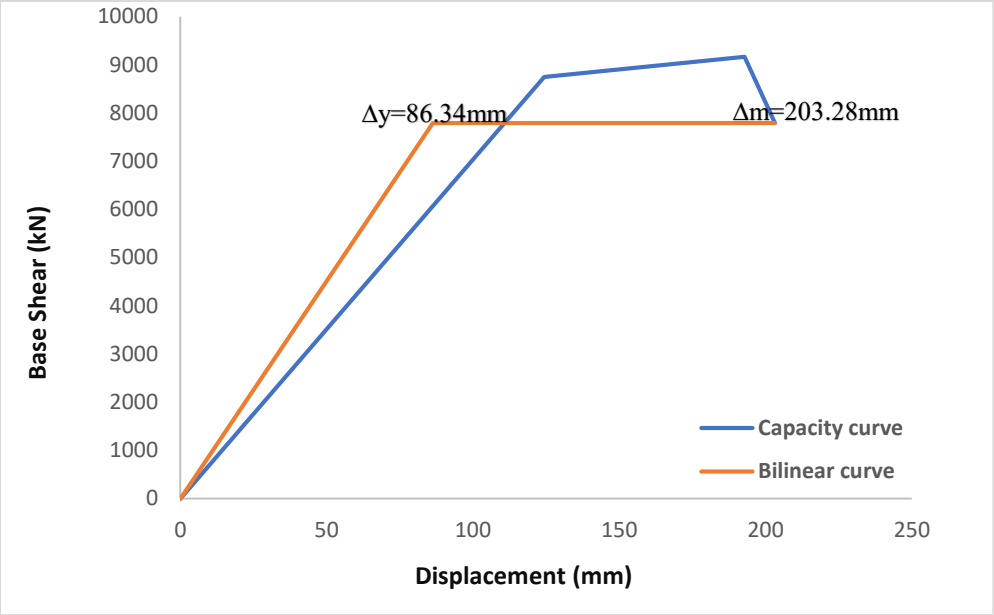

a) Model 9 (span length= 5m)

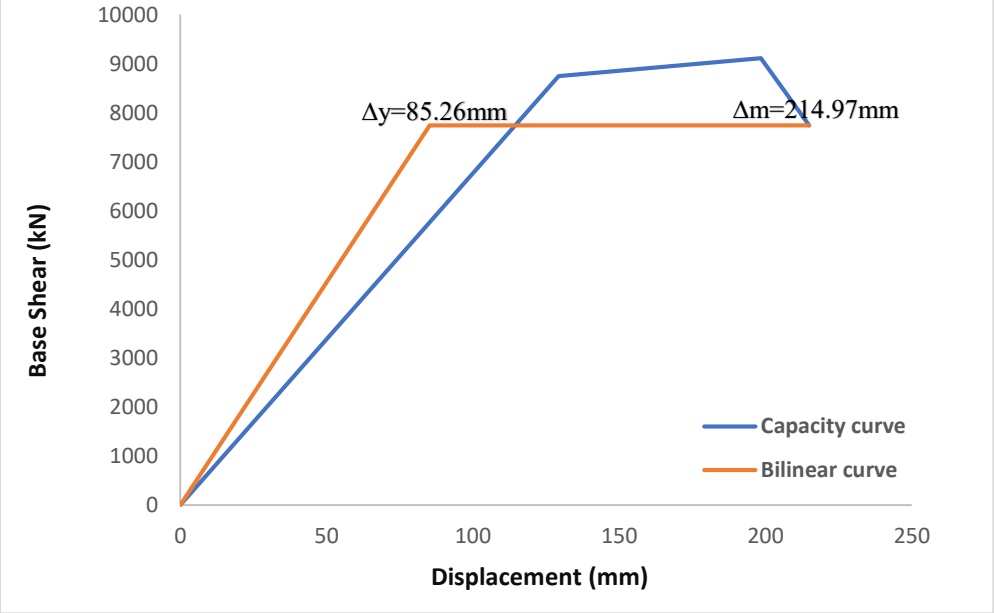

b) Model 10 (span length= 5.5m)

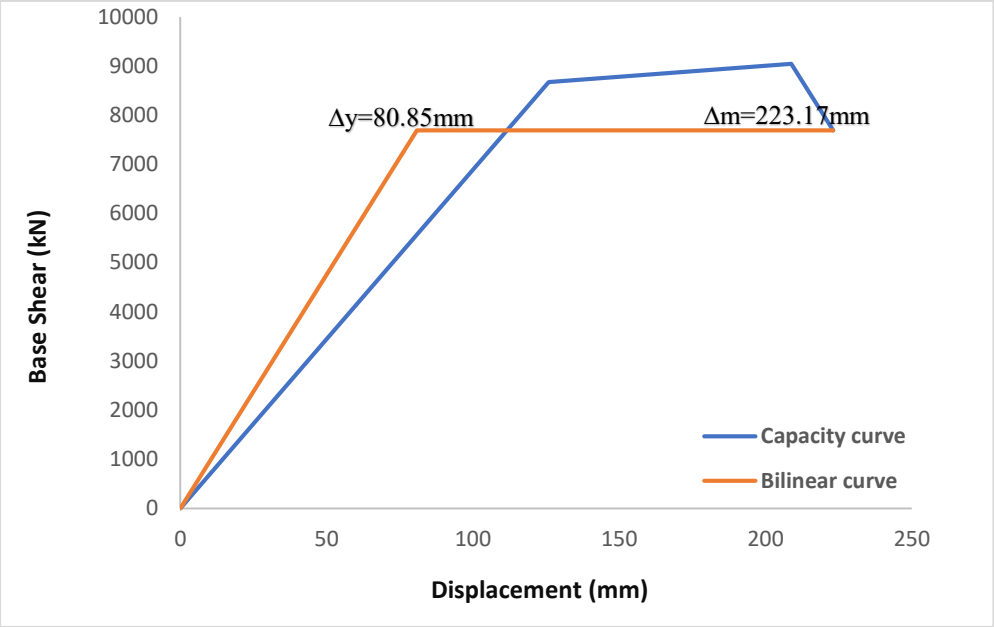

c) Model 11 (span length= 6m)

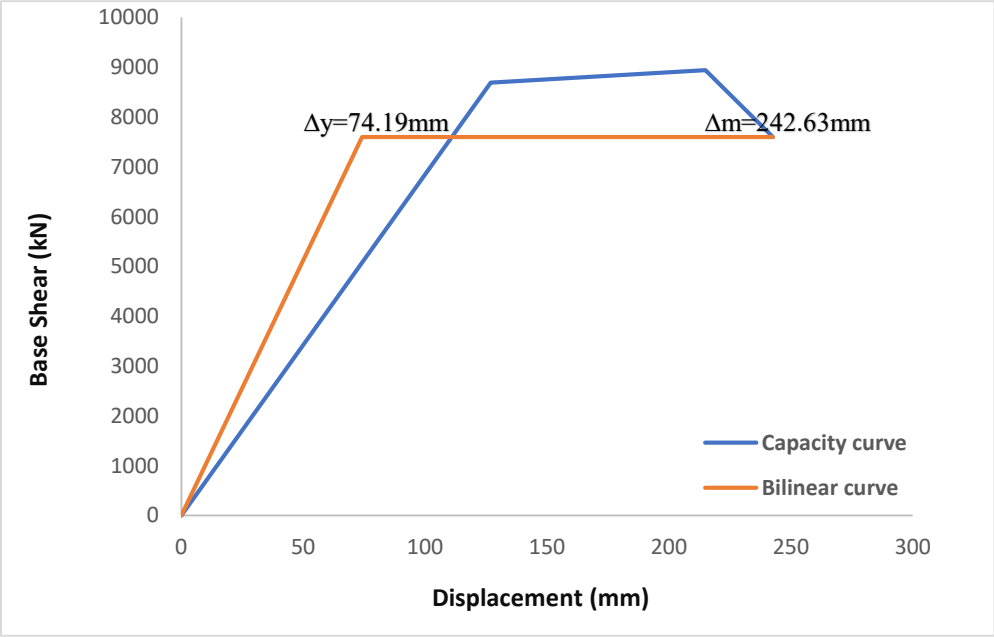

d) Model 12 (span length= 7m)

Figure A.1.3: Pushover (capacity) curve with bilinear curve for (4-story) with (($f'c$)= 250 kgf/cm^2, shear wall thickness = 300mm, shear wall position = edge)

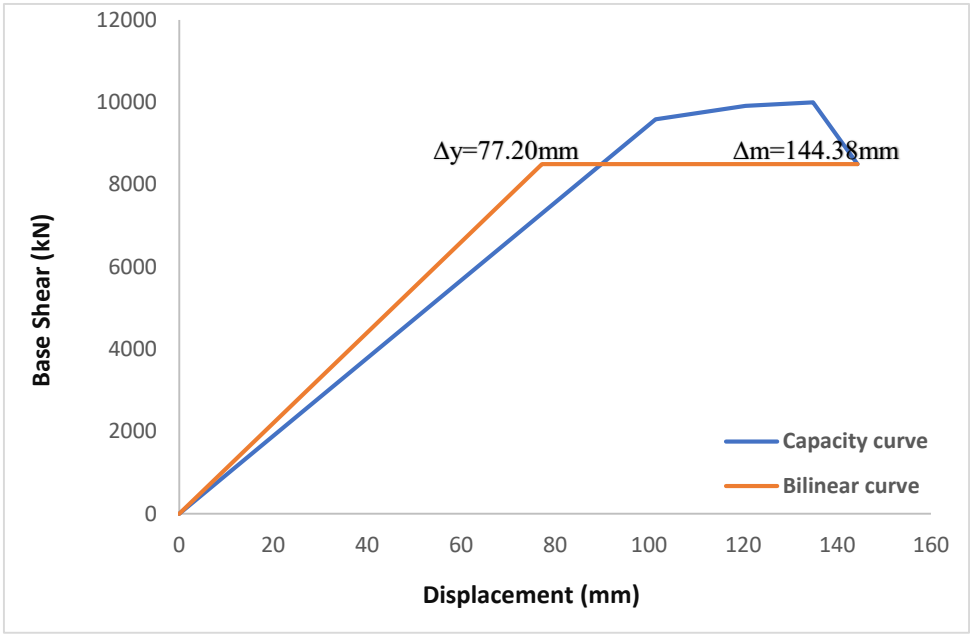

a) Model 13 (span length= 5m)

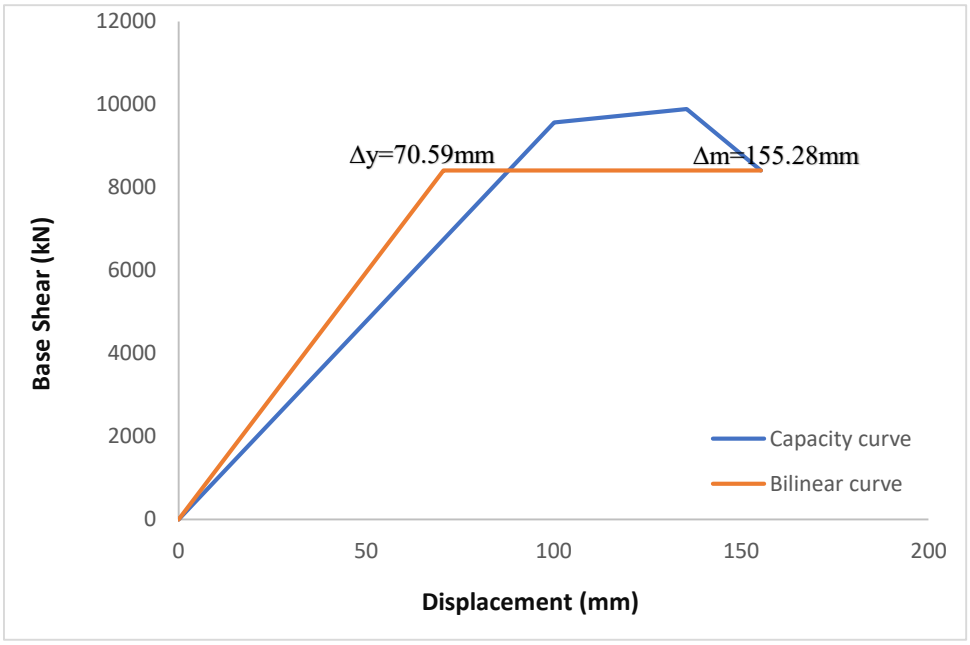

b) Model 14 (span length= 5.5m)

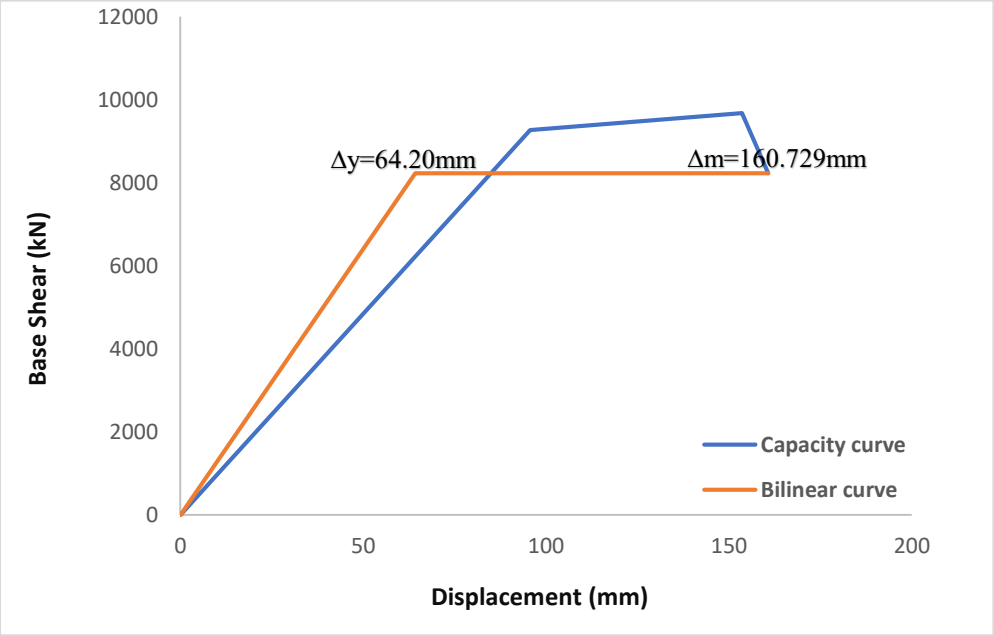

c) Model 15 (span length= 6m)

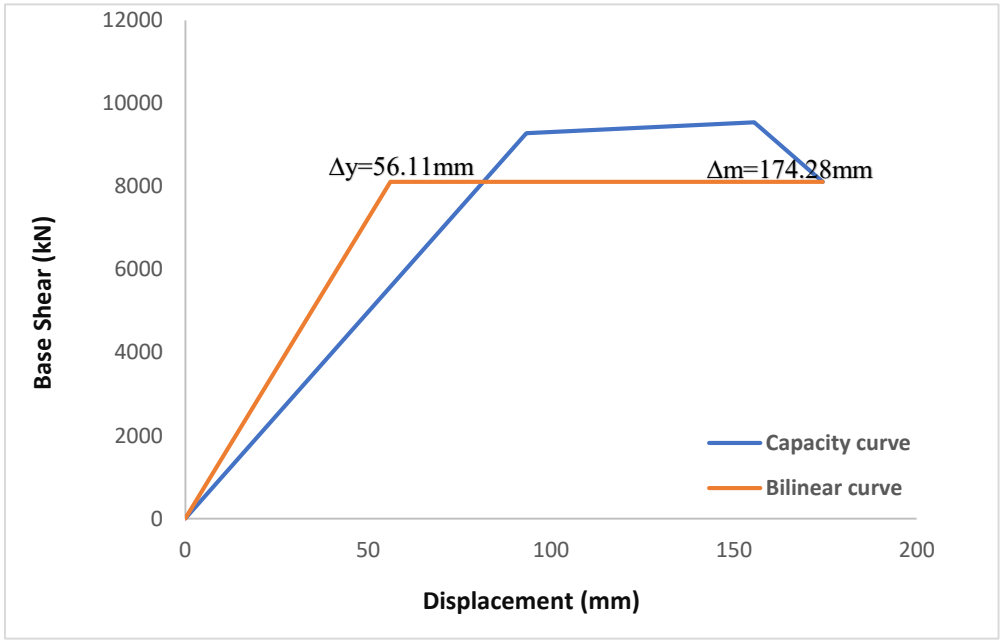

d) Model 16 (span length= 7m)

Figure A.1.4: Pushover (capacity) curve with bilinear curve for (4-story) with (($f'c$)= 250 kgf/cm^2, shear wall thickness = 300mm, shear wall position = middle)

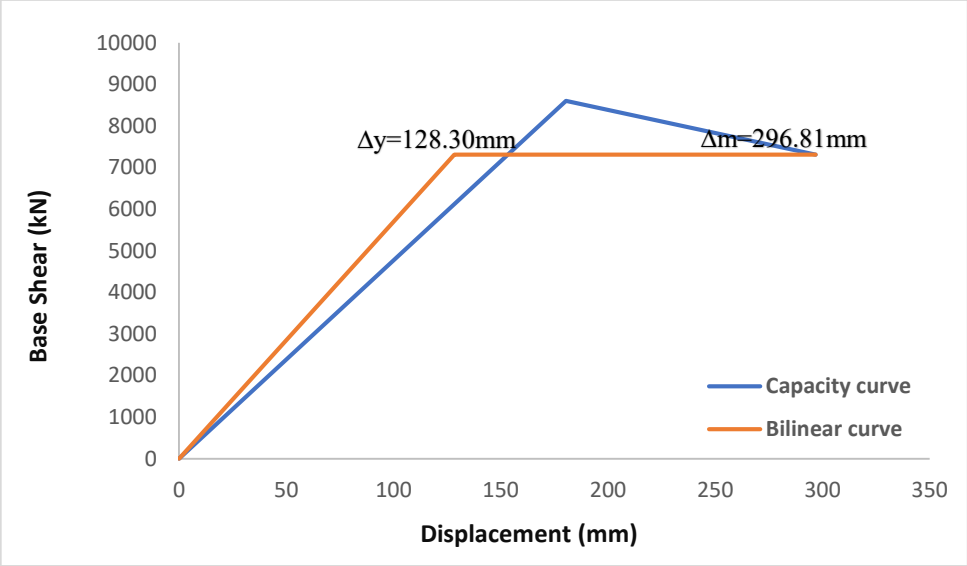

a) Model 17 (span length= 5m)

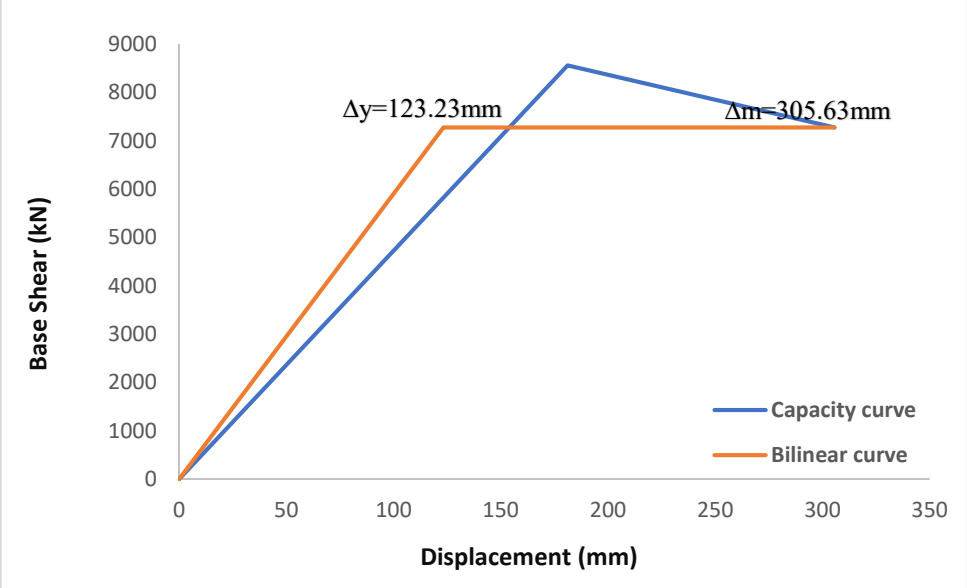

b) Model 18 (span length= 5.5m)

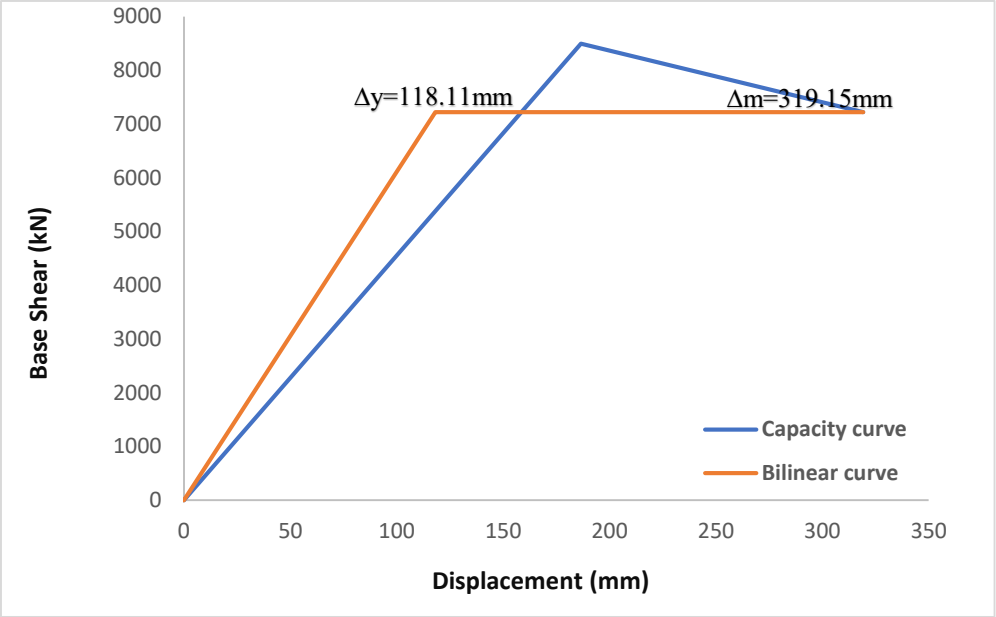

c) Model 19 (span length= 6m)

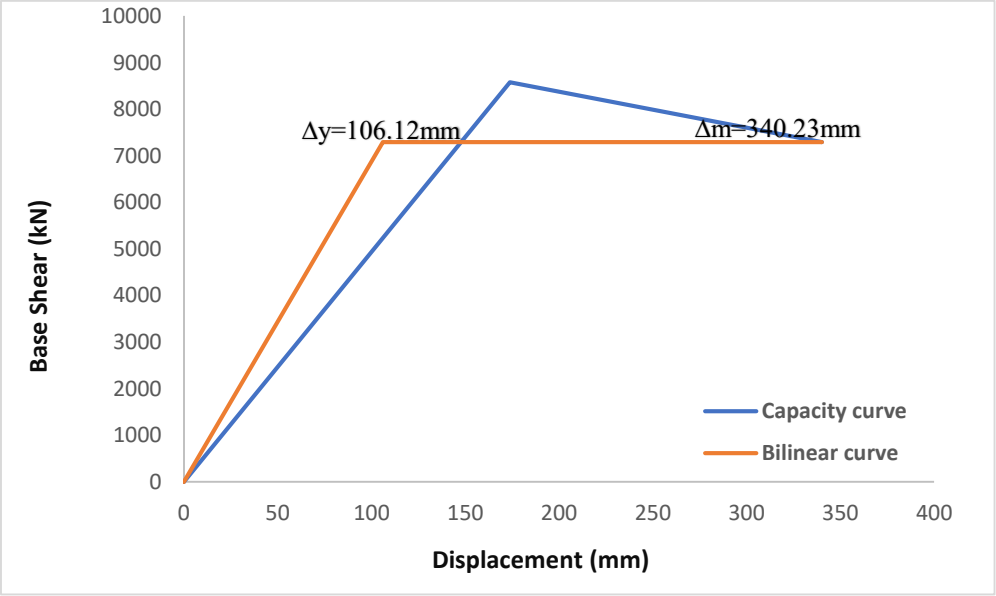

d) Model 20 (span length= 7m)

Figure A.1.5: Pushover (capacity) curve with bilinear curve for (4-story) with (($f'c$)= 300 kgf/cm^2, shear wall thickness = 250mm, shear wall position = edge)

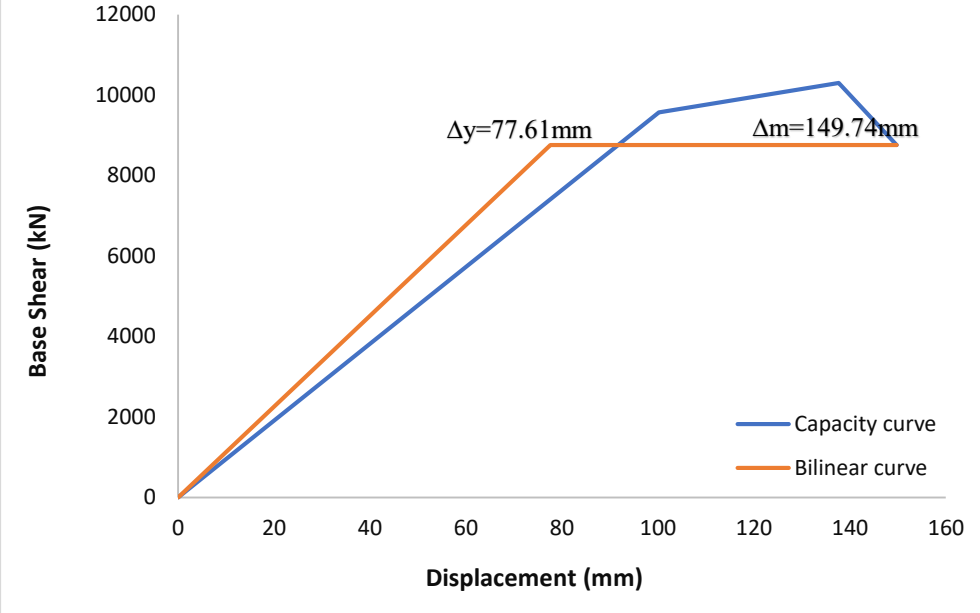

a) Model 21 (span length= 5m)

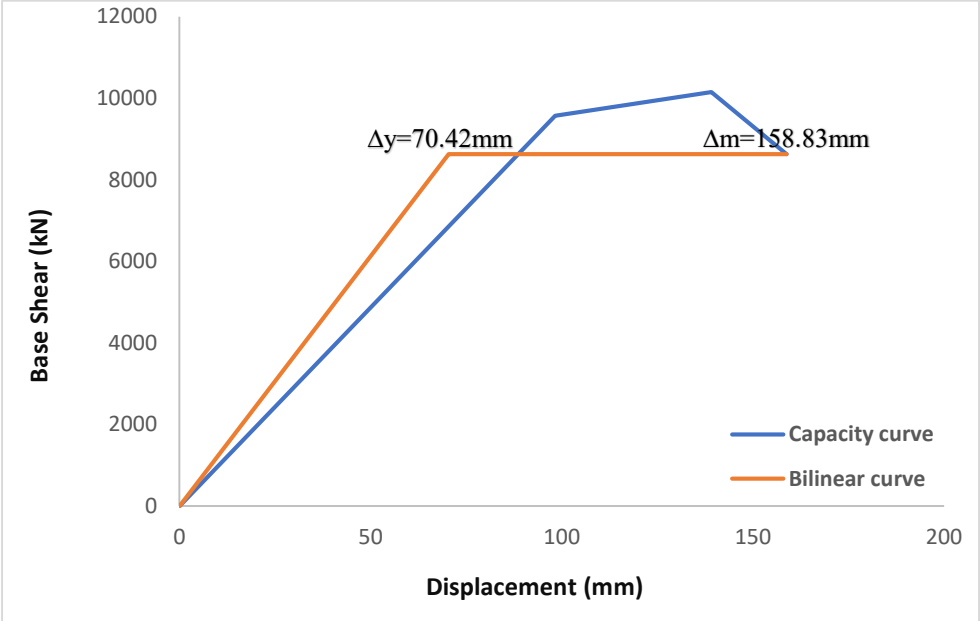

b) Model 22 (span length= 5.5m)

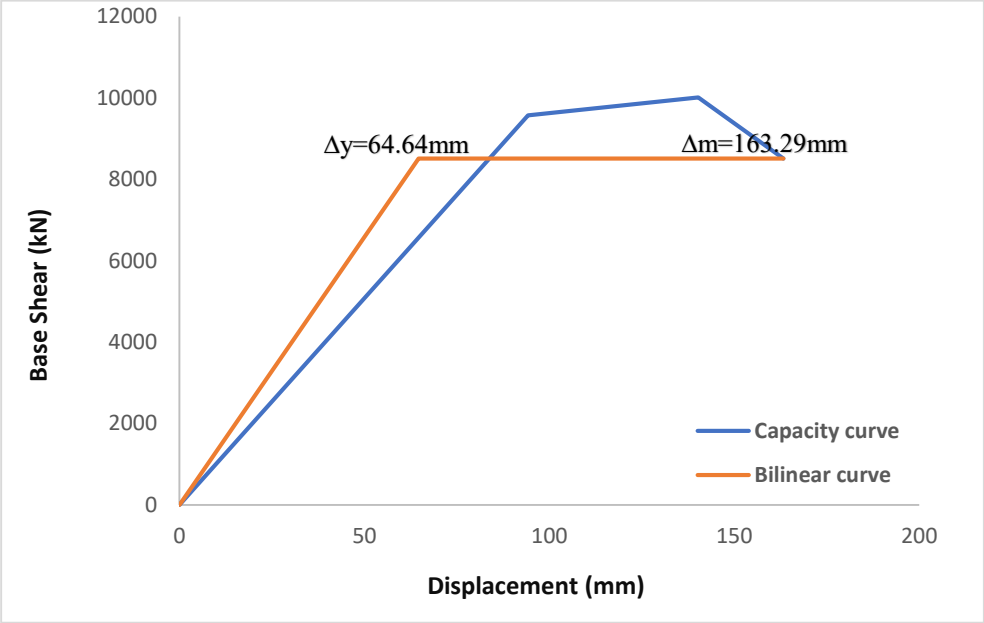

c) Model 23 (span length= 6m)

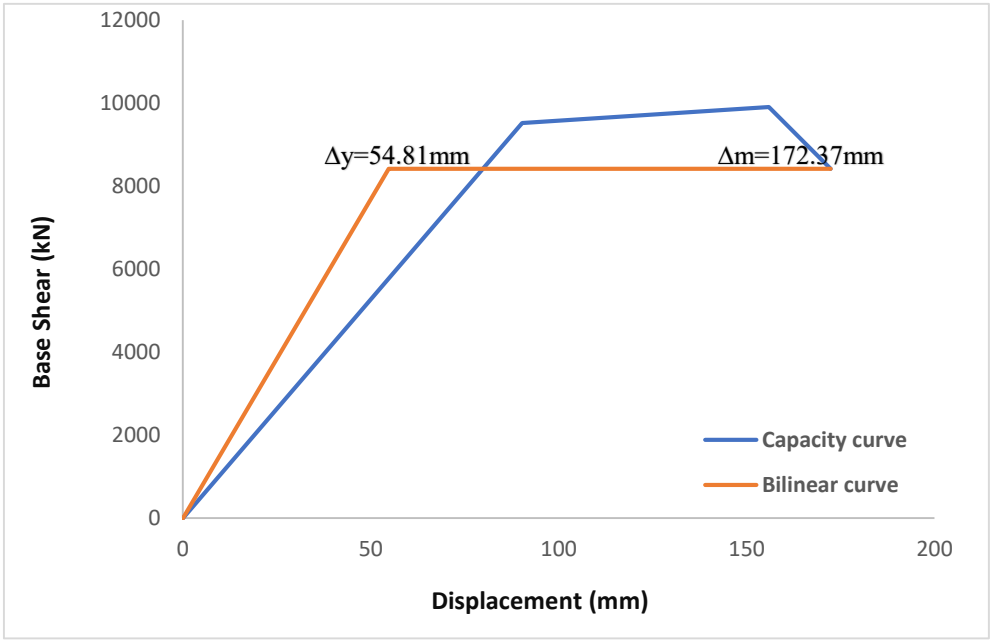

d) Model 24 (span length= 7m)

Figure A.1.6: Pushover (capacity) curve with bilinear curve for (4-story) with (($f'c$)= 300 kgf/cm^2, shear wall thickness = 250mm, shear wall position = middle)

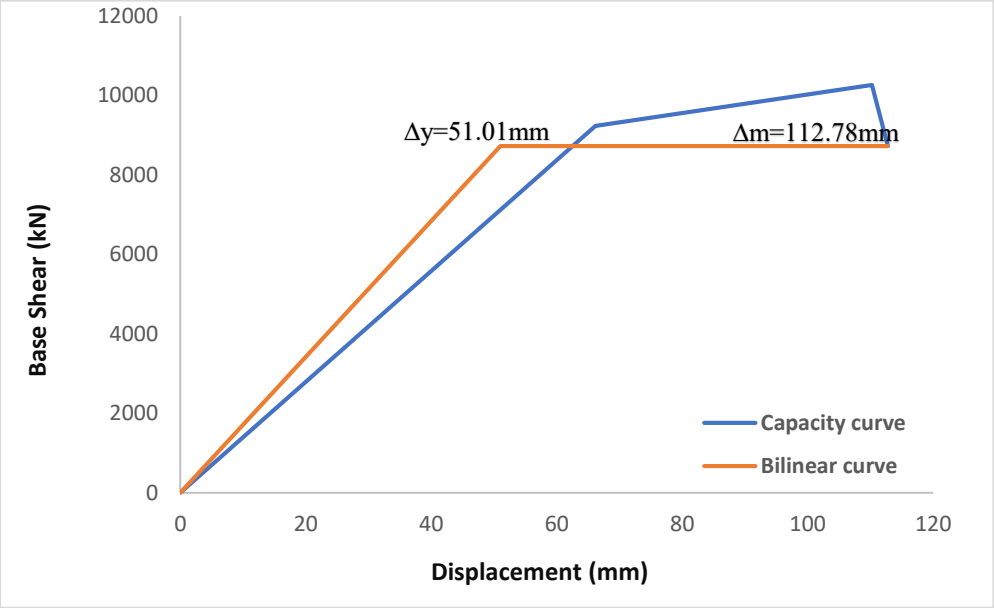

a) Model 25 (span length= 5m)

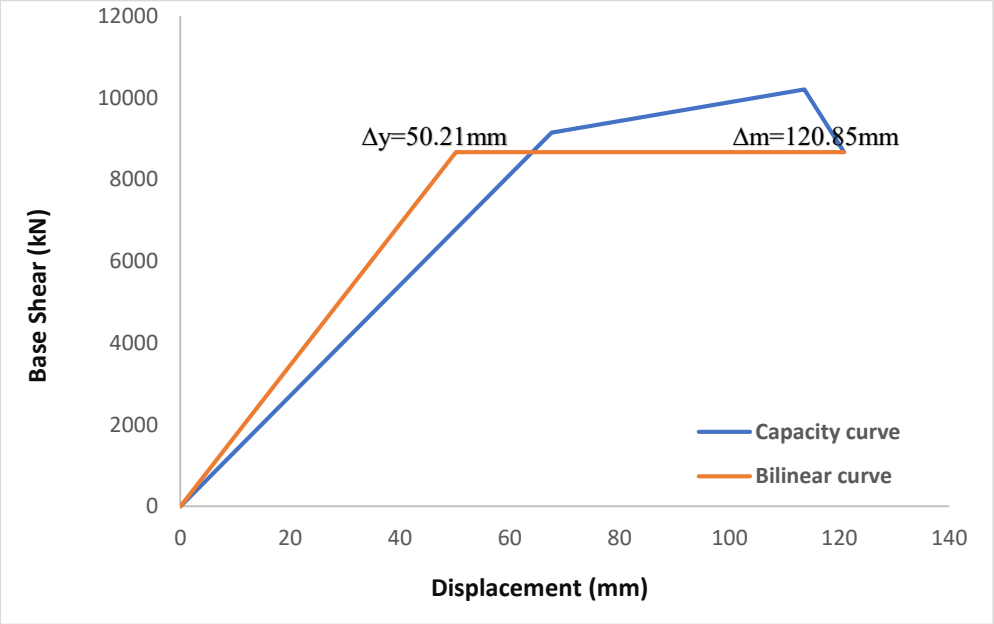

b) Model 26 (span length= 5.5m)

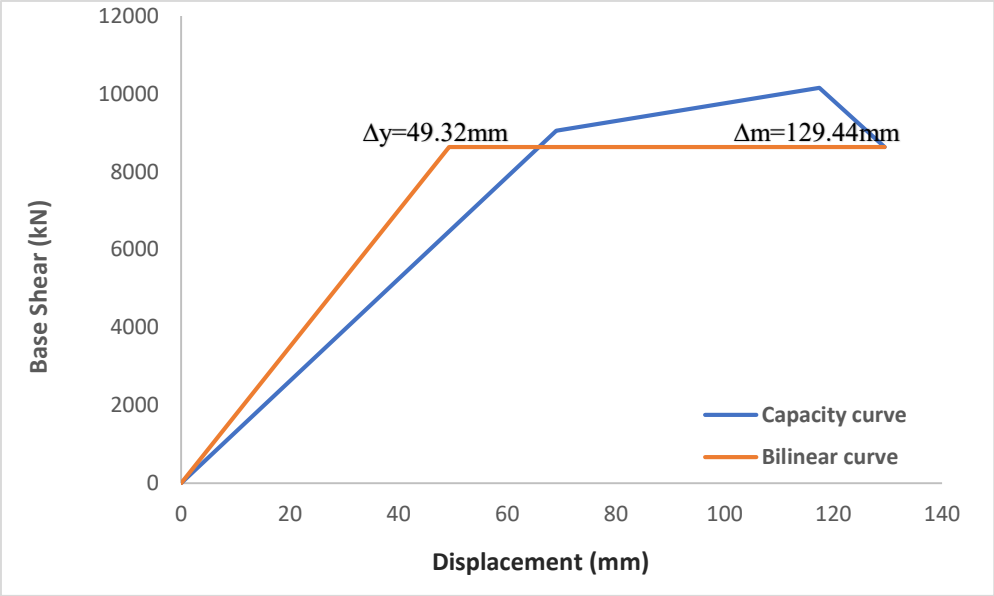

c) Model 27 (span length= 6m)

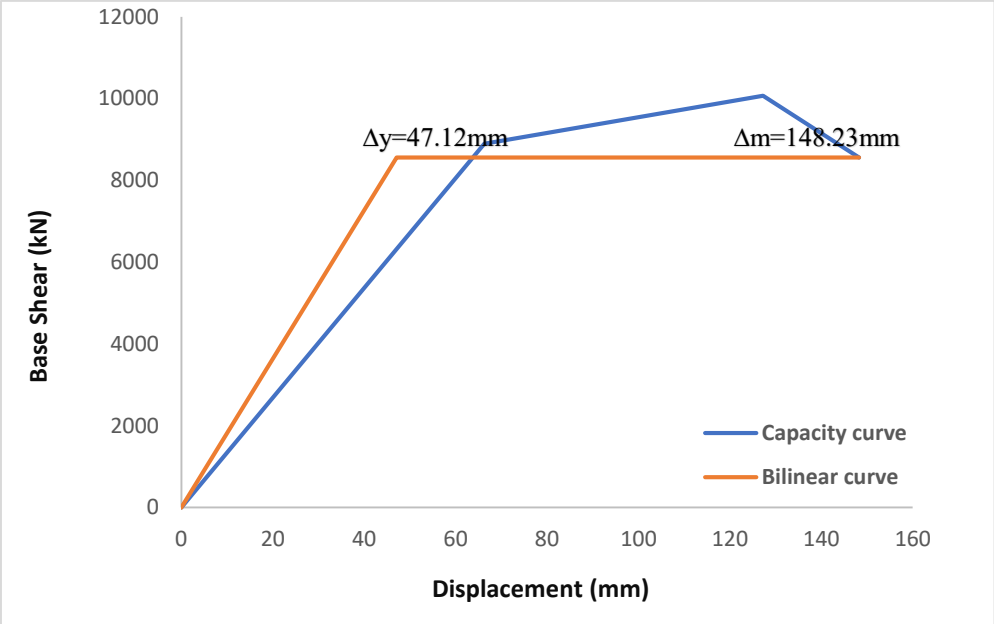

d) Model 28 (span length= 7m)

Figure A.1.7: Pushover (capacity) curve with bilinear curve for (4-story) with (($f'c$)= 300 kgf/cm^2, shear wall thickness = 300mm, shear wall position = edge)

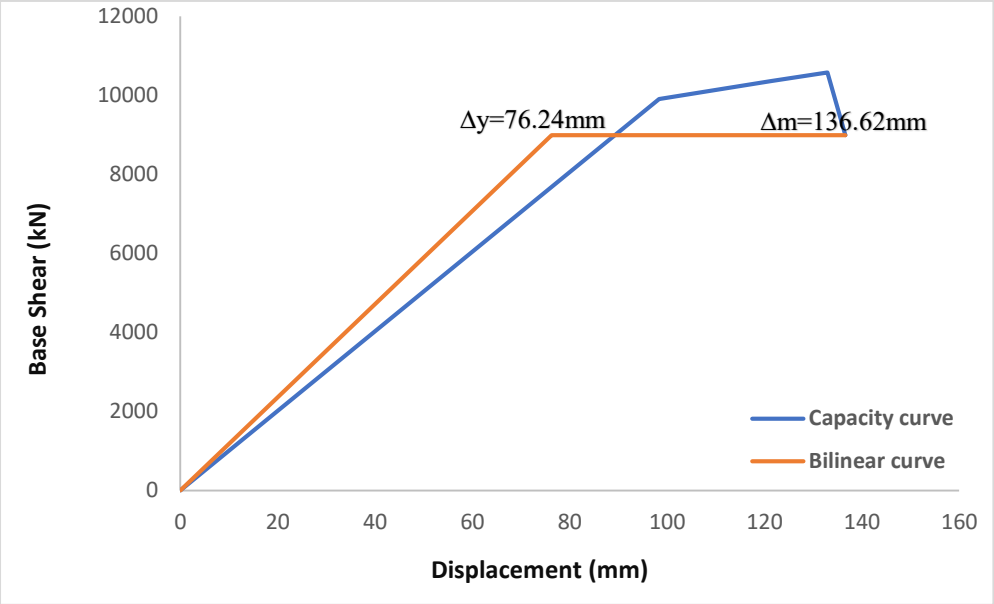

a) Model 29 (span length= 5m)

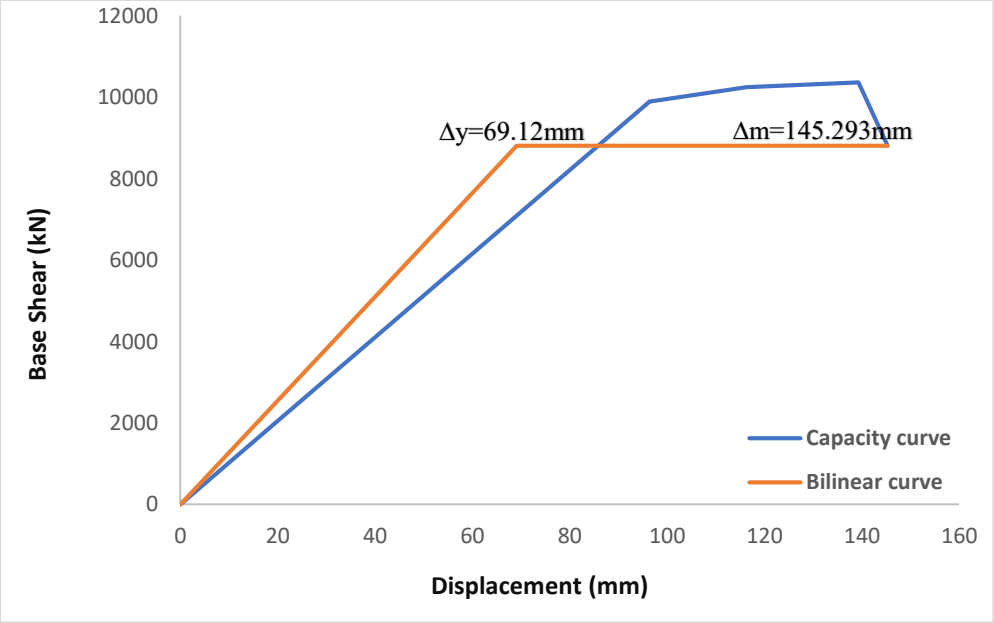

b) Model 30 (span length= 5.5m)

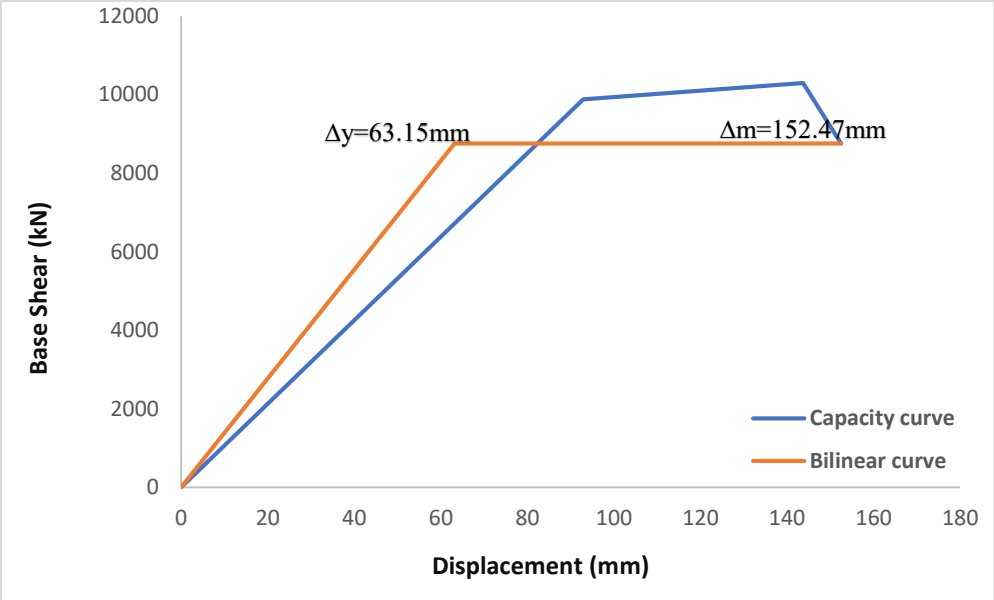

c) Model 31 (span length= 6m)

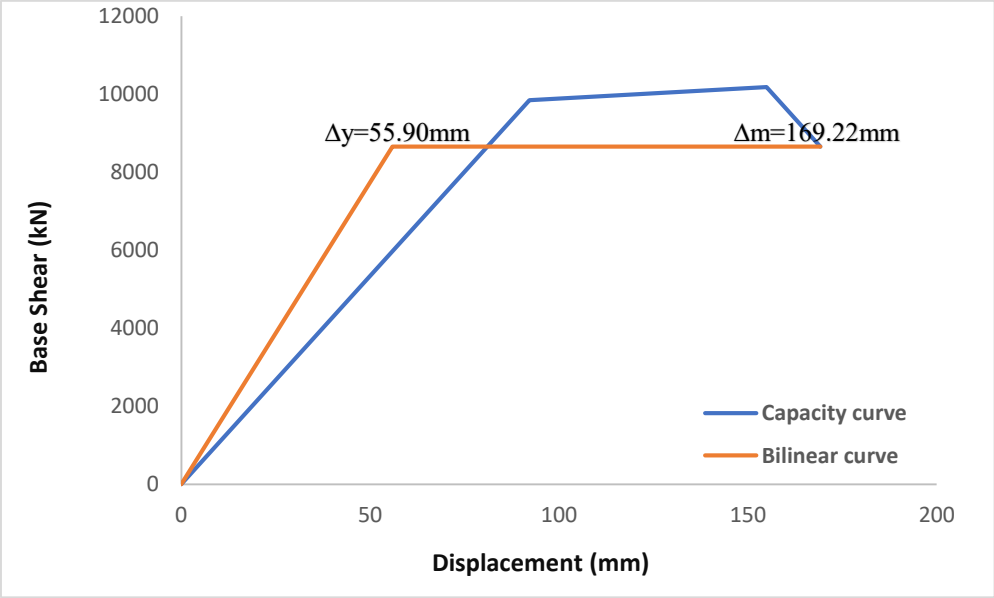

d) Model 32 (span length= 7m)

Figure A.1.8: Pushover (capacity) curve with bilinear curve for (4-story) with (($f'c$)= 300 kgf/cm^2, shear wall thickness = 300mm, shear wall position = middle)

APPENDIX 2

Pushover curves (capacity curves) for all models at mid-rise (8-story) buildings

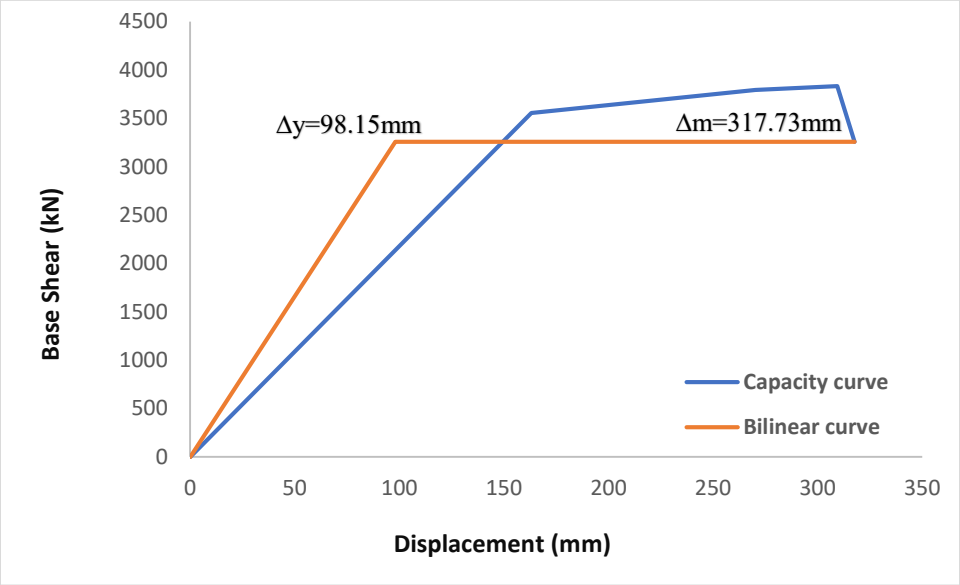

a) Model 33 (span length= 5m)

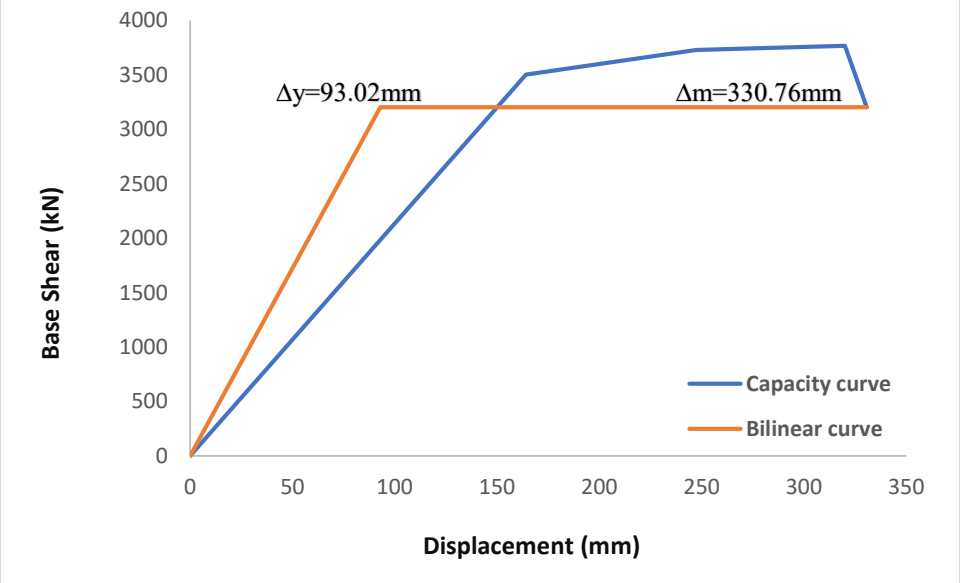

b) Model 34 (span length= 5.5m)

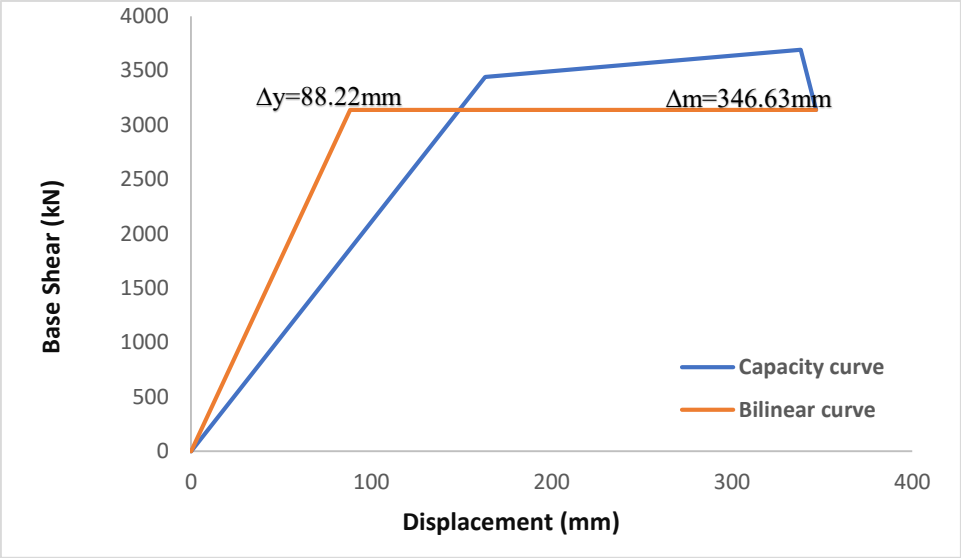

c) Model 35 (span length= 6m)

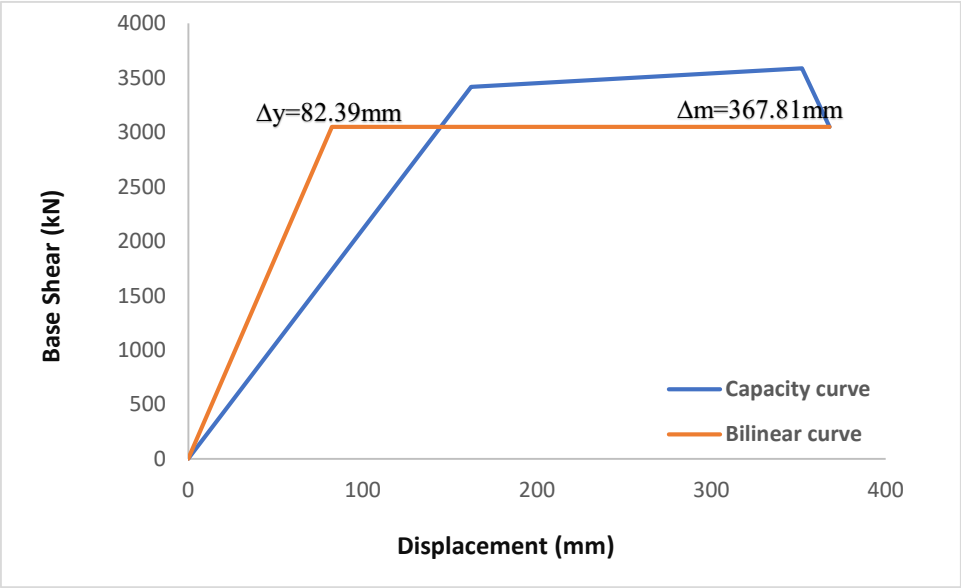

d) Model 36 (span length= 7m)

Figure A.2.1: Pushover (capacity) curve with bilinear curve for (8-story) with (($f'c$)= 250 kgf/cm^2, shear wall thickness = 250mm, shear wall position = edge)

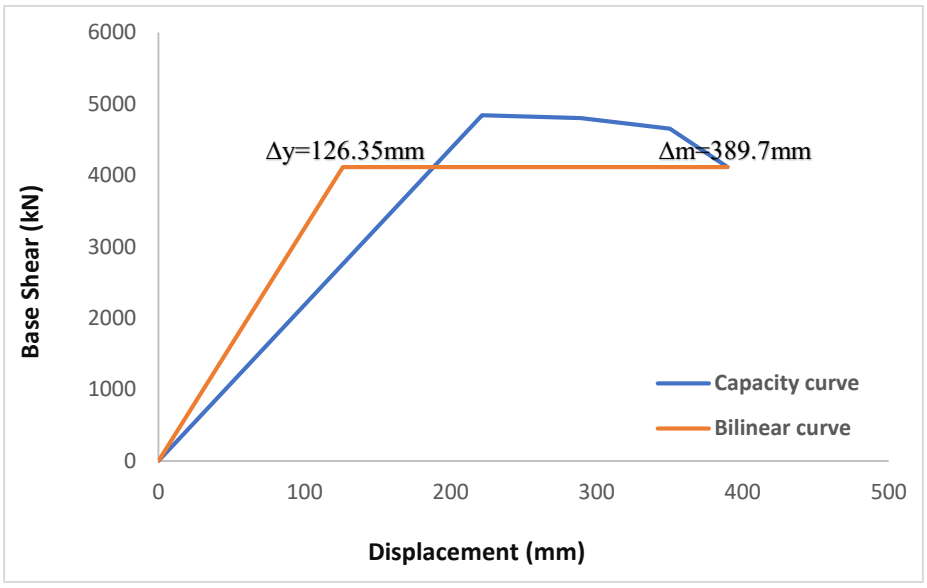

a) Model 37 (span length= 5m)

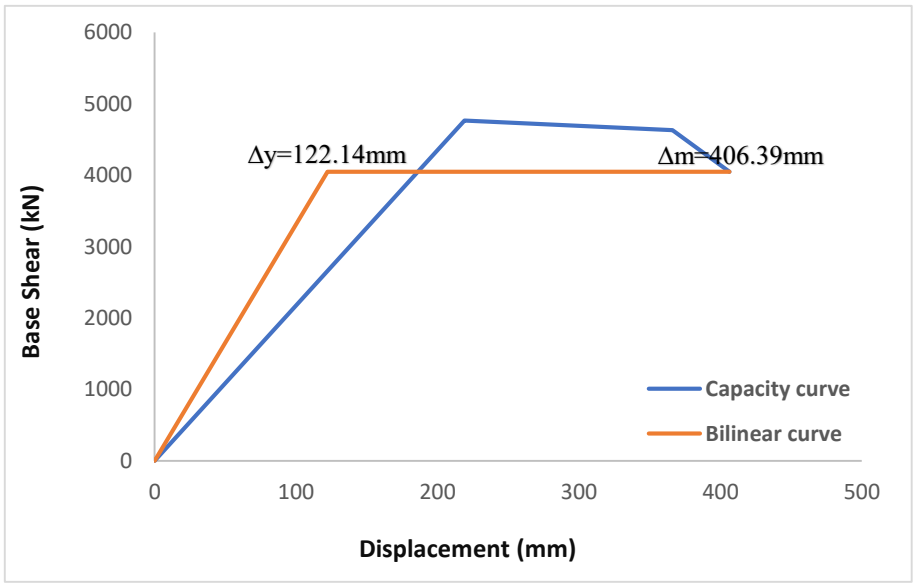

b) Model 38 (span length= 5.5m)

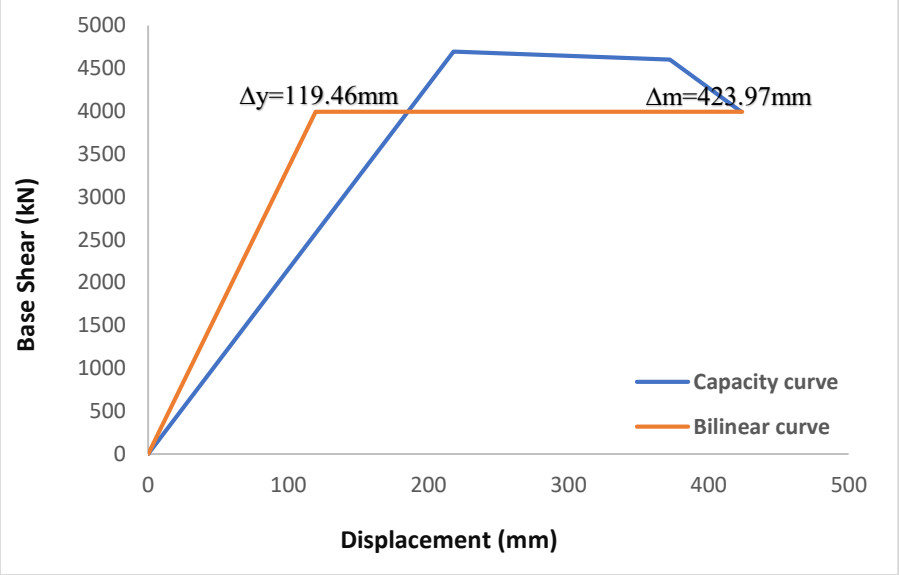

c) Model 39 (span length= 6m)

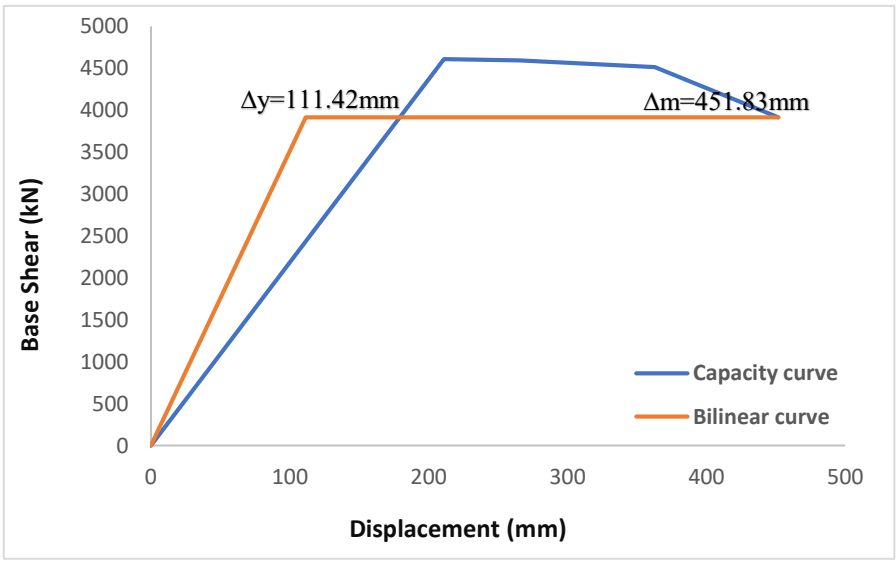

d) Model 40 (span length= 7m)

Figure A.2.2: Pushover (capacity) curve with bilinear curve for (8-story) with (($f'c$)= 250 kgf/cm^2, shear wall thickness = 250mm, shear wall position = middle)

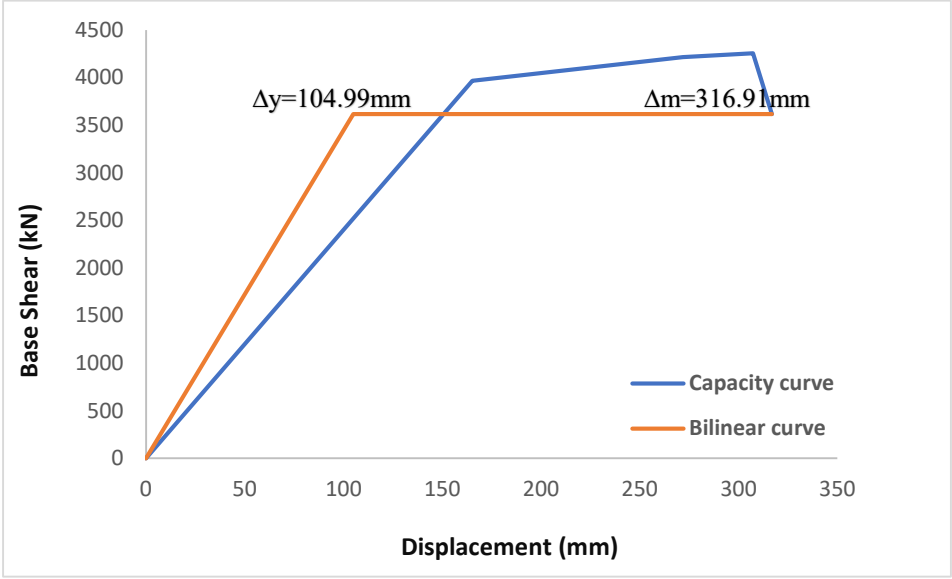

a) Model 41 (span length= 5m)

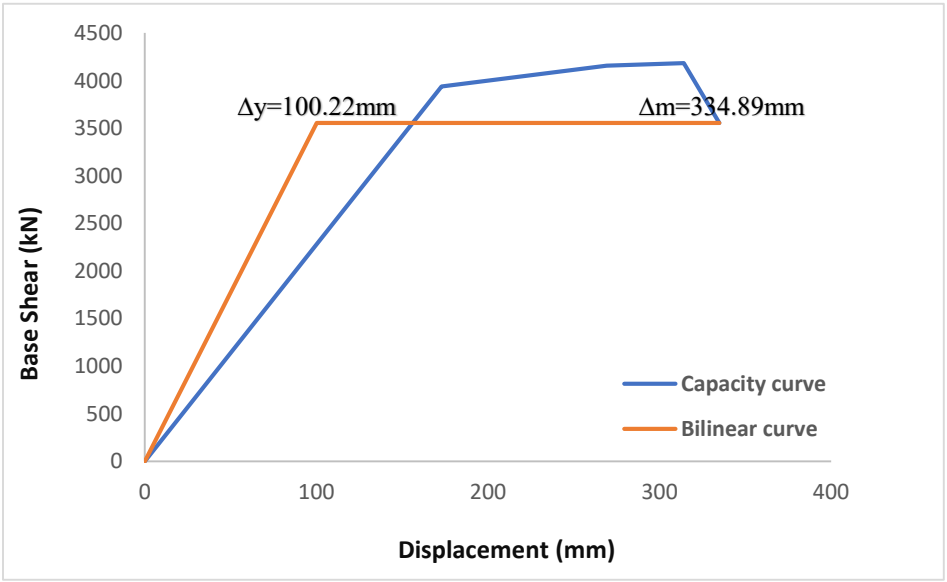

b) Model 42 (span length= 5.5m)

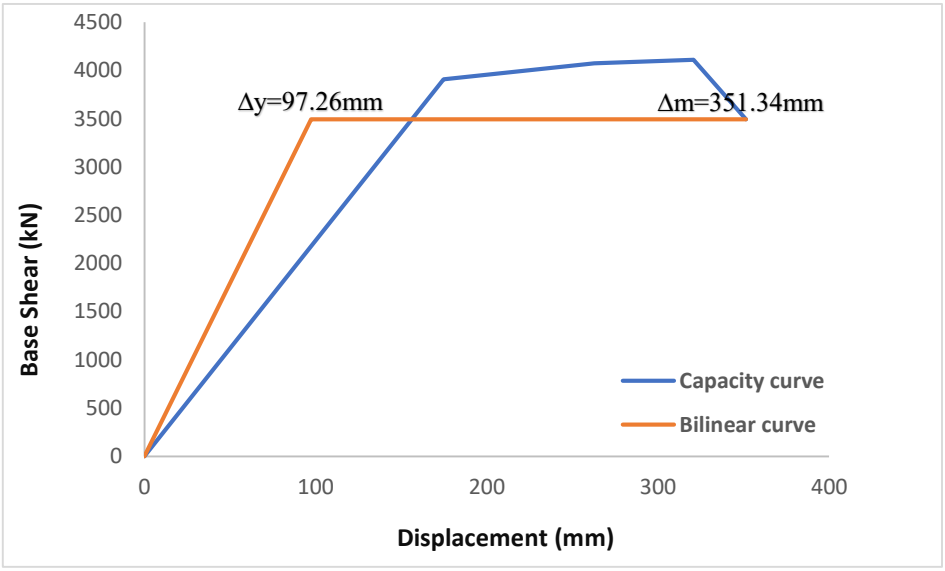

c) Model 43 (span length= 6m)

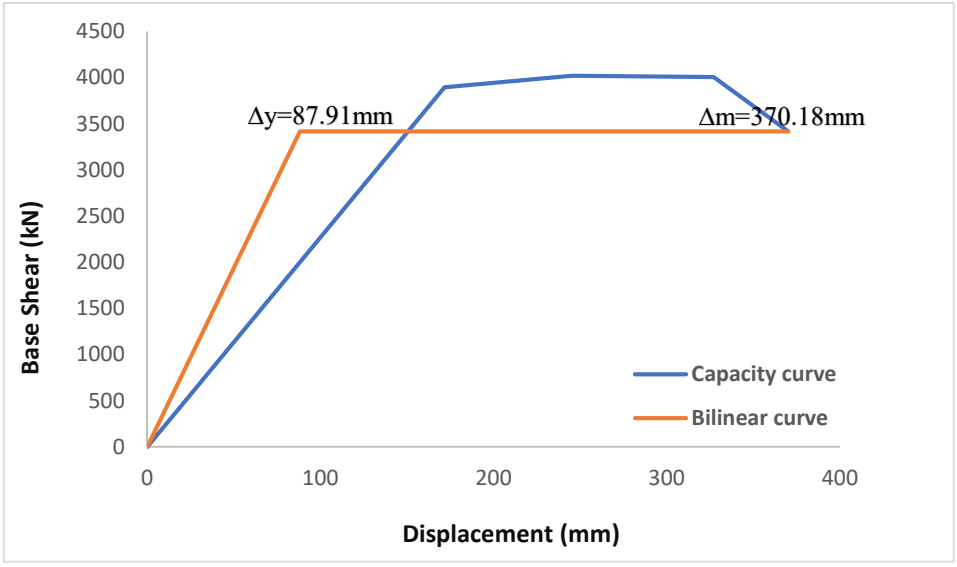

d) Model 44 (span length= 7m)

Figure A.2.3: Pushover (capacity) curve with bilinear curve for (8-story) with (($f'c$)= 250 kgf/cm^2, shear wall thickness = 300mm, shear wall position = edge)

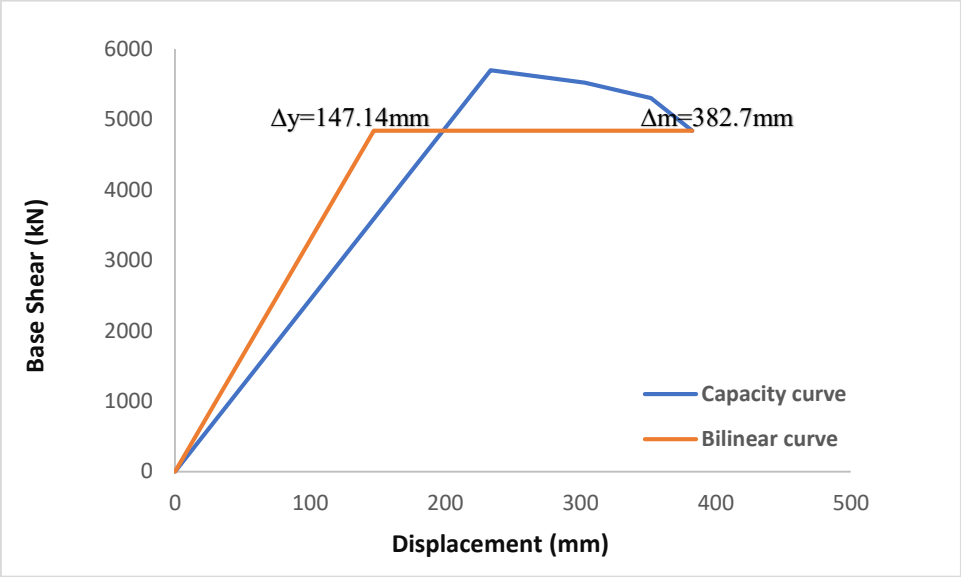

a) Model 45 (span length= 5m)

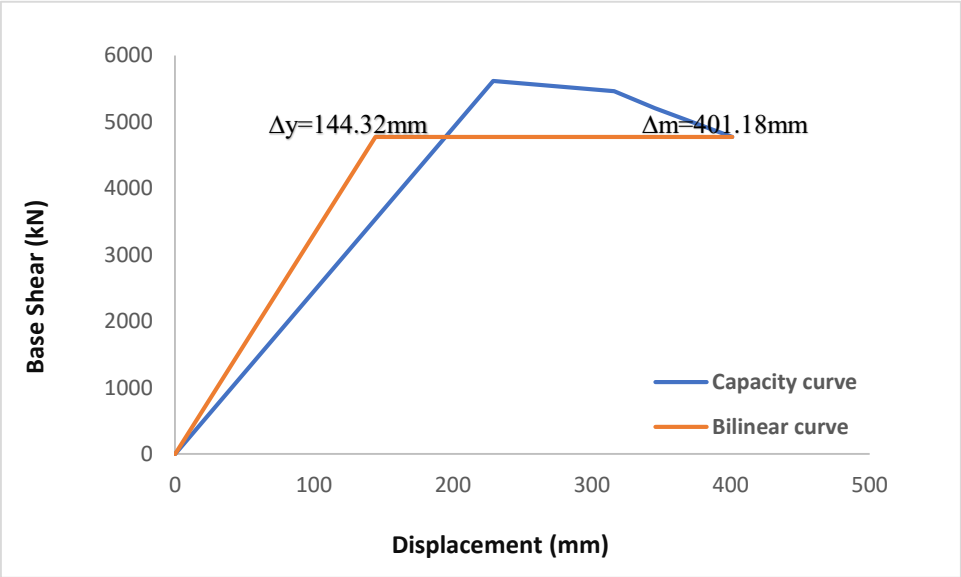

b) Model 46 (span length= 5.5m)

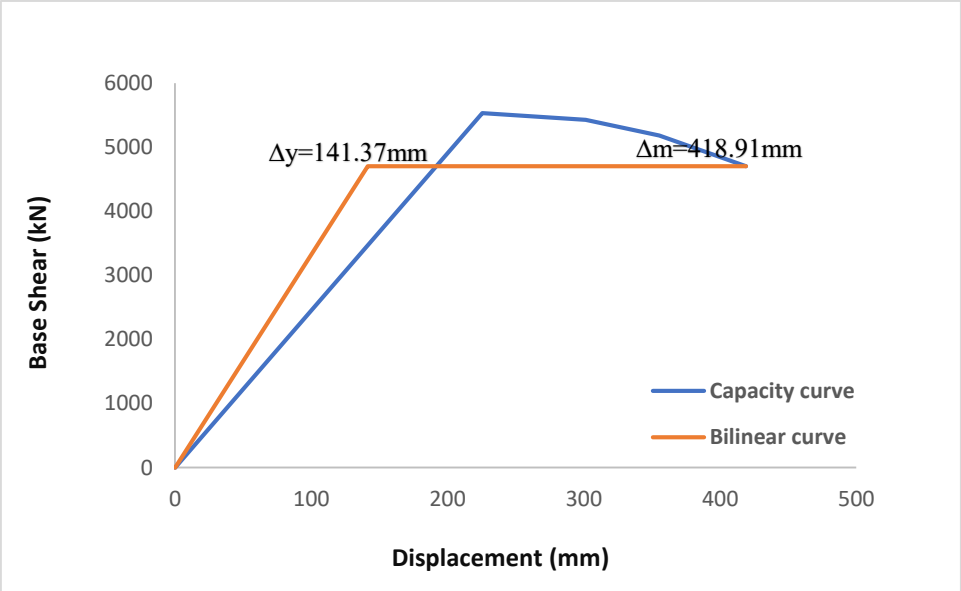

c) Model 47 (span length= 6m)

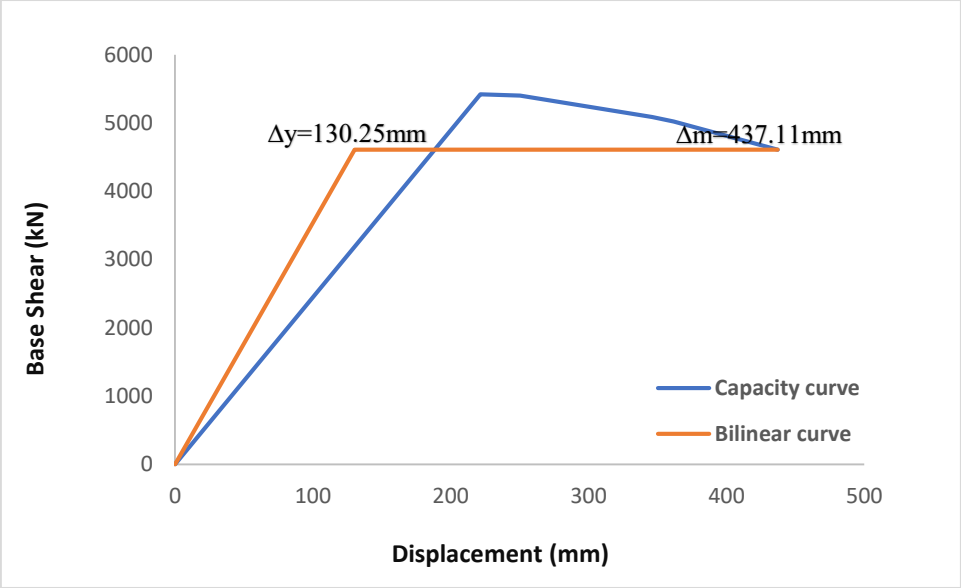

d) Model 48 (span length= 7m)

Figure A.2.4: Pushover (capacity) curve with bilinear curve for (8-story) with (($f'c$)= 250 kgf/cm^2, shear wall thickness = 300mm, shear wall position = middle)

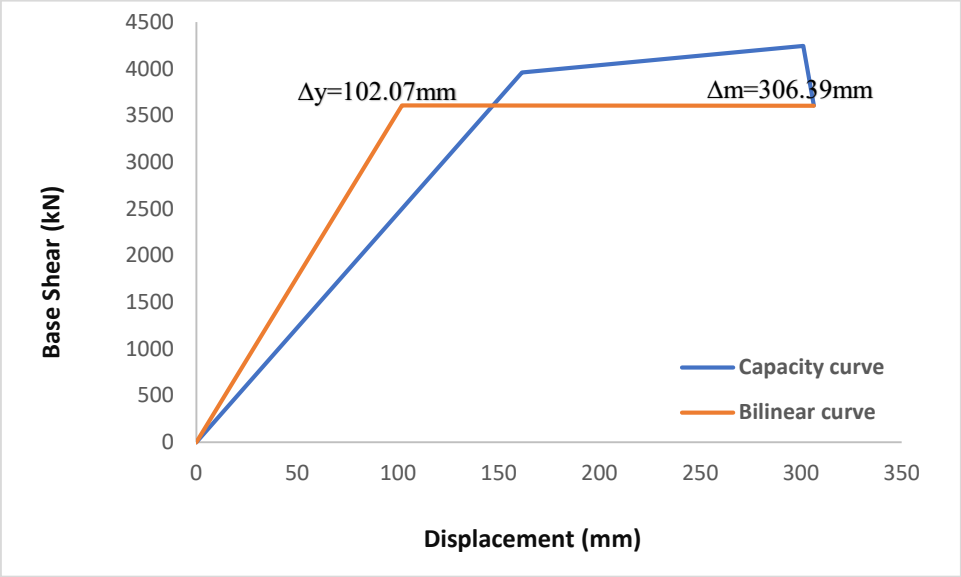

a) Model 49 (span length= 5m)

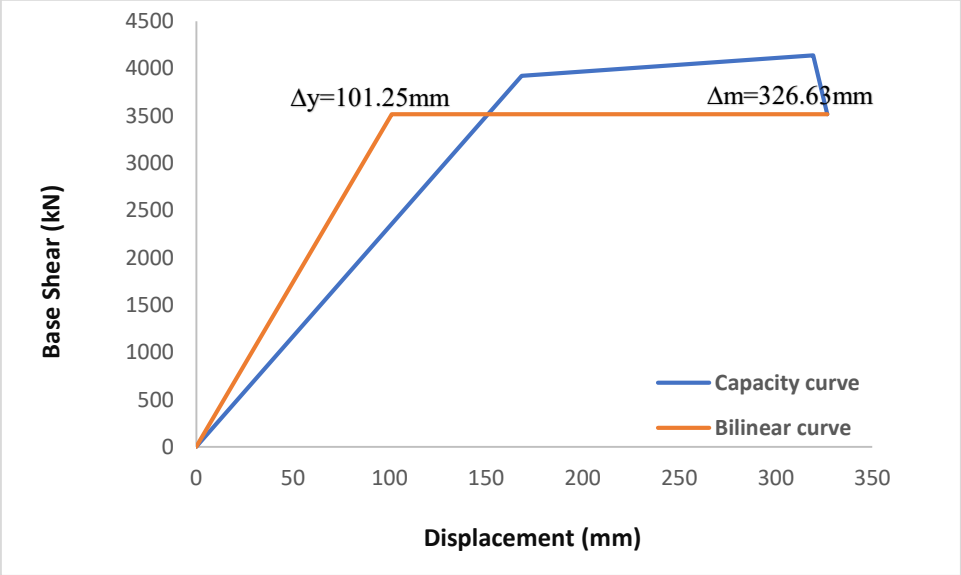

b) Model 50 (span length= 5.5m)

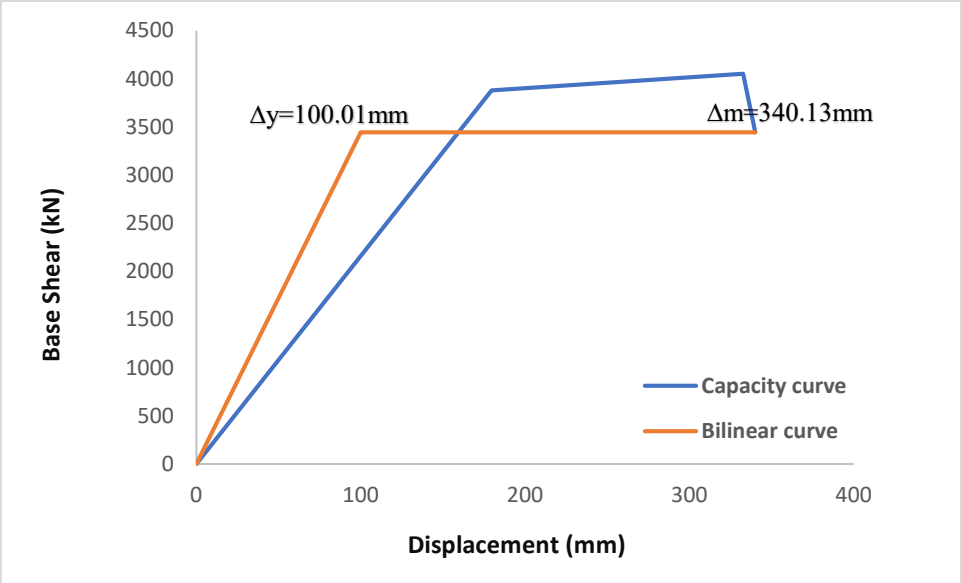

c) Model 51 (span length= 6m)

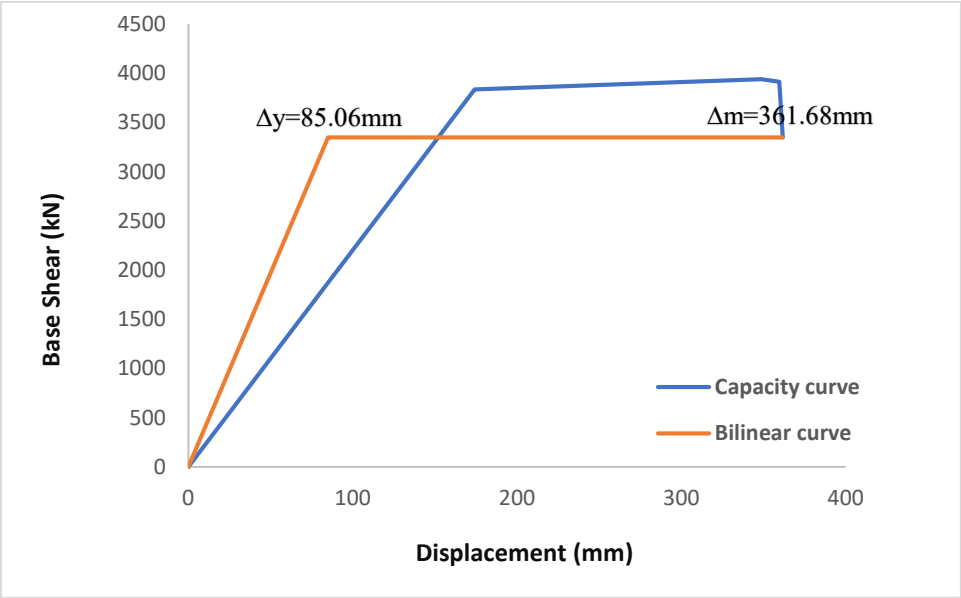

d) Model 52 (span length= 7m)

Figure A.2.5: Pushover (capacity) curve with bilinear curve for (8-story) with (($f'c$)= 300 kgf/cm^2, shear wall thickness = 250mm, shear wall position = edge)

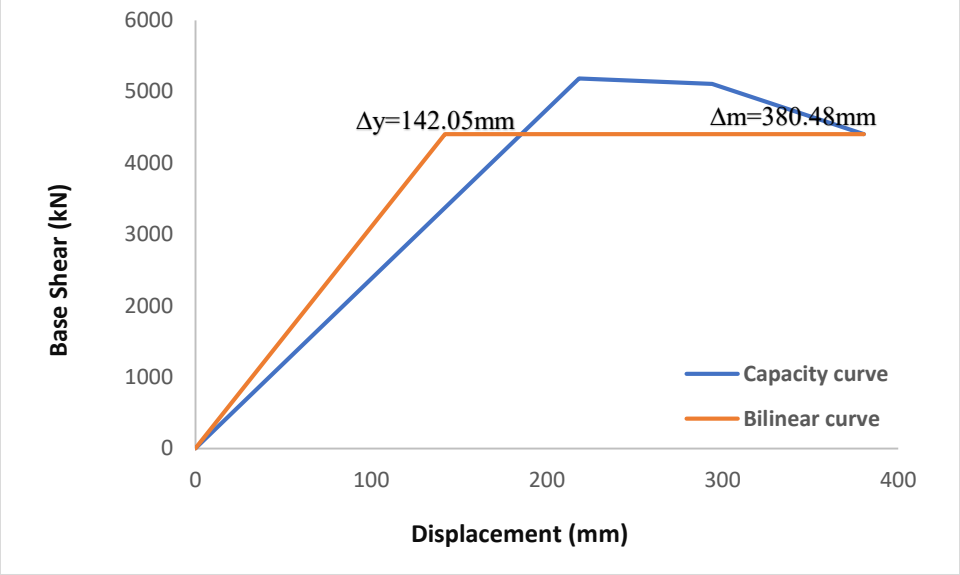

a) Model 53 (span length= 5m)

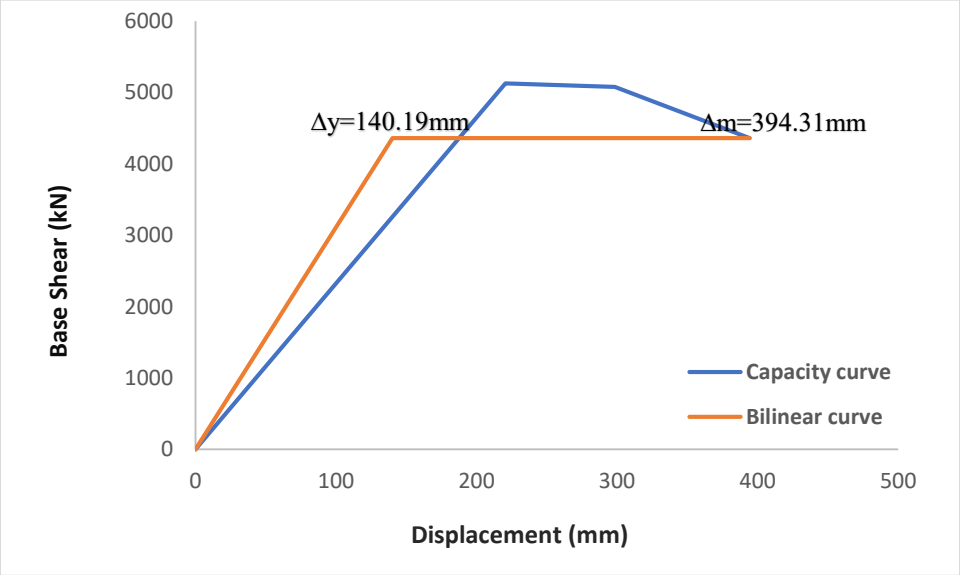

b) Model 54 (span length= 5.5m)

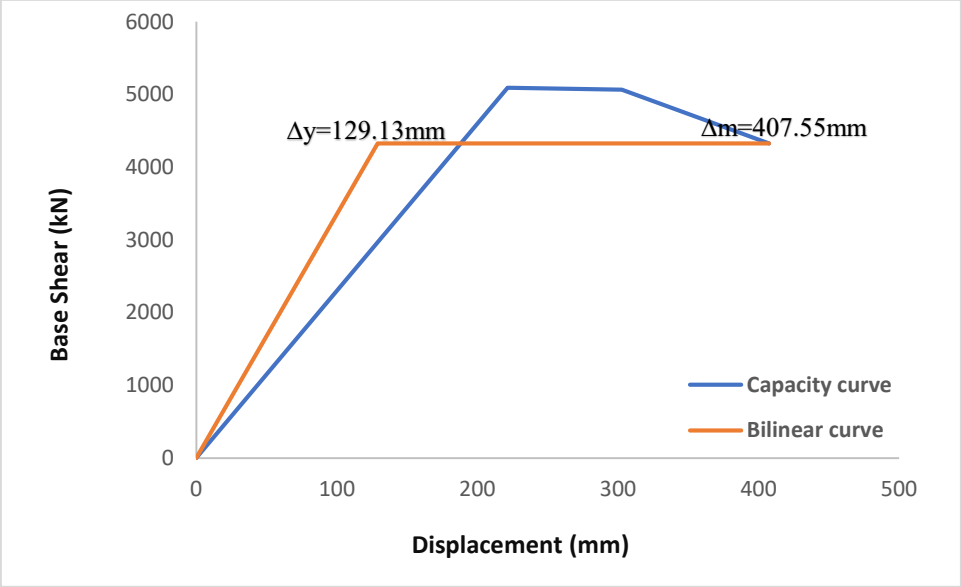

c) Model 55 (span length= 6m)

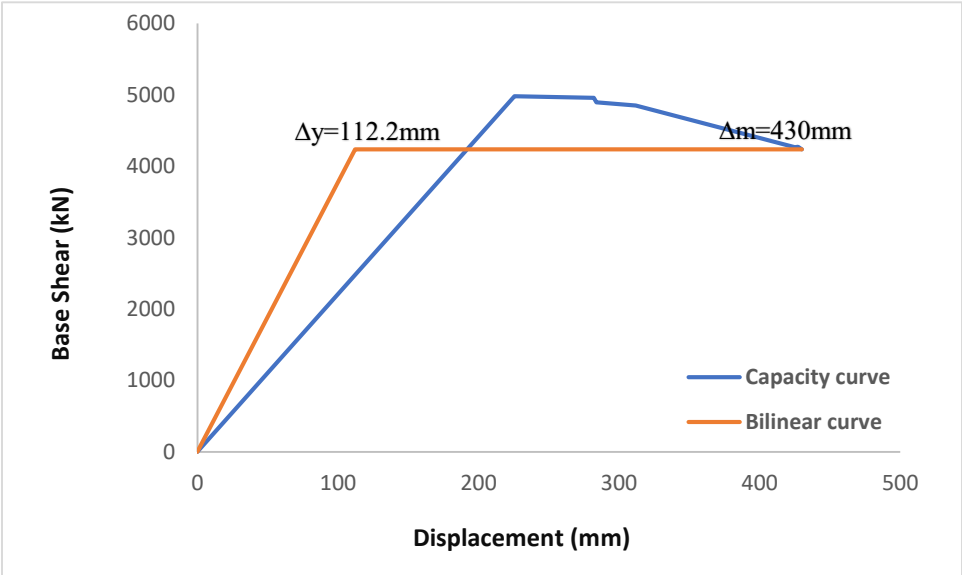

d) Model 56 (span length= 7m)

Figure A.2.6: Pushover (capacity) curve with bilinear curve for (8-story) with (($f'c$)= 300 kgf/cm^2, shear wall thickness = 250mm, shear wall position = middle)

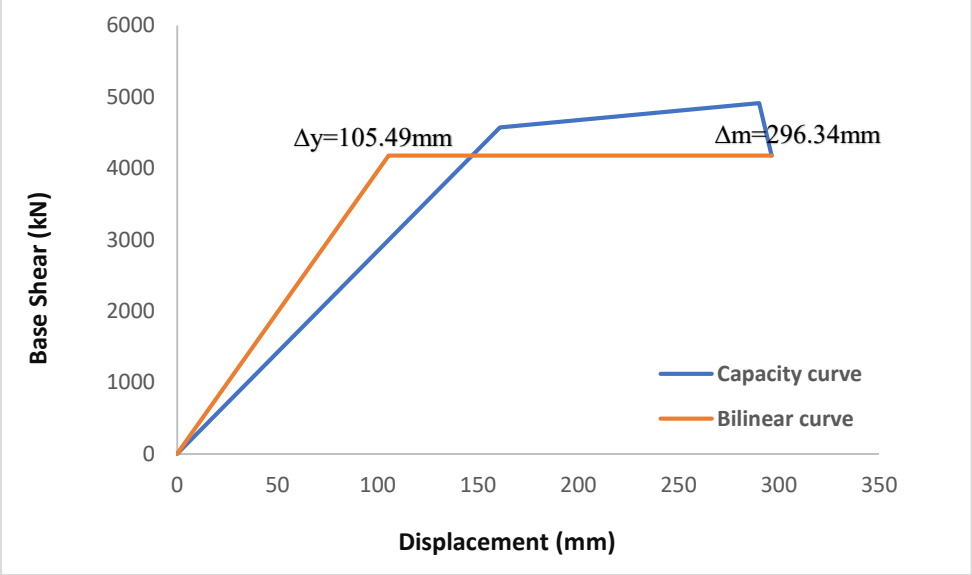

a) Model 57 (span length= 5m)

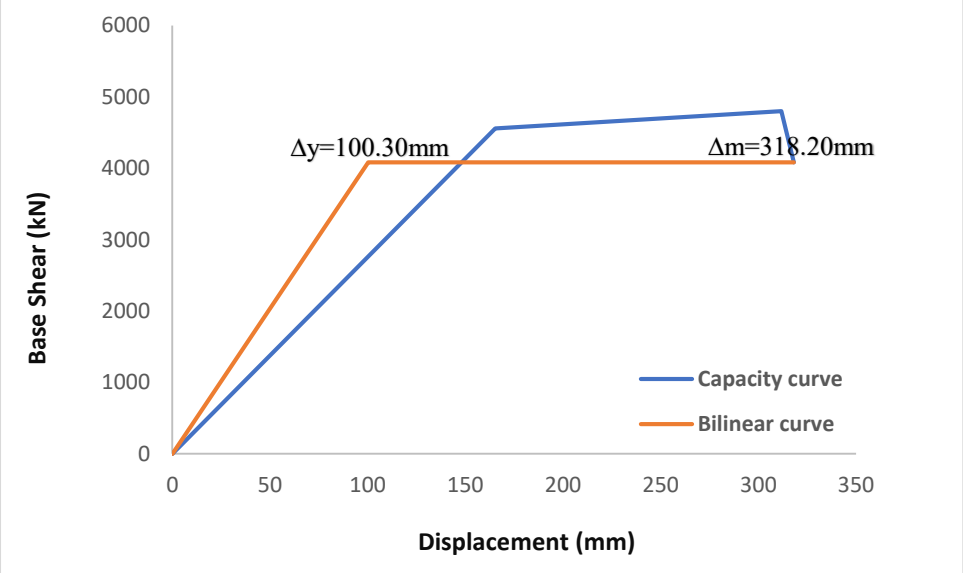

b) Model 58 (span length= 5.5m)

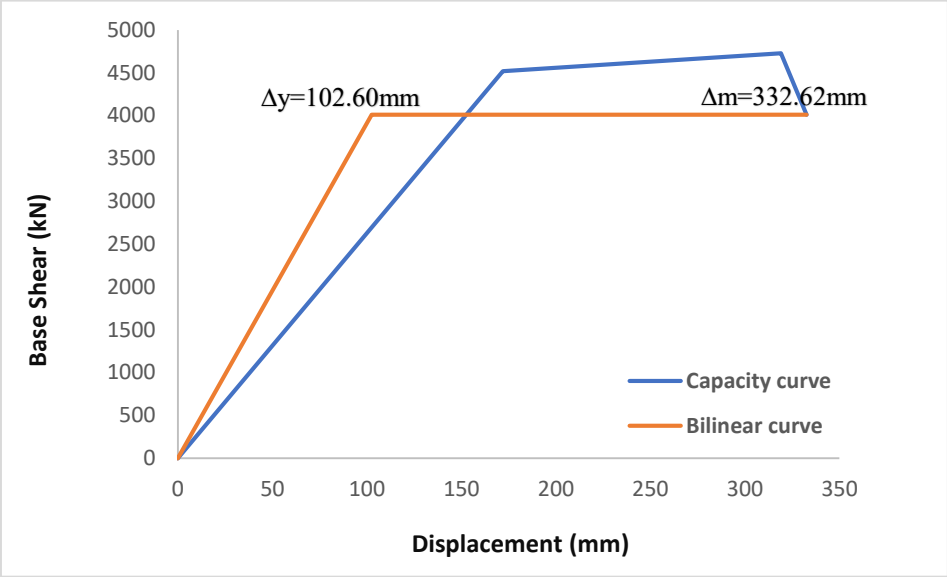

c) Model 59 (span length= 6m)

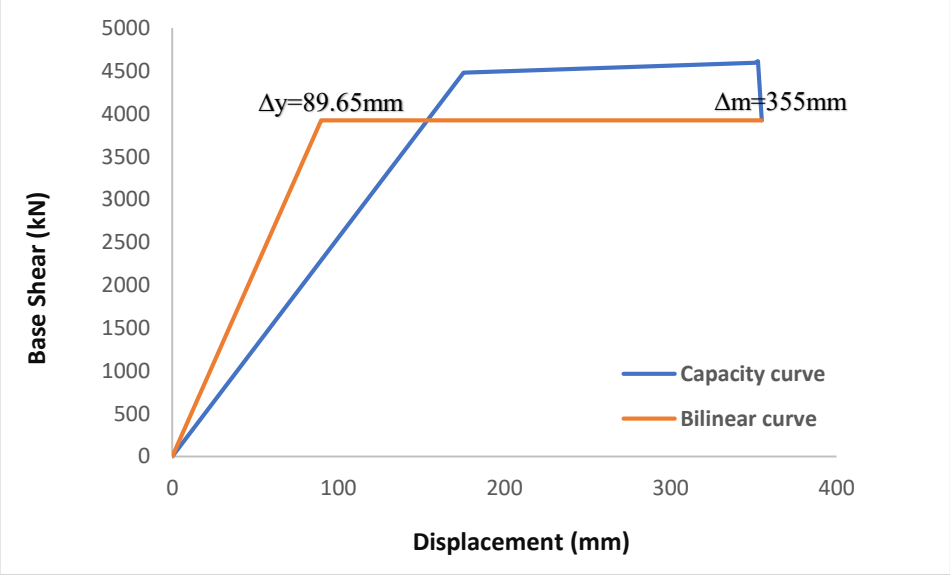

d) Model 60 (span length= 7m)

Figure A.2.7: Pushover (capacity) curve with bilinear curve for (8-story) with (($f'c$)= 300 kgf/cm^2, shear wall thickness = 300mm, shear wall position = edge)

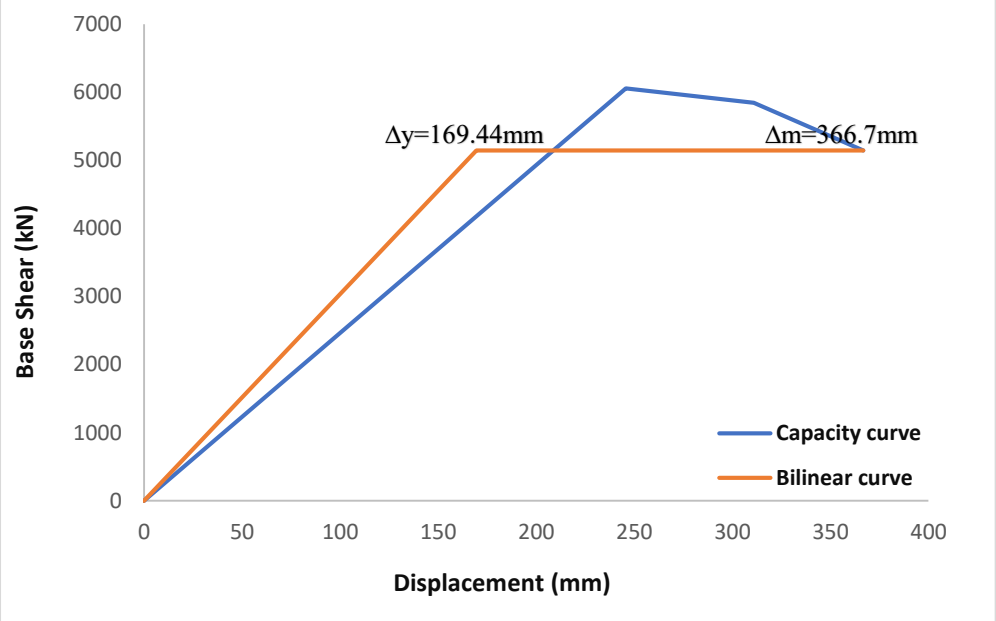

a) Model 61 (span length= 5m)

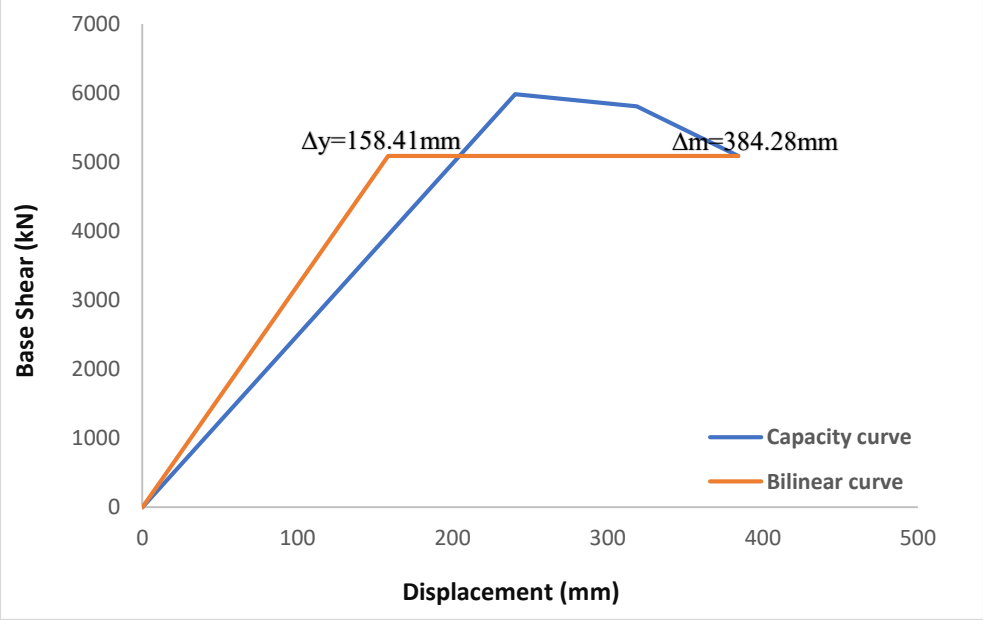

b) Model 62 (span length= 5.5m)

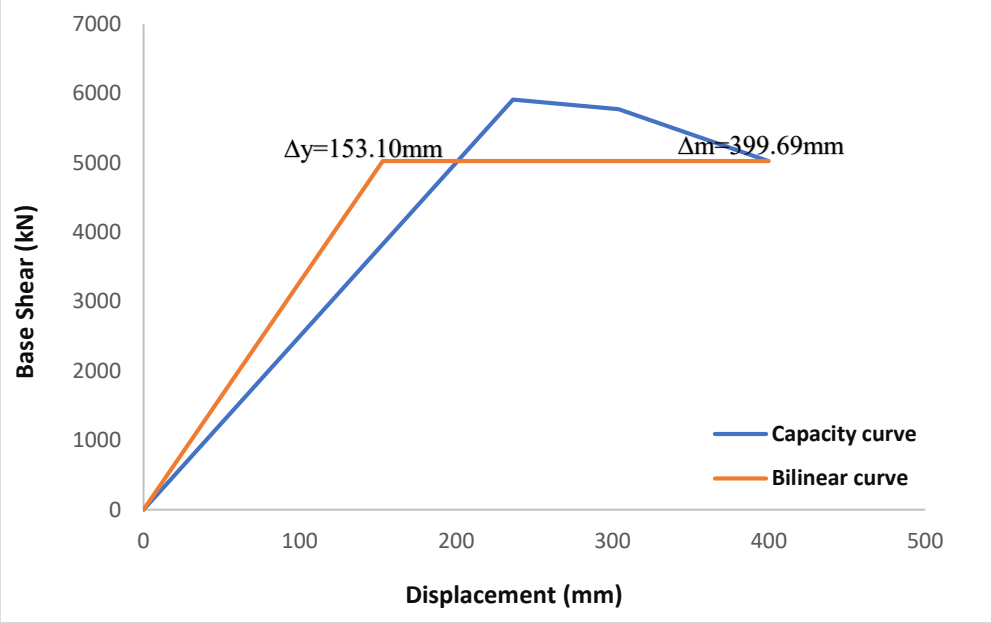

c) Model 63 (span length= 6m)

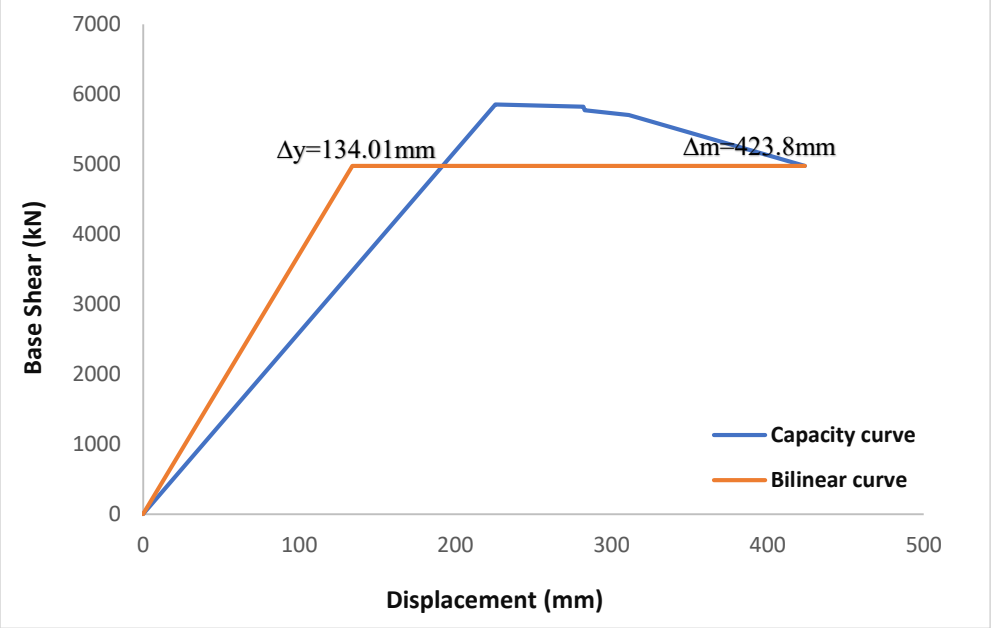

d) Model 64 (span length= 7m)

Figure A.2.8: Pushover (capacity) curve with bilinear curve for (8-story) with (($f'c$)= 300 kgf/cm^2, shear wall thickness = 300mm, shear wall position = middle)

APPENDIX 3

Pushover curves (capacity curves) for all models at high-rise (12-story) buildings

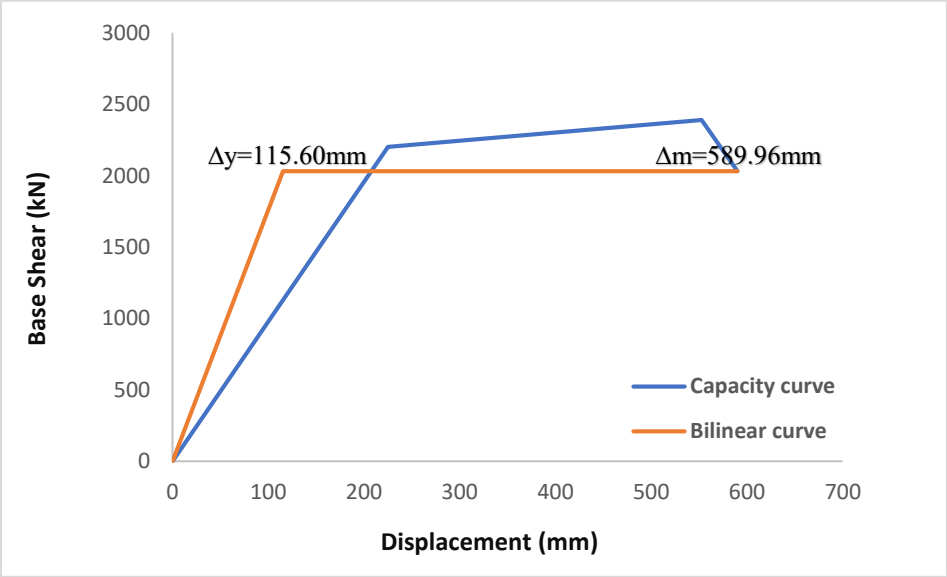

a) Model 65 (span length= 5m)

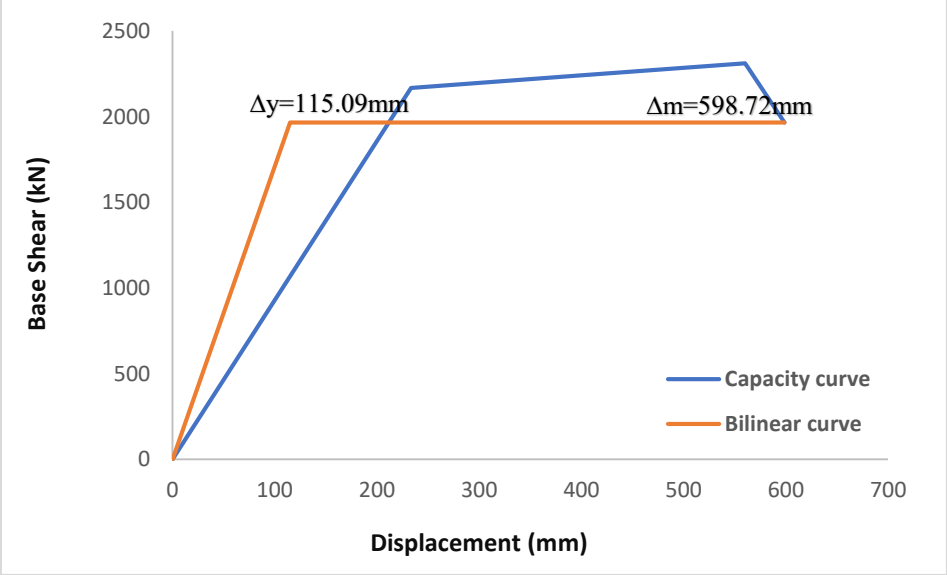

b) Model 66 (span length= 5.5m)

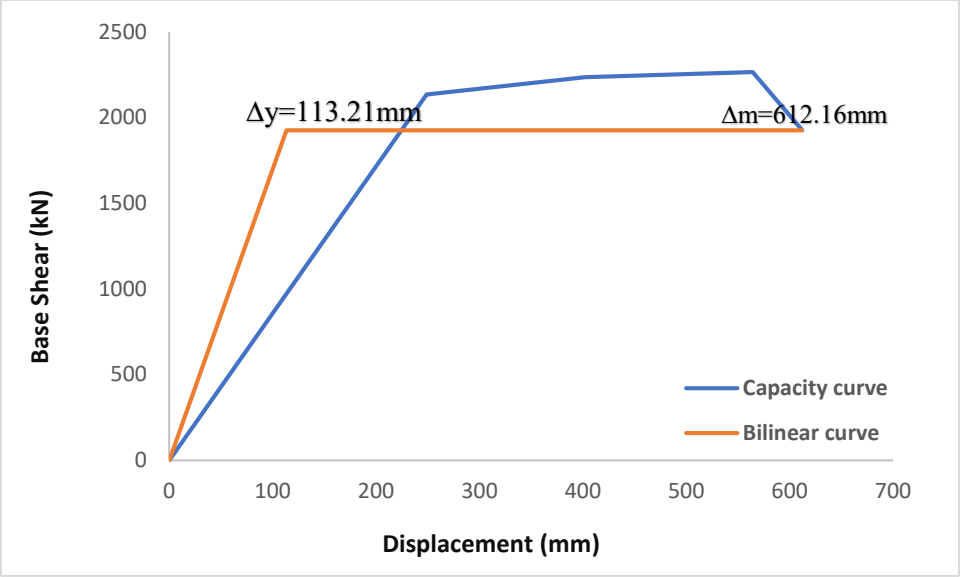

c) Model 67 (span length= 6m)

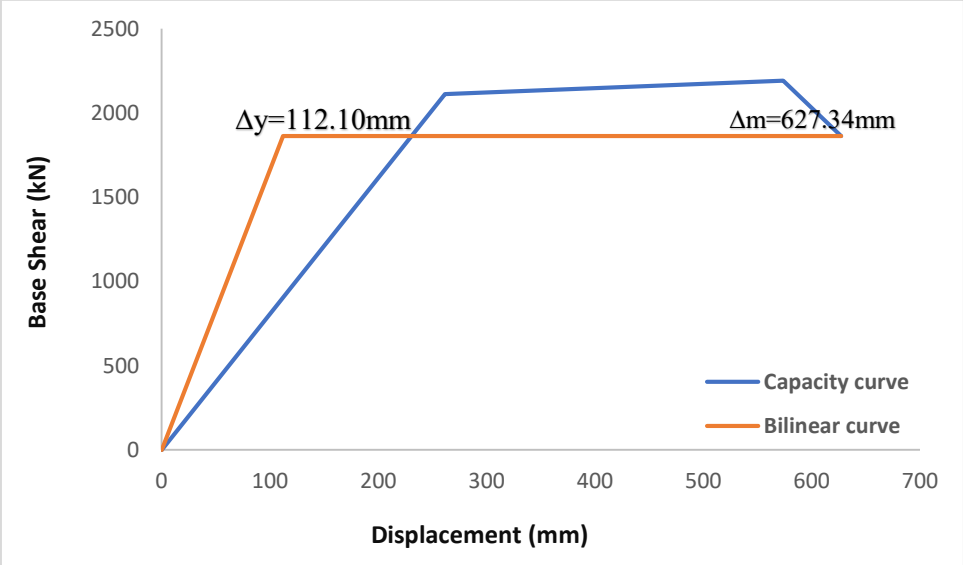

d) Model 68 (span length= 7m)

Figure A.3.1: Pushover (capacity) curve with bilinear curve for (12-story) with (($f'c$)= 250 kgf/cm^2, shear wall thickness = 250mm, shear wall position = edge)

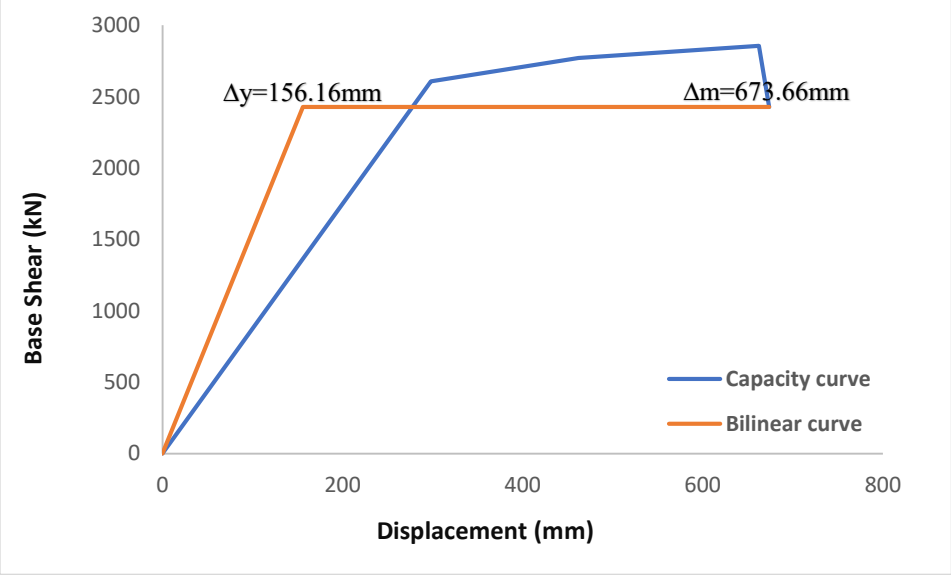

a) Model 69 (span length= 5m)

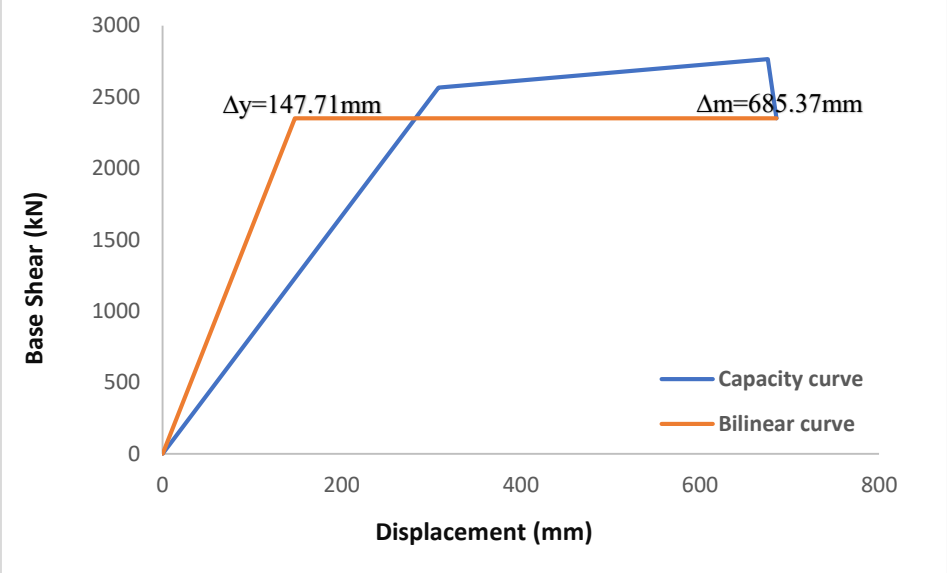

b) Model 70 (span length= 5.5m)

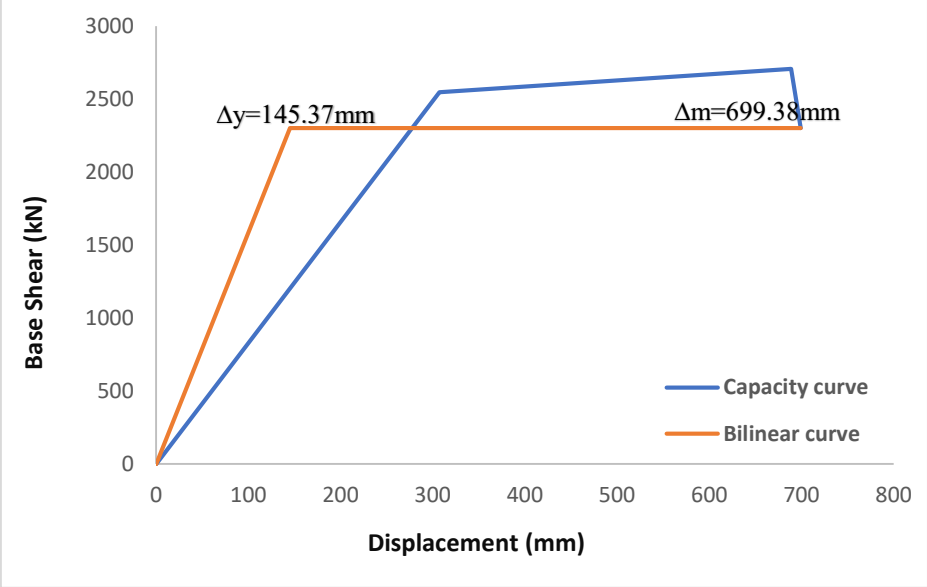

c) Model 71 (span length= 6m)

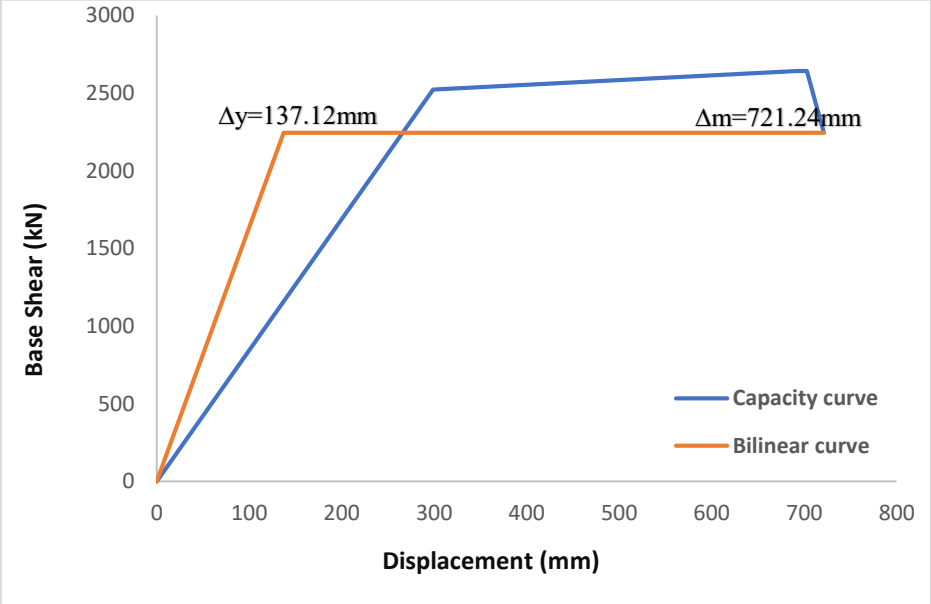

d) Model 72 (span length= 7m)

Figure A.3.2: Pushover (capacity) curve with bilinear curve for (12-story) with (($f'c$)= 250 kgf/cm^2, shear wall thickness = 250mm, shear wall position = middle)

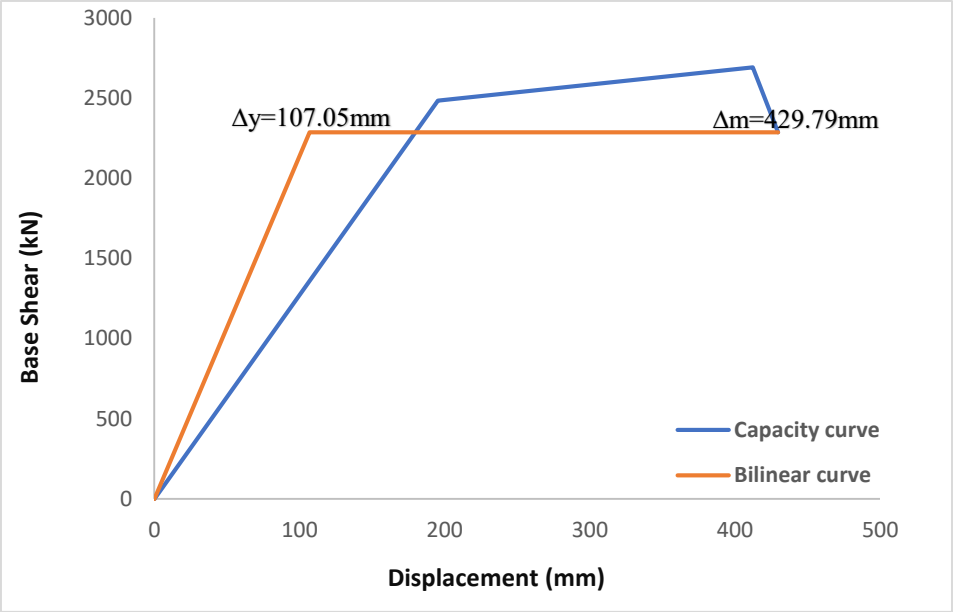

a) Model 73 (span length= 5m)

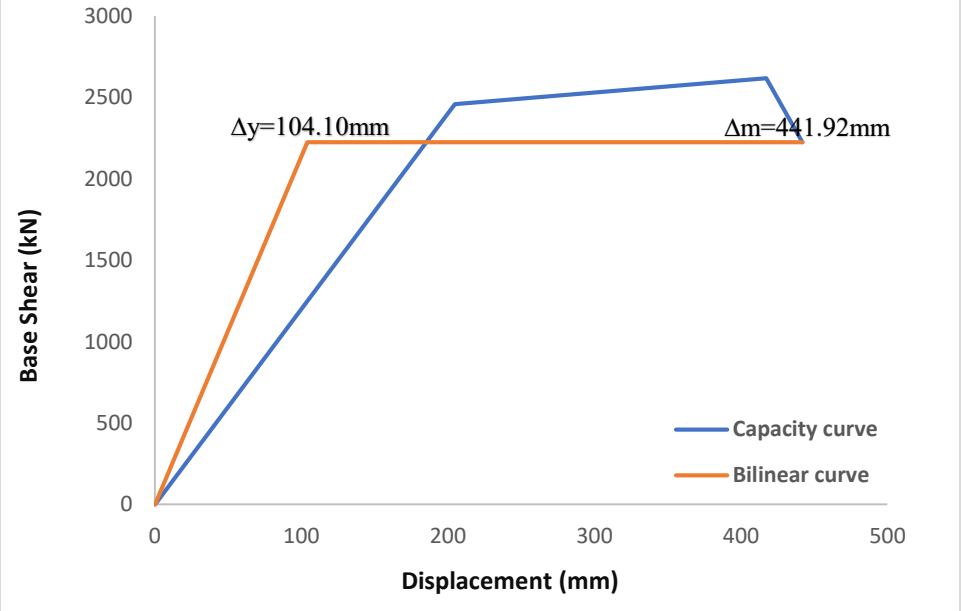

b) Model 74 (span length= 5.5m)

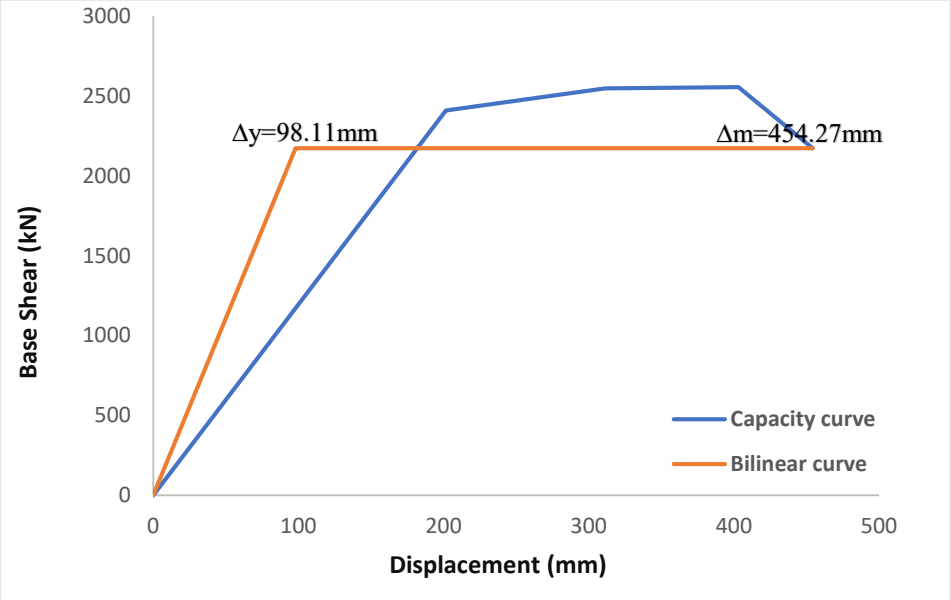

c) Model 75 (span length= 6m)

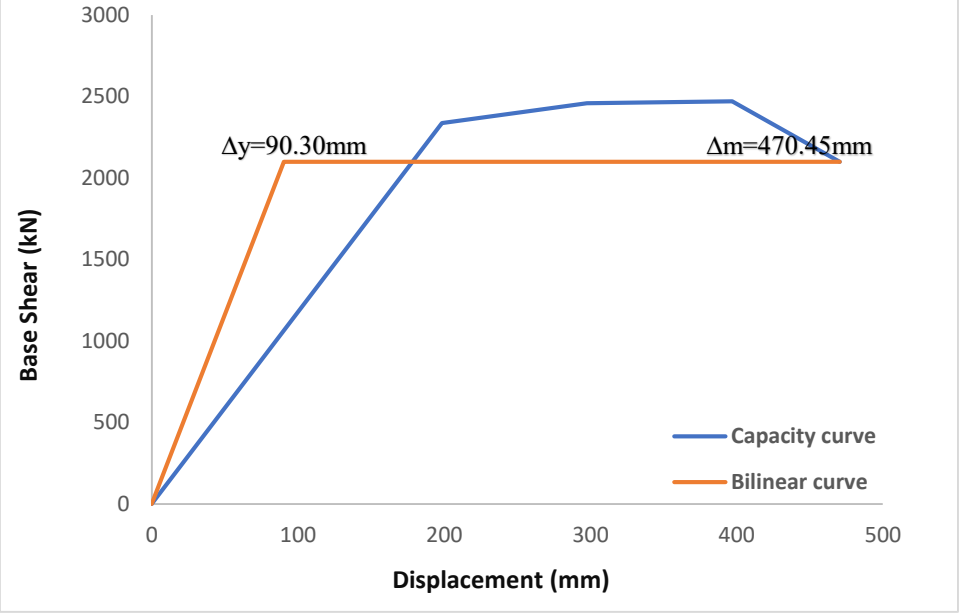

d) Model 76 (span length= 7m)

Figure A.3.3: Pushover (capacity) curve with bilinear curve for (12-story) with (($f'c$)= 250 kgf/cm^2, shear wall thickness = 300mm, shear wall position = edge)

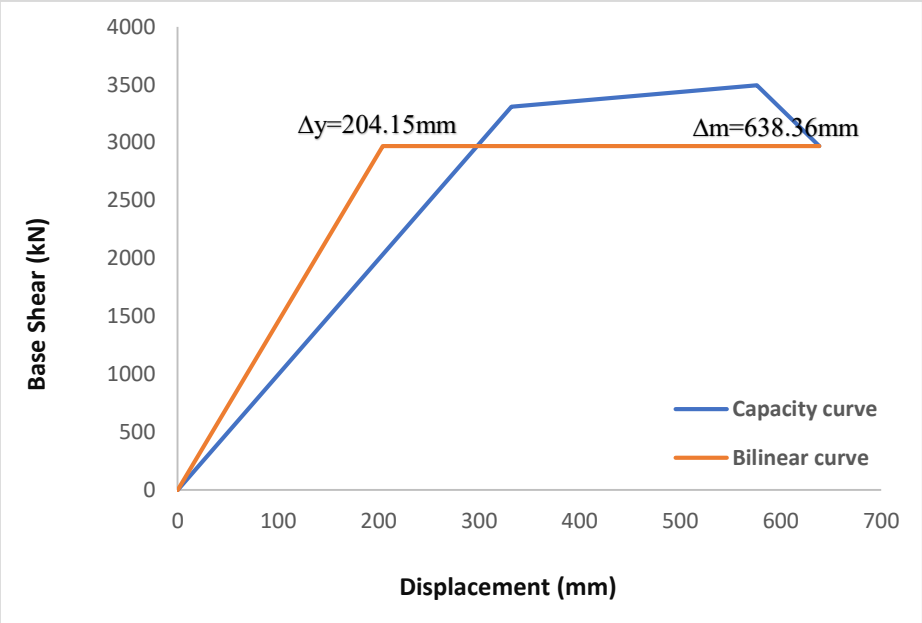

a) Model 77 (span length= 5m)

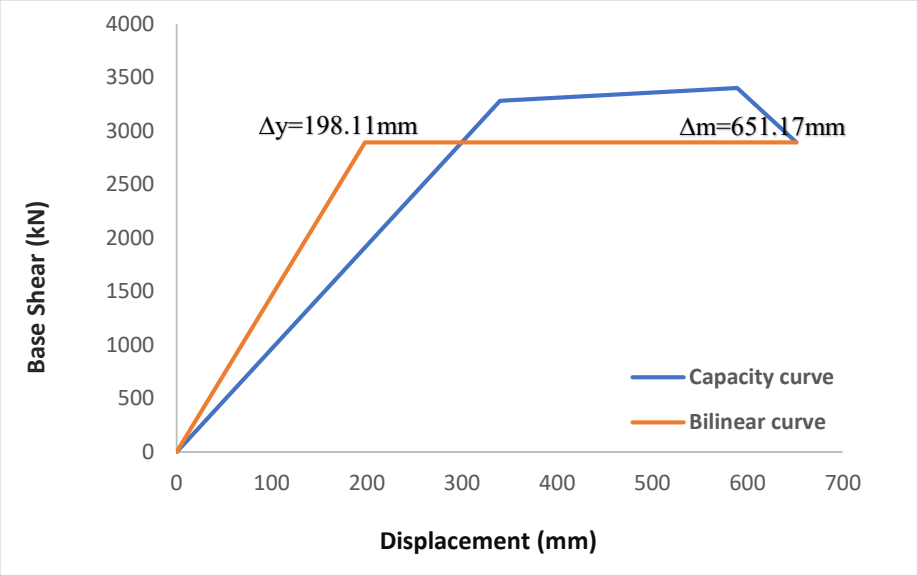

b) Model 78 (span length= 5.5m)

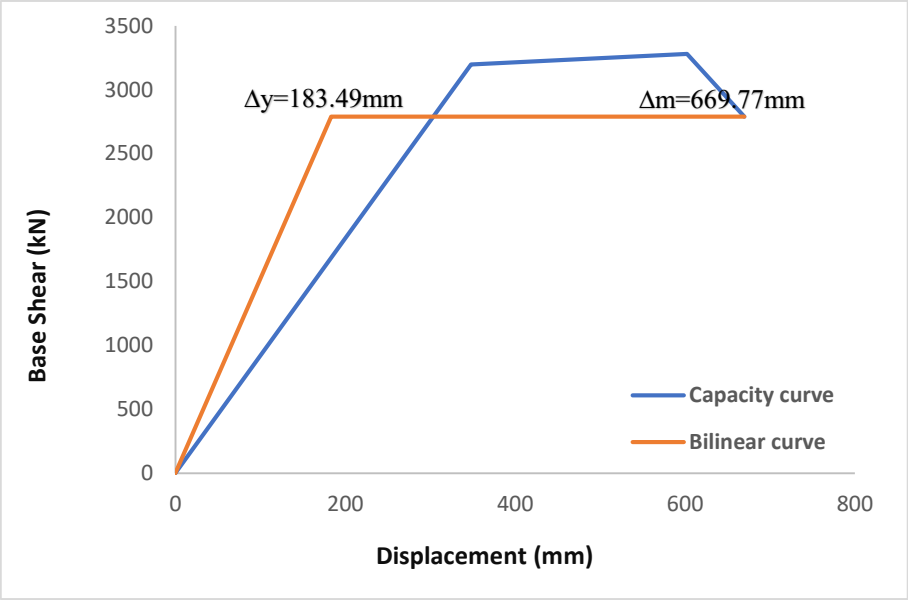

c) Model 79 (span length= 6m)

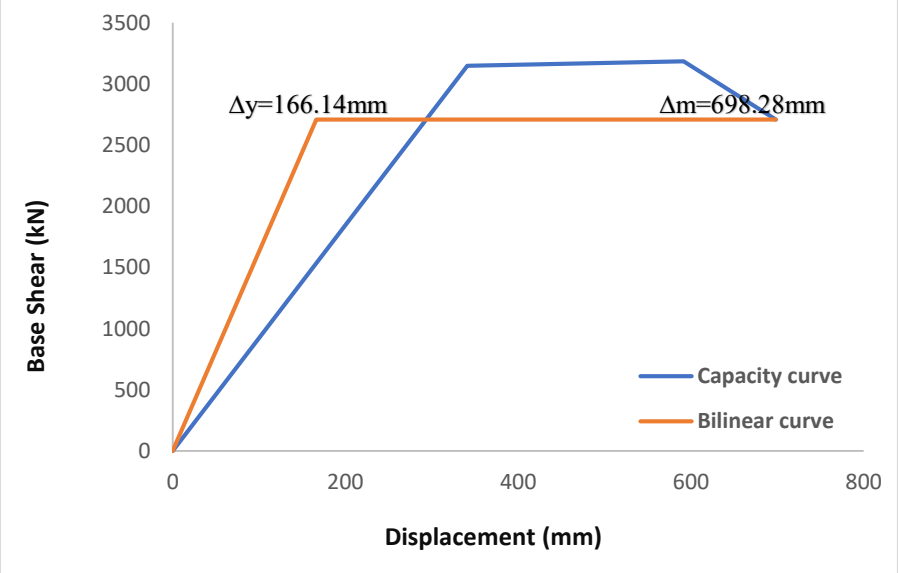

d) Model 80 (span length= 7m)

Figure A.3.4: Pushover (capacity) curve with bilinear curve for (12-story) with (($f'c$)= 250 kgf/cm^2, shear wall thickness = 300mm, shear wall position = middle)

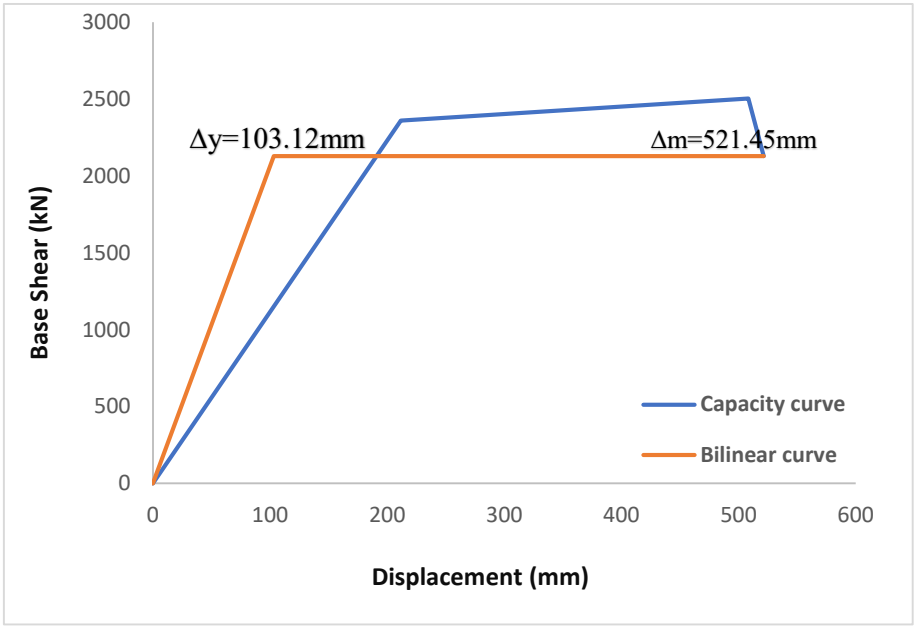

a) Model 81 (span length= 5m)

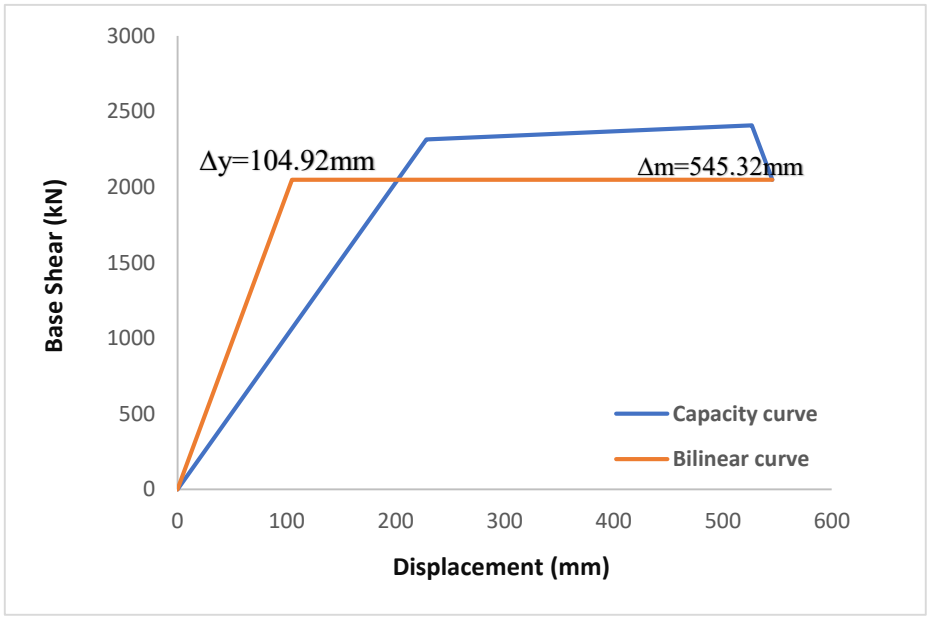

b) Model 82 (span length= 5.5m)

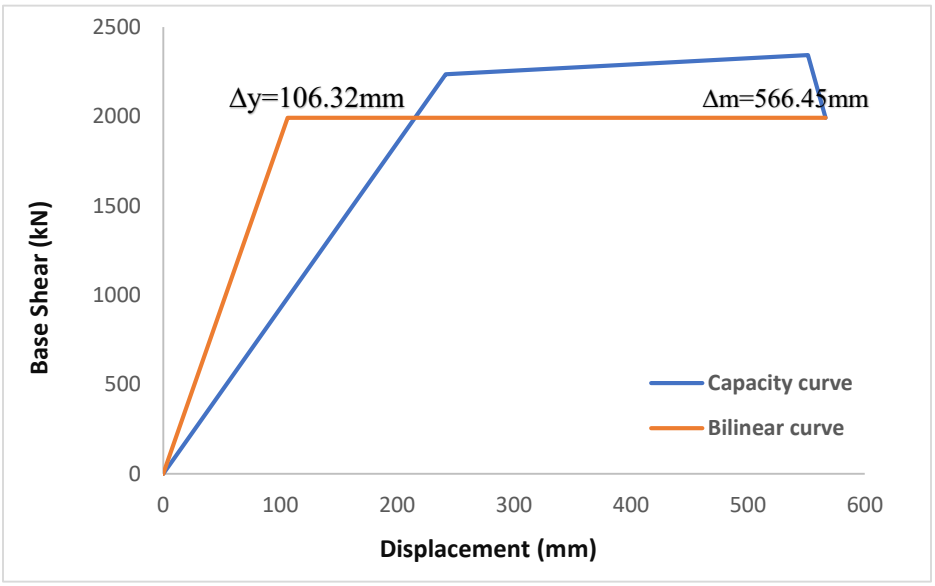

c) Model 83 (span length= 6m)

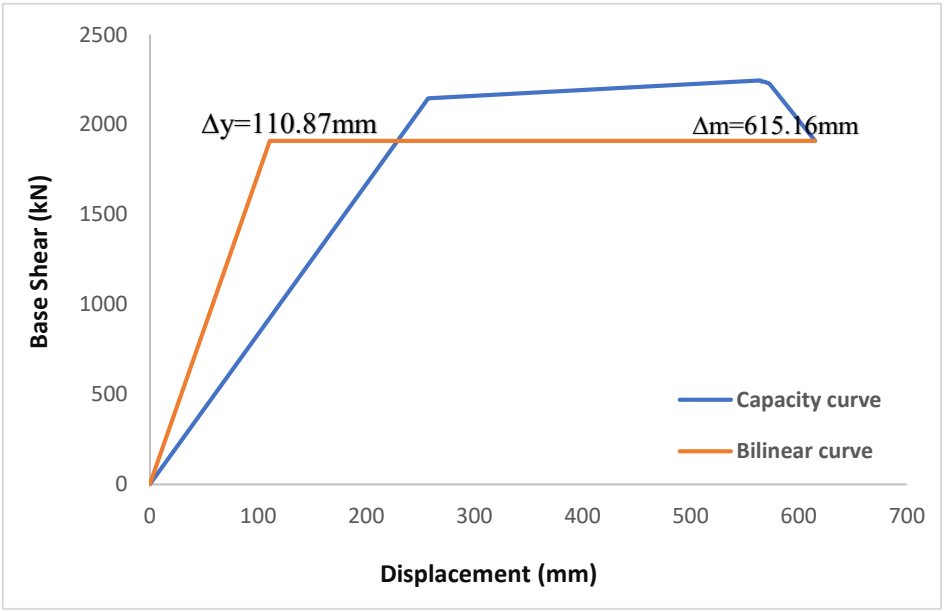

d) Model 84 (span length= 7m)

Figure A.3.5: Pushover (capacity) curve with bilinear curve for (12-story) with (($f'c$)= 300 kgf/cm^2, shear wall thickness = 250mm, shear wall position = edge)

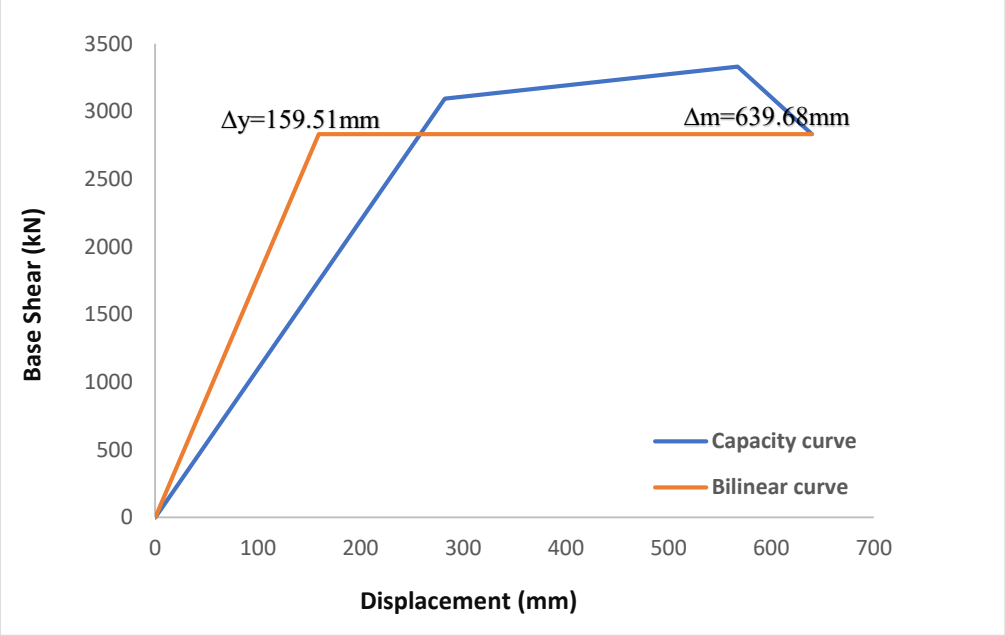

a) Model 85 (span length= 5m)

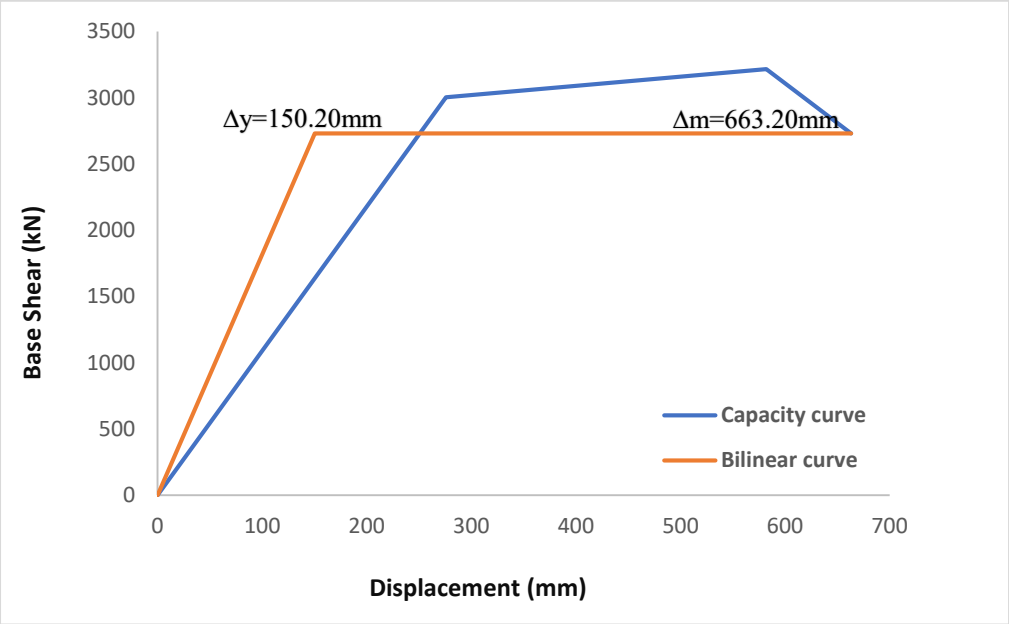

b) Model 86 (span length= 5.5m)

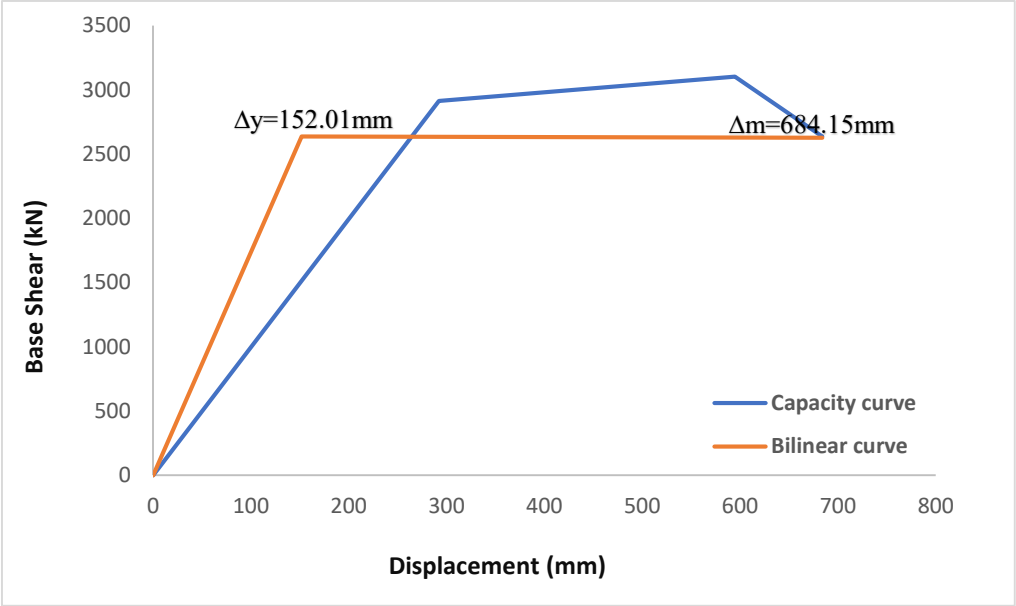

c) Model 87 (span length= 6m)

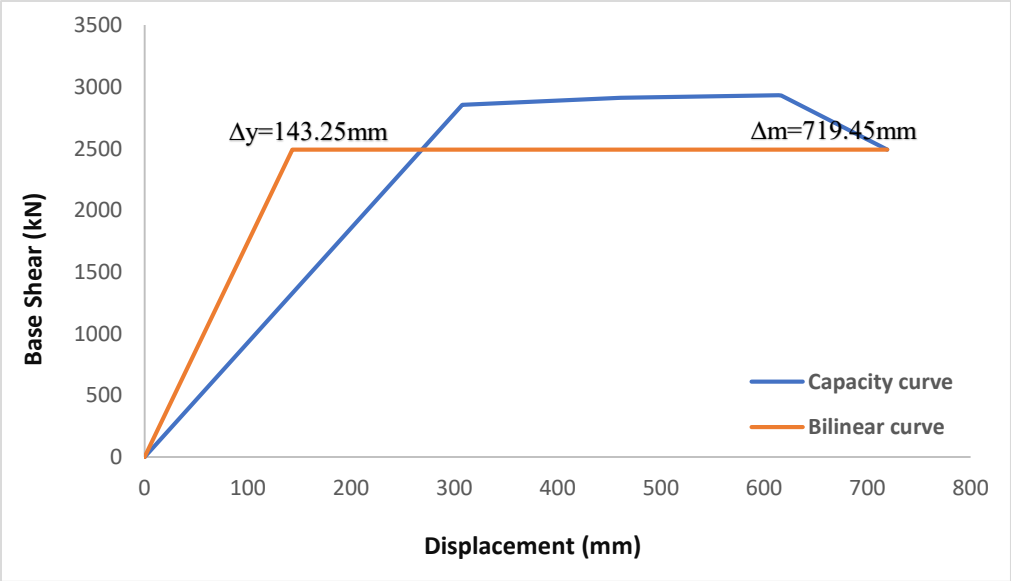

d) Model 88 (span length= 7m)

Figure A.3.6: Pushover (capacity) curve with bilinear curve for (12-story) with (($f'c$)= 300 kgf/cm^2, shear wall thickness = 250mm, shear wall position = middle)

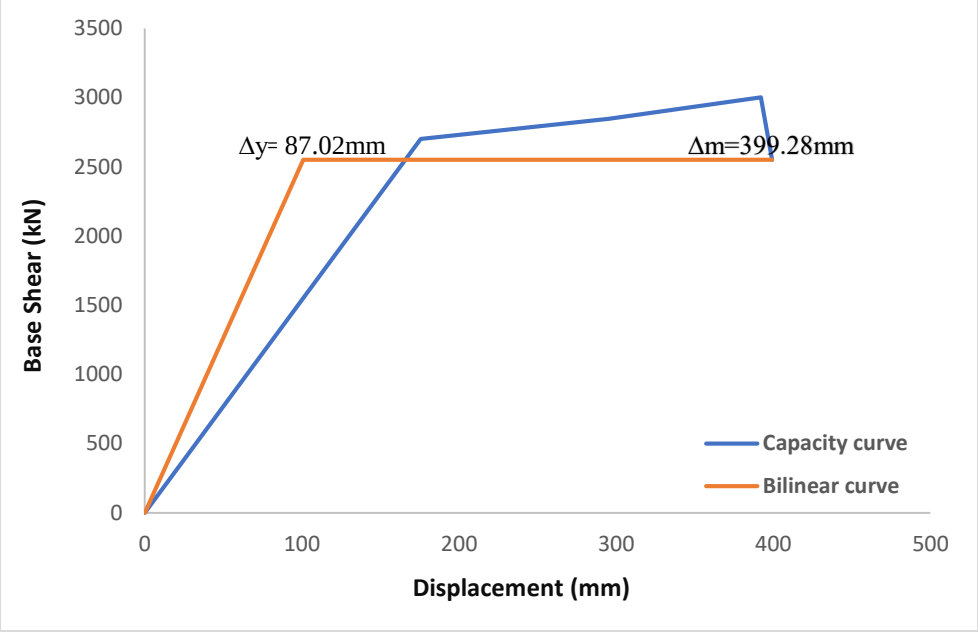

a) Model 89 (span length= 5m)

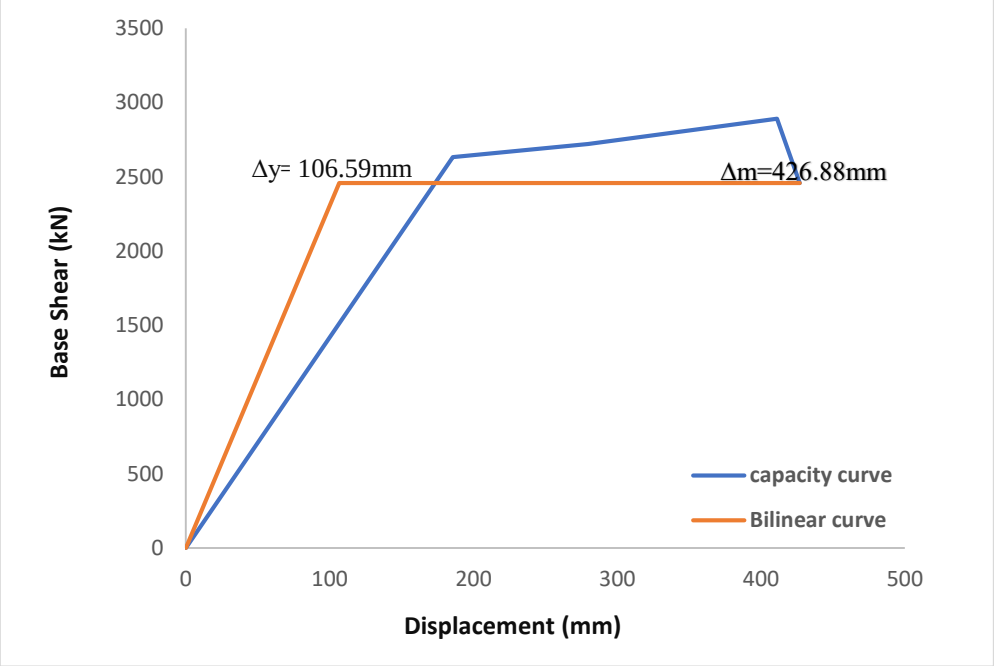

b) Model 90 (span length= 5.5m)

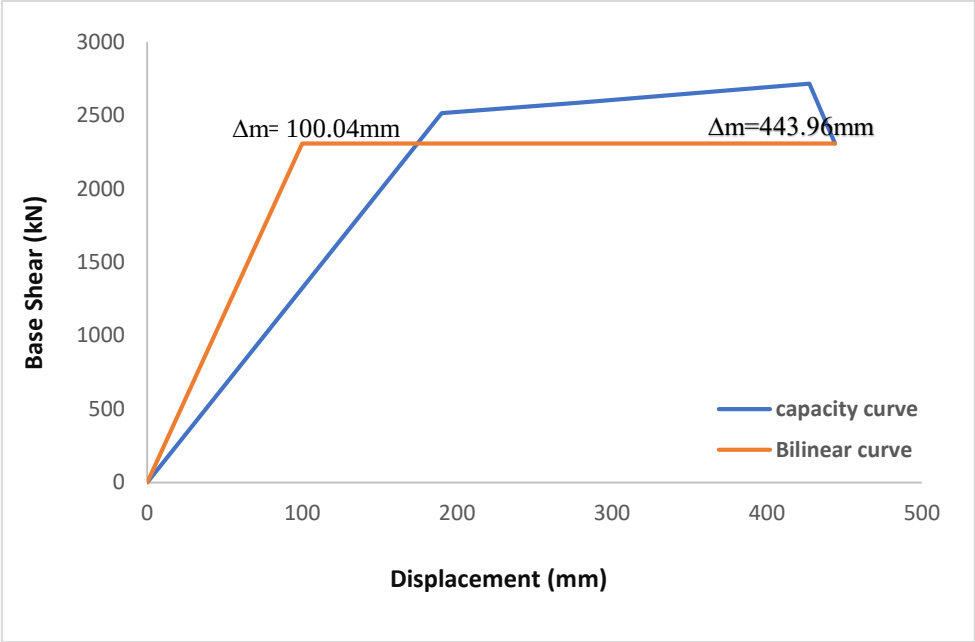

c) Model 91 (span length= 6m)

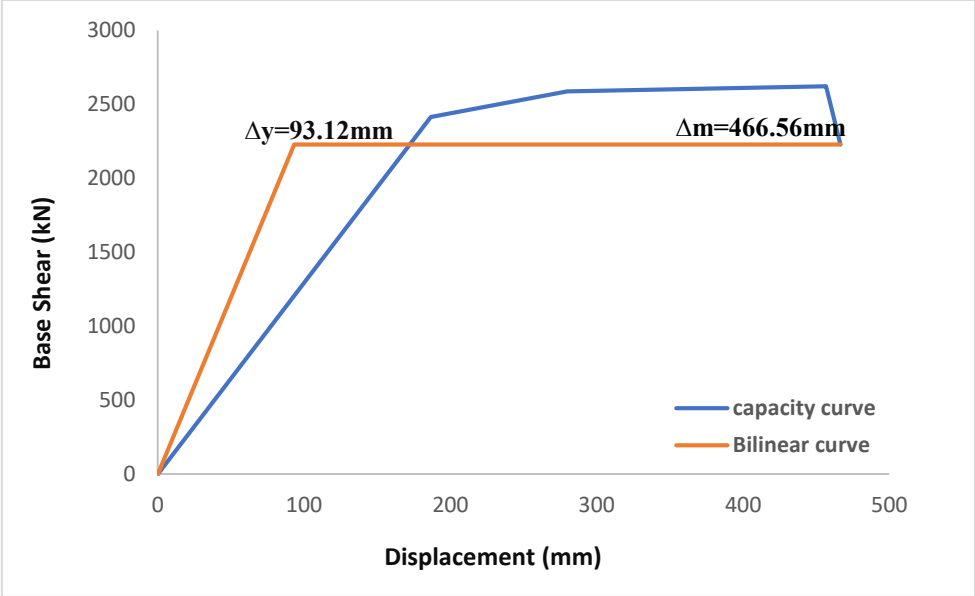

d) Model 92 (span length= 7m)

Figure A.3.7: Pushover (capacity) curve with bilinear curve for (12-story) with (($f'c$)= 300 kgf/cm^2, shear wall thickness = 300mm, shear wall position = edge)

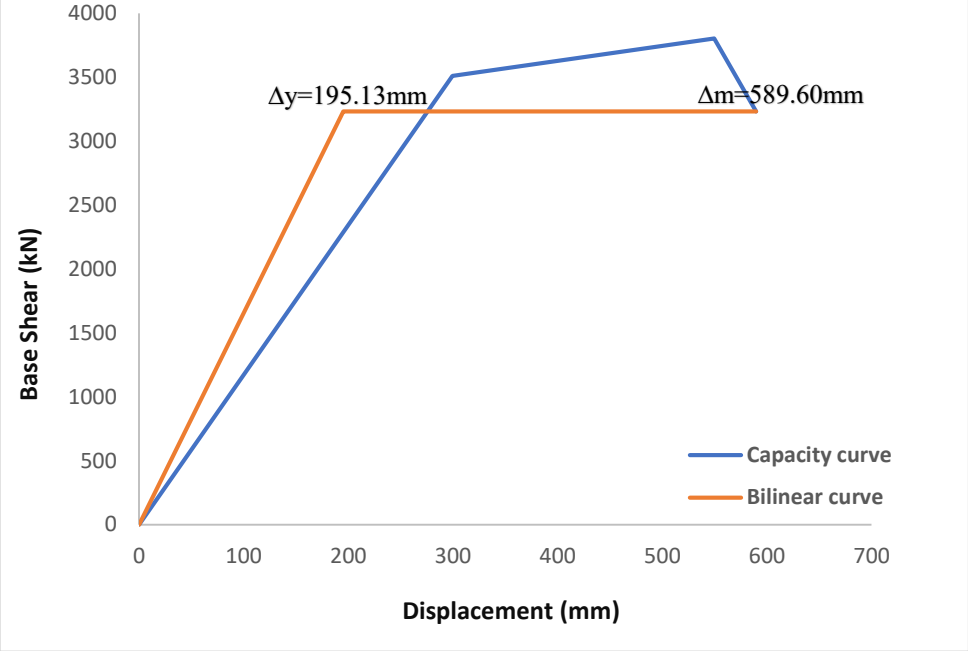

a) Model 93 (span length= 5m)

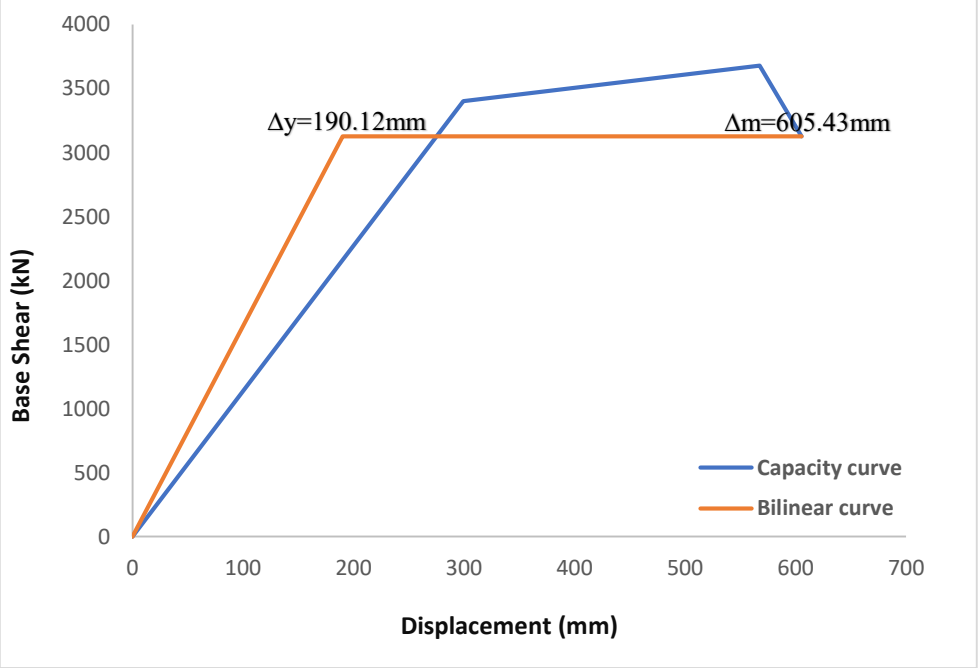

b) Model 94 (span length= 5.5m)

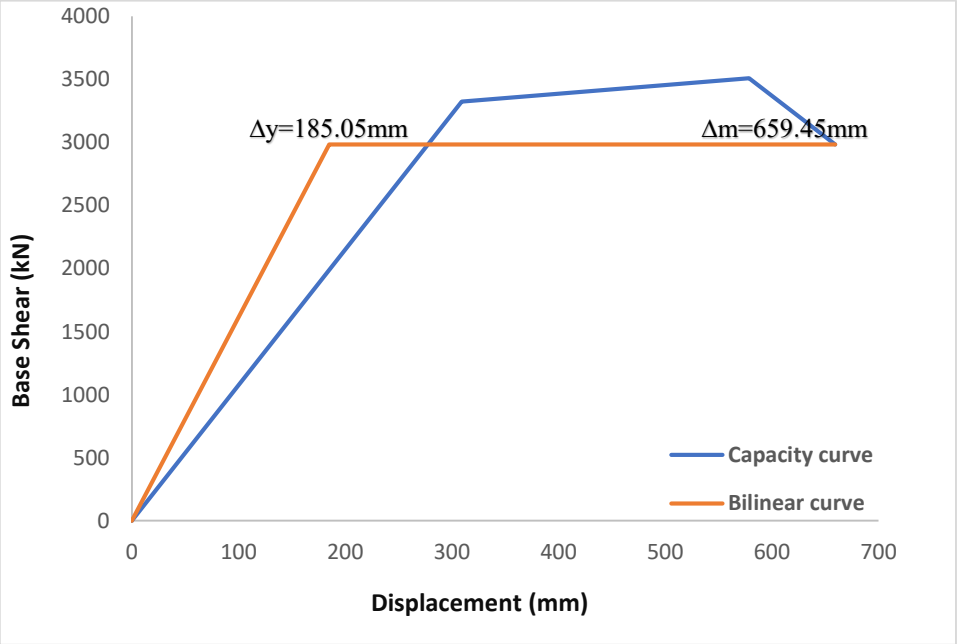

c) Model 95 (span length= 6m)

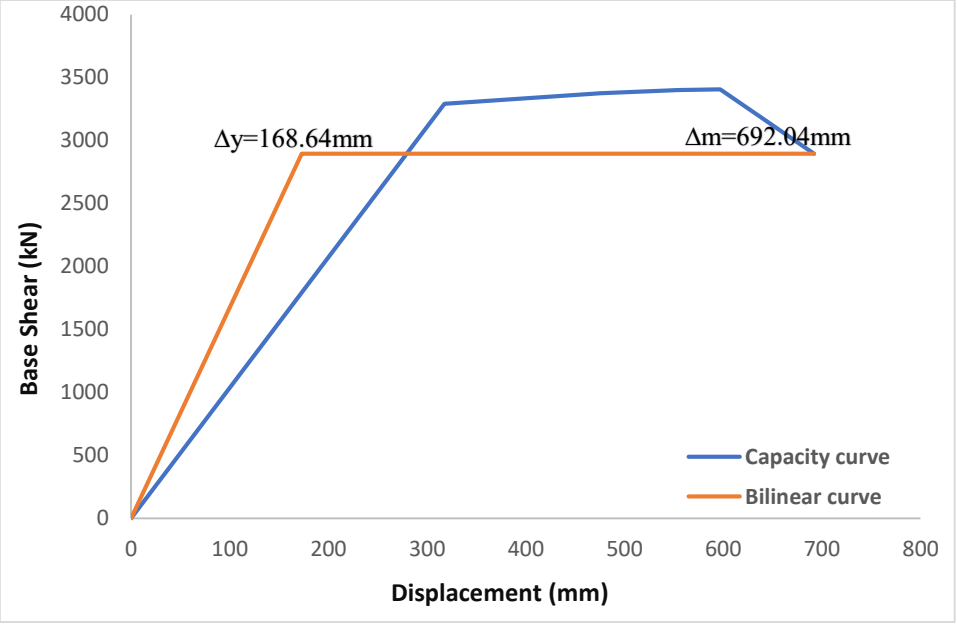

d) Model 96 (span length= 7m)

Figure A.3.8: Pushover (capacity) curve with bilinear curve for (12-story) with (($f'c$)= 300 kgf/cm^2, shear wall thickness = 300mm, shear wall position = middle)

APPENDIX 4

Plagiarism and Ethical Rules Contract Form

YAKIN DOĞU ÜNİVERSİTESİ
NEAR EAST UNIVERSITY

Lisansüstü Programlar
Graduate Studies

İntihal ve Etik Kurallar Sözleşmesi Formu
Plagiarism and Ethical Rules Contract Form

_____2020-2021_____ Akademik Yılı /Academic Year _____Fall_____ Dönemi/ Semester

Ben aşağıda imza sahibi, çalışmalarımda kullanılan ve sunulan tüm bilgileri Yakın Doğu Üniversitesi, Fen Bilimleri Enstitüsü tarafından belirlenen akademik kurallar ve etik çerçeveye uygun şekilde düzenleyeceğimi belirtirim. Aynı zamanda, bu kurallar ve çerçeve uyarınca, kayıtlı bulunduğum program süresince üreteceğim tüm çalışmaların sonuçlarına ait olmayan ve çalışmalarımda kullanacağım tüm materyal ve kaynakları uygun şekilde alıntılanacağımı da beyan ederim. Çalışmalarımın alıntılama konusunda orjinallik açısından kontrol edileceği de bilgim dahilindedir.

I hereby declare that all information utilized in my work will be obtained and presented in accordance with the academic rules and ethical guidelines of the Graduate School of Applied Sciences, Near East University. I also understand that as required by these rules and conduct, I will be fully citing and referencing all materials and results that are not original to my academic studies/essays/analyses. In addition, I am aware that my work will be checked through various plagiarism detection software (such as Ithenticate and Turnitin) for originality.

Açık İsim/ Full Name: SHAHRAM JKHSI QASIM

Öğrenci Numarası/Student No: 20193875

Ana Bilim Dalı/ Department: Civil Engineering Department

İmza/Signature:

Tarih /Date: 28/10/2020

APPENDIX 5

Similarity Report

Skip to Main Content
Assignments
Students
Grade Book
Libraries
Calendar
Discussion
Preferences

About this page

This is your assignment inbox. To view a paper, select the paper's title. To view a Similarity Report, select the paper's Similarity Report icon in the similarity column. A ghosted icon indicates that the Similarity Report has not yet been generated.

Thesis_Shahram Jkhsi Qasim_20193875

Inbox | Now Viewing: new papers ▼

Submit File Online Grading Report | Edit assignment settings | Email non-submitters

Delete Download move to...

	Author	Title	Similarity	web	publication	student papers	Grade	response	File	Paper ID	Date
☐	Shahram Jkhsi Qasim	Abstract	0% 0%	0%	0%	N/A	--	--	download paper	1494023313	25-Jan-2021
☐	Shahram Jkhsi Qasim	Conclusions	0% 0%	0%	0%	N/A	--	--	download paper	1493406606	24-Jan-2021
☐	Shahram Jkhsi Qasim	Chapter 1	1% 1%	1%	0%	N/A	--	--	download paper	1484974485	09-Jan-2021
☐	Shahram Jkhsi Qasim	Chapter 2	2% 2%	2%	2%	N/A	--	--	download paper	1484974571	09-Jan-2021
☐	Shahram Jkhsi Qasim	Chapter 4	6% 6%	5%	3%	N/A	--	--	download paper	1491792579	22-Jan-2021
☐	Shahram Jkhsi Qasim	Chapter 3	11% 11%	9%	7%	N/A	--	--	download paper	1491792302	22-Jan-2021
☐	Shahram Jkhsi Qasim	Full Thesis_Shahram Qasim	13% 13%	11%	7%	N/A	--	--	download paper	1494032123	25-Jan-2021